Universidade de Aveiro
2018
Departamento de Engenharia de Materiais e Cerâmica

Soraia Alexandra Ramos Coelho

MATERIAIS HÍBRIDOS ORGÂNICO-INORGÂNICOS DE BOROSSILICATO POR SOL-GEL, PARA A ENGENHARIA DE TECIDOS ÓSSEOS

HYBRID ORGANIC-INORGANIC BOROSILICATE MATERIALS BY SOL-GEL FOR BONE TISSUE ENGINEERING

Universidade de Aveiro
2018

Departamento de Engenharia de Materiais e Cerâmica

Soraia Alexandra Ramos Coelho

MATERIAIS HÍBRIDOS ORGÂNICO-INORGÂNICOS DE BOROSSILICATO POR SOL-GEL, PARA A ENGENHARIA DE TECIDOS ÓSSEOS

HYBRID ORGANIC-INORGANIC BOROSILICATE MATERIALS BY SOL-GEL FOR BONE TISSUE ENGINEERING

Dissertação apresentada à Universidade de Aveiro para cumprimento dos requisitos necessários à obtenção do grau de Mestre em Mestrado Integrado de Engenharia de Materiais, realizada sob a orientação científica da Doutora Isabel Margarida Miranda Salvado, Professora Associada do Departamento de Engenharia de Materiais e Cerâmica da Universidade de Aveiro, e do Doutor José Carlos Martins de Almeida, Investigador do mesmo departamento.

“There are no limits to what you can accomplish, except the limits you place on your own thinking”

Brian Tracy

The jury

President

Prof. Doutor Jorge Ribeiro Frade
Professor Catedrático da Universidade de Aveiro

Commitee

Doutor Luís Miguel Mota Ferreira
Investigador do Centro de Ciências e Tecnologias Nucleares - Instituto Superior Técnico, Universidade de Lisboa

Profª. Doutora Isabel Margarida Miranda Salvado
Professora Associada da Universidade de Aveiro (Orientadora)

acknowledgments

Firstly, I would like to thank my supervisors, Professor Isabel Salvado and Doctor José Carlos Almeida, for providing me with the opportunity to work with them and in the field of my interests. Specially, I owe my sincere gratitude to Dr. José Carlos for his continued support, patience and motivation, always trying to share his knowledge and positive thinking.

To Professor Maria Helena Fernandes, I am grateful for her help and advices in the field of biomaterials.

From the University of Erlangen, Nuremberg, my acknowledgements to Irem and Professor Aldo R. Boccaccini, and his group, for their collaboration in studies of *in vitro* biocompatibility.

Also, I would like to acknowledge the technical staff of the Department of Materials Engeneering (DEMAC), Eng.ª Célia, Eng.º Artur, as well as Celeste from the Chemical Department, and Dr.ª Rosário Soares from the Central Analysis Laboratory of the University of Aveiro.

From the laboratory, where I spent most of the time, I would like to thank Dr.ª Erika for her constant availability, advices and help every time I needed it.

To my friends, João Couto, Joana Morgado and Marisa Conceição, and my twin sister Catia Coelho, I want to thank for their unconditional support and for allowing me to have moments of distraction when I needed the most. To one of my dearest and oldest friends, Rita Azevedo, for helping me reviewing the thesis.

I would like to give a special thanks to my boyfriend, Nathaniel Roque, for always listening to my worries, for supporting me and encouraging me.

Finally, I must express my very profound gratitude to my parents specially my mother, for providing me with the chance to have a master's degree, and for their support and continuous encouragement throughout my years of study, always believing in me and in my capacities.

palavras-chave

Materiais híbridos, polidimetilsiloxano, borossilicato, sol-gel, bioatividade, citocompatibilidade, angiogénese

resumo

Materiais híbridos baseados no sistema polidimetilsiloxano (PDMS)-SiO_2-CaO, preparados por sol-gel, têm-se revelado um grupo de biomateriais promissores em várias aplicações desde a regeneração de tecidos ósseos a sistemas de libertação de fármacos. Estes híbridos são biocompatíveis e possuem propriedades bioativas e osteogénicas que possibilitam a fixação dos osteoblastos e o crescimento do tecido ósseo. Para além do cálcio, a incorporação de iões terapêuticos, como o boro (B), permite estimular a regeneração óssea e angiogénese, tornando-se uma alternativa ao uso de fatores de crescimento angiogénicos. A combinação destes iões no material híbrido orgânico-inorgânico preparado pelo método sol-gel é uma novidade.

Desta forma, o presente trabalho teve como objetivo produzir um material híbrido bioativo e biocompatível, baseado no sistema PDMS-SiO_2-B_2O_3-CaO capaz de libertar iões de cálcio e boro a fim de estimular a angiogénese. Com isto surgiu a necessidade de entender o efeito do boro e do cálcio na estrutura e microestrutura do material e, consequentemente, a influência destes na atividade biológica. Para alcançar tais objetivos, cinco composições diferentes com concentrações de boro distintas foram preparadas, usando os mesmos precursores e técnica de sol-gel. Os materiais resultantes apresentavam-se na forma de monólito e com diferentes estruturas e microestruturas entre eles.

Da análise estrutural do material, que foi realizada por espectroscopia de Infravermelhos por Transformada de Fourier (FT-IR) e por Ressonância Nuclear Magnética (NMR), verificou-se a presença de ligações híbridas (Si-O-Si) entre a fase orgânica (PDMS) e a fase inorgânica (TEOS), assim como ligações características de borosiloxano (B-O-Si). A partir dos resultados de ressonância nuclear magnética do boro (^{11}B) verificou-se que a presença do ião modificador (cálcio) nas composições faz alterar a coordenação do boro, de trigonal (BO_3) para tetraédrico (BO_4), e que estes encontram-se ligados ao silício. Verificou-se que o aumento da concentração de boro no sistema híbrido tem como consequência a diminuição dos valores da área superficial especifica (SSA), obtidos pela técnica de Brunauer-Emmet-Teller (BET), assim como da mesoporosidade do material. Por outro lado, as micrografias, obtidas por Microscopia Eletrónica de Varrimento (SEM), mostraram um aumento da macroporosidade com a adição do boro. Os testes de bioatividade realizados *in vitro*, por imersão do material num fluído corporal simulado (SBF), revelaram a capacidade do material em se degradar, libertando iões de cálcio e boro no líquido sobrenadante, assim como em depositar uma camada de fosfato de cálcio à superfície, sugerindo bioatividade. Isto sugere o potencial destes materiais híbridos para serem utilizados na área da regeneração de tecidos ósseos.

A relação entre a estrutura, microestrutura e libertação iónica foram discutidas de forma a identificar as formulações que irão continuar para posteriores estudos com linhas celulares específicas relacionadas com a angiogénese,

keywords

Hybrid Materials, polydimetilsiloxane, borosilicate, sol-gel, bioactivity, cytocompatibility, angiogenesis

abstract

Polydimethylsiloxane (PDMS) - SiO_2 - CaO based hybrid materials, prepared by sol-gel, have proven to be very promising materials in tissue engineering applications and drug delivery systems. These hybrid materials present biocompatible, osteogenic and bioactive properties, that will support osteoblast attachment and bone growth. The incorporation of therapeutic ions, such as boron (B), is known to stimulate bone regeneration and angiogenesis, which makes it an alternative to the use of vascular growth factors, due to its low cost, high stability and potentially greater safety. The combination of such ions in hybrid materials prepared by the sol-gel method is a novelty.

The main purpose of this work was to produce, by sol-gel method, bioactive and biocompatible hybrid materials within the system PDMS-SiO_2-B_2O_3-CaO capable of releasing calcium and boron to stimulate angiogenesis. Another purpose was to achieve a better understanding of the effect of boron in the structure and microstructure of this material. For that, five different compositions with different amounts of boron were prepared using the same precursors and sol-gel route, resulting in different monolithic materials, with distinct structures and microstructures. The material's structure was analysed by Fourier Transform Infrared Spectrometry (FT-IR) and solid state Nuclear Magnetic Resonance (NMR) techniques, that expose the presence of hybrid bonds (Si-O-Si) between organic (PDMS) and inorganic phase (TEOS), as well as borosiloxane bonds (B-O-Si). From the results of nuclear magnetic resonance of ^{11}B it was found that the presence of the modifier ion (calcium) in the compositions changes the boron coordination, from trigonal (BO_3) to tetrahedral (BO_4). These groups are attached to silicon. Thus, it was verified that the increase of boron amount in the system led to a decrease in the specific surface area (SSA), obtained by BET method, as well as the mesoporosity of the material. On the other hand, SEM micrography's showed an increase in macroporosity with the boron concentration. The bioactivity tests performed *in vitro* by immersion of the materials in Kokukos's simulated body fluid (SBF), demonstrated that the material was able to form a layer of calcium phosphate on its surface, and to release therapeutic ions in the supernatant liquid. Thus, this suggests the potential of these materials to be used in the field of tissue regeneration.

The relationship among structure, microstructure and ion release were discussed aiming the identification of the formulations that will continue for further studies with specific angiogenesis-related cell lines

Table of Contents

List of Figures

List of Tables

List of Acronyms and Abbreviations

a.u.	Arbitrary Units
BET	Brunauer-Emmett-Teller method
ca.	*Circa*
CaAc	Calcium acetate
EDS	Energy Dispersive X-ray Spectroscopy
FT-IR	Fourier Transform Infrared Spectroscopy
HA	Hydroxyapatite
ICP	Inductively Coupled Plasma
IR	Infrared
ISO	International Standard Organization
IUPAC	International Union of Pure and Applied Chemistry
IPA	Isopropanol
MAS	Magical Angle Spinning
NMR	Nuclear Magnetic Resonance
ORMOSIL	Organically modified silicate
ppm	Parts-per-million
PCL	Poly ε-caprolactone
PDMS	Polydimethylsiloxane
PTMO	Polytetramethylene oxide
PVA	Polyvinyl alcohol
pH	Potential of Hydrogen
SEM	Scanning Electron Microscopy
SBF	Simulated Body Fluid
SSA	Specific Surface Area
TEOS	Tetraethyl Orthosilicate
TEB	Triethylborate
TMB	Trimethylborate
XRD	X-Ray Diffraction

List of Symbols

δ_a	Bending (asymmetric) vibrational mode
δ_s	Bending (symmetric) vibration mode
δ	Chemical shift (NMR)
$D_{(Q)}$	Cross-linked D-Q structural unit
D^n	Difunctional structural unit
n	Number of bridging oxygen atoms surrounding Si
ν_a	Stretching (asymmetric) vibrational mode
ν_s	Stretching (symmetric) vibrational mode
T	Temperature
Q^n	Tetrafunctional structural unit
r	H_2O/TEOS molar ratio
wt.%	Weight percent

Chapter 1

Introduction

The present thesis is divided in five chapters. Chapter I – Introduction, the current one, summaries the background and the main objectives of this thesis. Chapter II address the literature review about bone tissue, tissue engineering, biomaterials, particularly, hybrid materials and the importance and influence of their therapeutic ions in the material structure and biological behaviour. Chapter III presents the experimental procedure and the characterization techniques performed to the material. In Chapter IV it is exposed the data from the analysis and its discussion. Ultimately, Chapter V presents the conclusions of this work and the possible future works.

1.1. Background

The increase in the human longevity has led to a continuous search for new materials, in order to provide a better quality of life for the human being. However, bone defects, caused by diseases or injuries, are consider a serious health problem that affect both the elderly and young people. Bone treatments are generally done using bone grafts, however they have shown several limitations, over the years, which have encouraged the development of artificial materials. The scientific progress has given rise to new approaches, in which the biomaterials not only have the aim of replace (structural role), but also are focused on the regeneration (functional role). These materials integrate the Tissue Engineering (TE) field, which is based on the repair and regeneration of damaged tissues and organs (particularly in bone tissues) as a result of diseases, injuries or aging [1,2]. This multidisciplinary field makes use of biomaterials, cells and growth factors, and for the success of its processes, the biomaterials need to present certain characteristics: biocompatibility, bioactivity, and some need to be biodegradable, porous and with mechanical behaviour similar to the host bone [3–5]. Since bone is considered a hybrid structure with an extracellular matrix mainly consisting of an organic (collagen) and an inorganic (apatite) phase, many researchers have been tried to produce a hybrid material that can combine these two phases for the regeneration of bone tissues.

The search for a material with mechanical properties close to those of human bone produced a new family of hybrid materials, named organically modified silicates (ORMOSILs), that take advantage of the synergy between inorganic silica (SiO_4) domains, based on sol-gel bioactive glass compositions, and organic polydimethylsiloxane, PDMS ($((CH_3)_2.SiO_2)_n$, domains [6–9]. These domains interact at a nanoscale, allowing the combination of the mechanical and bioactive properties of the inorganic phase, with the flexibility and controlled degradation rate of the organic phase. Several studies have shown that hybrid materials based on PDMS-SiO_2 system and produced by the sol-gel

process, are potential biomaterials for various applications, such as bone tissue engineering, scaffold production, and controlled drug delivery systems [7].

Sol-gel process has already been used in the preparation of inorganic materials, such as silicate-based bioactive glasses, make them with better features and properties for biomedical applications. This process was attracted much attention due to the possibility of controlling both the materials composition and morphology, providing the synthesis of the products at low temperatures, and with high degree of homogeneity and purity at a molecular level. The resulting sol-gel materials tend to be more porous and with higher surface area, which contributes to an excellent rate of degradation/reabsorption while occurs the formation of hydroxyapatite layer (HA) on the surface of the material. This layer is an indicator of the materials' potential bioactivity and are responsible for the development of strong chemical bond between the materials and the bone tissue [4].

The conception of the calcium-phosphate layer (bioactivity) is due to the ionic dissolution products from the material, which are also responsible for its osteoconductive, osteogenic and angiogenic properties. In this way, the biological behaviour can be improved by the incorporation of chemical elements, as therapeutic agents, into the composition of the materials. It is the case of calcium (Ca) and boron (B) ions, which are known to be involved in the bone metabolism and to play a physiological role in angiogenesis, grow and mineralization of bone tissues [4,10–14].

Calcium ion is one of the main constituents of biological apatite – inorganic phase of the human bone, thus it is obvious its importance and presence in the material. However, one of the major drawbacks pointed regarding the utilization of these hybrids, has been the use of calcium nitrate as the calcium source in sol-gel processing. These nitrates are potentially harmful due to the toxicity of the formed nitrites as by-products and they only can be extracted at temperatures above 400ºC. Still, in this case it is not possible, because the polymer used in the material will degrade [15]. An alternative was the use of calcium acetate as calcium source for PDMS-SiO_2-base hybrids, to produce a cytocompatible material. The use of this precursor is not very common and its application in this hybrid system is also new. Therefore, the way calcium is arranged in the silica network and the chemical bonds that are established are important factors to study.

In addition to calcium, the boron effects are also important and, as far as the authors know, the preparation of hybrids with the presence of these two ions is a novelty [16–19]. Hence, the way the boron behaves in PDMS-SiO_2-CaO hybrid system, when and how it is incorporated in the silica network during the sol-gel reactions, what links it establishes and with which chemical groups, are aspects that need to be considered, since they are going to affect the structure and microstructure of the final materials.

1.2. Objectives

The main purpose of the present work is to develop a sol-gel procedure to produce biocompatible PDMS-SiO_2-B_2O_3-CaO hybrid materials, for application in bone tissue engineering. It is intended that these hybrid materials have the capacity of releasing calcium and boron simultaneously, in order to induce osteogenesis and angiogenesis, which are fundamental to the repair and growth of bone tissue. Another objective is to study the influence of Ca and B ions on the structure and microstructure of materials. The material's structure and microstructure will be analysed by Fourier Transform Infrared Spectrometry (FT-IR), X-ray Diffraction (XRD), Nuclear Magnetic Resonance (NMR), Scanning Electron Microscopy (SEM) and nitrogen adsorption (BET). The bioactivity will be evaluated *in vitro* by immersion of the materials in Kokubos's simulated body fluid (SBF) and a subsequent surface analysis will be done by SEM and XRD. The supernatant soaking liquid will be analysed by Inductively Coupled Plasma Spectroscopy (ICP), to determine, in particularly, the concentrations of calcium boron in the liquid. Finally, the cytocompatibility assays will be performed *in vitro* in a cellular medium, and it will be carried out by the University of Erlangen, Nuremberg, Germany. The cell biology studies will be designed to investigate the possible cytotoxicity of the samples and to determine the effect of samples on osteoblast and mesenchymal stem cell activity, and differentiation ability.

At the end of the project, one expects to have a better understanding of the relationship between preparation conditions, structure and microstructure, and to relate those parameters with the *in vitro* acellular and cellular behaviour of the developed materials.

Chapter 2

State of the art

2.1. Bone tissue

The development achieved at a scientific level and the search for new materials over time have allowed the increase in longevity of mankind. However, the increase in life expectancy results in the aging of the population, arising a higher probability of diseases or injuries in elder people. Bone defects are the most common problem and can arise due to trauma, osteoporosis or tumour removal. In addition, they are difficult to recover, since bone regeneration speed decreases with the age.

The bone is a dynamic, highly vascularized, self-repairing connective tissue that plays important roles in our body. Its responsibilities include supporting muscles, protecting internal organs and being able to respond to multiple stimuli, while adapting its shape and properties to mechanical and metabolic changes. This constant reorganization of the tissue is due to the presence of a mineral reservoir, namely calcium and phosphorus ions, and bone cells, that allow the elimination of the old bone and the constant formation, resorption and repairment of the matrix [5].

The bone tissue is a mineralized tissue with two macrostructures: the cortical bone (or compact bone) and the trabecular or cancellous bone (spongy bone). The main difference between them is the porosity. The cortical bone corresponds to the outer layer of the bone and it is dense, with only 10% of porosity. Also, it is well vascularized and mineralized [20]. Its interior is formed by a set of channels, Volkmann and Havers channels, that contains nerves and blood vessels. The trabecular bone is the inner part of the bone and it is constituted by an irregular and interconnected porous structure, with 50 to 90% of porosity. This interconnected network is called trabeculae and has in its inner bone marrow and stem cells. Unlike the compact bone, the cancellous bone has a higher surface area, because it is less dense, which makes it weaker and more flexible. Its Young's modulus and compressive strength are around 20 times inferior than those of the cortical bone [5]. However, the greater surface area contributes to the diffusion of nutrients and growth factors, making it more metabolically active than compact bone [21]. Figure 1 shows and identified the different macrostructures of the bone, and its components.

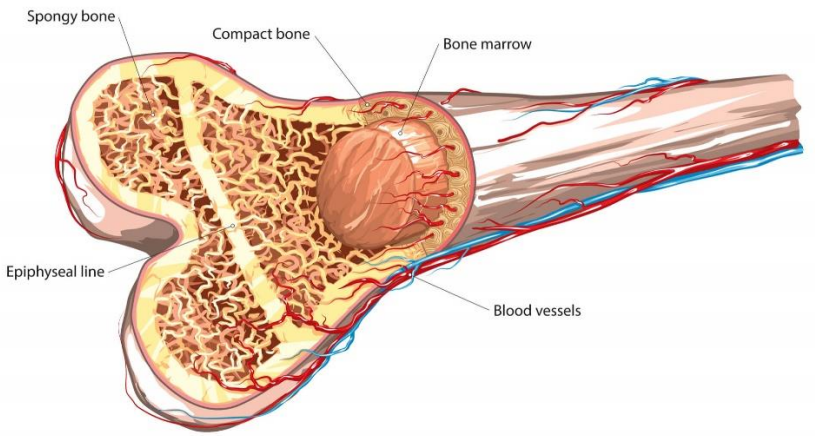

Figure 1 - Example of bone tissues.

Regarding the composition, the bone tissue consists of an extracellular matrix with two components: an organic phase (30%) composed by proteins, mainly type I collagen fibbers (natural polymer); and a mineral inorganic phase (70%) constituted essentially by calcium and phosphate salts, being the major salt hydroxyapatite (HA) ($Ca_{10}(PO_4)_6(OH)_2$. The ratio of calcium to phosphate varies between 1.3 and 2.0 (per weight). Other minerals are present but in smaller amount (Mg, Na, K, Zn, Sr, C). The HA crystals are small (10 to 100 nm) and are distributed along the collagen fibbers. This junction of hydroxyapatite and collagen fibbers combines their main properties, that are compressive strength and tensile strength respectively, allowing the hardening and characteristic strengthening of the bone tissue. While collagen possesses a Young's modulus of 1-2 GPa and a tensile strength of 50-1000 MPa, the mineral hydroxyapatite has ~ 130 GPa and ~100 MPa [22]. Both components are fundamental for the proper functioning and performance of the bone. From a material's science perspective, the bone is a hybrid material of a polymer-ceramic (organic-inorganic), with a hierarchical structural organization of its constituents [3,5,22].

As said before, the bone is a highly dynamic form of connective tissue which undergoes continuous remodelling to optimally adapt its structure to changing functional demands. This remodelling, that consists in the elaboration, maintenance and resorption of bone tissue, results from the interaction of three cell types: osteoblasts, osteocytes and osteoclasts [5]. All of them have defined tasks and are essential for the maintenance of a healthy bone tissue:

- *Osteoblasts:* arise from the mesenchymal stem cells (MSC) present in the bone marrow, which differentiate into osteoblasts through the growth factors in the body. These cells are responsible for the synthesis of the organic part and, then, for the mineralization of the bone tissue.

- *Osteocytes:* inactive osteoblasts that are trapped in the bone matrix, occupying the spaces known as lacunae. They play important functions in skeletal maintenance.
- *Osteoclasts:* are involved in the process of reabsorption of the old bone tissue [5,23,24].

The bone is constantly remodelled by the resorption of osteoclasts followed by the formation of a new bone by osteoblasts. These processes of self-regeneration of the extracellular bone matrix are done by the differentiation of the osteoblasts and occurs in three stages. First occurs the proliferation of cells, in which the expulsion of proteins by the osteoblasts results in the non-mineralized component of the matrix (organic phase). Subsequently, the matrix maturation is achieved by the cross-linking of the proteins, which allows the formation of a more compact and stable structure. At this stage, the matrix is called "osteoid". Finally, the mineralization of the matrix occurs, through which the calcium and phosphate (and other inorganic minerals) precipitate and deposit on the collagen fibbers connecting with them, resulting in the inorganic component of the bone matrix [25]. After some time, these inorganic precipitates become crystals of hydroxyapatite.

Besides osteoblasts, mesenchymal stem cells also generate blood vessel cells, whose active formation is essential for the cell survival, and so, for the bone development, since they allow the transport and exchange of oxygen, nutrients and growth factors. The bone is a highly vascularized tissue, with its skeletal integrity being maintained by the connection and interaction between blood vessels and bone cells [11]. There are several growth factors and cytokines that are involved in the neoangiogenesis of the bone, such as vascular endothelial growth factor (VEGF), basic fibroblast growth factor (bFGF), transforming growth factor beta (β-TGF), and linterleukina 6(IL-6) and linterleukina 8 (IL-8), respectively [11].

***

However, this ability of spontaneous regeneration that the bone possesses is not always enough. In those cases of fracture or disease the process can be speeded up with the use of implants. More and new medical procedures have been requested, for repairing bone defects or losses of tissues or organs, as a result of trauma, injury, disease or aging [1]. Current treatments are based on grafts (transplants), that have the purpose of restoring some of the lost functionalities. According to their origin, they can be classified as autografts, allografts and synthetic grafts. Autografts are the gold standard, which involves transplanting bone from another part of the patient's own body to the defect site. Although they are the most preferred, there may be complications, since the bone is limited in supply, and it can give rise to chronic pain and infection in the patient. Allograft is another alternative, in which a bone or organ is taken from another person, and it is available from a bone bank. Still, it

is expensive and potentiates risks of disease transmission from donor to host. Synthetic grafts (alloplastic materials) are also used as substitutes and are usually made of metal or ceramic protheses. Although metals provide immediate mechanical support at the site of the defect, they are stronger and stiffer than bone and have limitations in terms of integration capacity with the surrounding tissue, which can lead to failure because of infection. Another problem is the different size of the ions. Ceramic materials have the advantage of being based on hydroxyapatite, which is similar to the bone mineral phase. However, they have low tensile strength and are brittle, making it impossible to be used in locations of significant torsion or bending [5,26].

Even though these therapies have saved and improved countless lives, they remain imperfect solutions. The costs, the risks of transplantation, the reconstruction and the durability of the implants are some of their biggest limitations.

2.2. Tissue Engineering

A new promising approach and solution has emerged: Tissue Engineering (TE). Langer and Vacanti defined it as "an interdisciplinary field that applies the principles of engineering and the life sciences toward the development of biological substitutes that restore, maintain, or improve the tissue functions" [1]. Tissues such as skin, bone and cartilage have been successfully regenerated. This can potentially overcome the problem of a shortage of living tissues and organs available for transplantation [1,2]. In contrast to the classic biomaterials approach, it aims to develop materials focused on the regeneration of damaged tissue, instead of just replacing them [4].

In this field, tissue scaffold is the most common biomaterial used, and it serves as a three-dimensional (3D) temporary structure for cells to migrate, proliferate and differentiate and, consequently, synthesize a new tissue or organ with a desired shape and dimension [3,4]. Generally, the materials are seeded with cells, growth factors, or can be subjected to mechanical or environmental chemical stimuli. These cells can be cultured in two different ways: *in vitro* or *in vivo*. *In vitro*, the cells harvested from the patient (osteogenic cells in the case of bone) are seeded in a controlled environmental with the synthetic biomaterial and left to proliferate. Then, the biomaterial formed is implanted back into the patient. *In vivo*, the biomaterial is directly implanted into the defect, to guide and stimulate tissue repair in situ, seeded with cells or not [2,4,27]. In Figure 2 it is represented a scheme of the *in vitro* strategies, where cells are seeded in a scaffold and, posteriorly, incorporated in the patient [28].

In this way, the biomaterial choice for creating scaffolds, monoliths or powders, should considerate the structural characteristics desirable for the formation of optimized tissue [4,5].

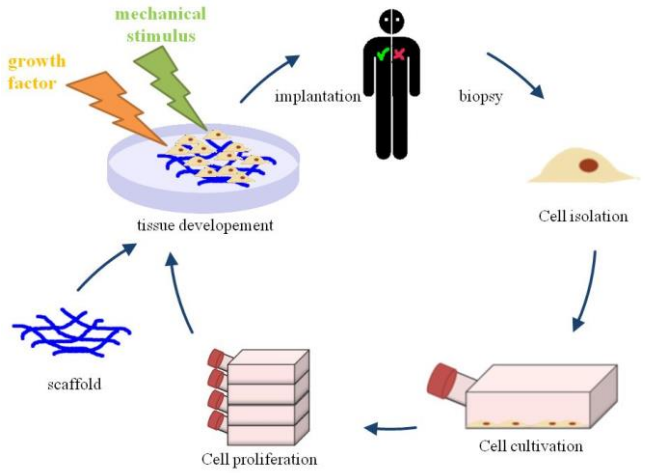

Figure 2 - Tissue engineering in vitro: a combination of cells, biomaterial scaffolds, biofactors and mechanical stimulus, for the development of a functional biomaterial that can later be placed in the patient. Adapted by [28].

2.3. Biomaterials

In 1991 at the 2nd Chester Conference, biomaterial was defined as " all material intended to contact biological systems to evaluate, treat, strengthen or replace any tissue, organ or function of the organism" [25,29]. As said before, in TE the biomaterial should meet certain criteria, and maintain its properties and structural characteristics during its implantation and throughout its period of useful use, without causing damages to the physiological environment surrounding [29,30]. In this way, an ideal bone substitute material, specially the scaffolds, should be [26,31]:

- *Biocompatible,* which means to be well integrated in the host's tissue without eliciting any toxic and inflammatory response, i.e., it must be accepted biologically by the organism [4,27];
- *Biodegradable,* that is, it should degrade through interactions with the body, so that the cells can produce their own extracellular matrix. The by-products should be non-toxic and easily resorbed or excreted by the body. It is important that the degradation occurs at a controlled rate that matches the production of new tissue [4,23,27];
- *Bioactive,* eliciting specific biological responses at the interface of the material, which results in the formation of a chemical bond between the tissues and the material [3,4,32];
- *Osteoconductive and Osteoinductive,* to promote adhesion and proliferation of the osteogenic cells in order to produce the bone matrix [5], and to induce them to the bone healing site and stimulate the osteogenic differentiation pathway [5,23];
- *Porous,* with an interconnected porosity involving micro and macropores to ensure cellular penetration, their uniform distribution, and tissue vascularization which is important in the

diffusion of nutrients among the cells. Pore size is important and is directly related to the vascularization. So, a material must consist of macropores (diameter > 50 nm) to allow the entrance, migration and growth of the cells, the exit of products from degradation and the circulation of vessels to deliver nutrients to the cells. This results in a rapid vascularization and, consequently, in a swift osteogenesis (formation of bone tissue). On the other hand, smaller pores (micropores with a diameter of 0.2 – 2 nm) are crucial to allow local adhesion [4,23], but this porosity compromises mechanical properties such as compressive strength.

The selection of the most appropriate material in bone tissue engineering applications is a very important step towards the construction of a tissue engineered product. Up until now several materials, mostly ceramics/glass, polymers of natural or synthetic origins, or composites of ceramic-polymer, have been proposed [4]. Within the ceramics, silicate-based bioactive glasses (BGs) have gained much attention in the biomedical field, owed to their ability to enhance osteogenesis and angiogenesis. This is mainly due to the ionic dissolution products released from the material [13,31,33].

2.3.1. Bioactive glass (BG)

The first bioactive glass (BG), commercially named Bioglass®45S5, was invented by Professor Larry Hench, in the late 1960s, and it was produced by conventional method of melting [3,4,33]. This was a silicate glass based on a quaternary SiO_2-CaO-Na_2O-P_2O_5 oxide system [3,4], and it was the first case in which an inorganic material was able to achieve a spontaneous chemical bond with the bone tissue and create a stable and tightly bonded interface [4]. Their bone bonding ability has been attributed to the formation of a hydroxycarbonate apatite (HCA) layer on the surface of the glass, when in contact with body fluid [3,4]. The HCA layer formed is similar to the bone mineral phase, allowing the development of a strong bond between the bioactive glasses and the bone tissue [3,34]. This ability to form HA-like layer or calcium-phosphate layer, when immersed in simulated body fluid (SBF) *in vitro,* is often taken as the indication of its bioactivity, and this bioactivity *in vitro* is an indication of the bioactive potential of a material *in vivo* [4]. However, recent studies have proven that despite the material not forming HA-like layer in a SBF, it demonstrates extensive bonding to the bone. The opposite may also happen [4].

Mechanism of HCA layer formation

The bone bonding occurs through the formation of HCA layer between the materials and the bone tissue. This layer is developed as a result of a sequence of chemical reactions on the surface of the bioactive glass implant, that release soluble ionic species. These reactions can be divided in five surface reactions, as described by Hench based on Bioglass 45S5 [4,35–37]:

Stage 1: occurs a controlled diffusion, where an ion exchange reaction happens between the glass network modifiers (Na^+ and Ca^{2+}) and H^+ ions (or H_3O^+) from the solution, which leads to hydrolysis of the silica groups and the creation of silanol (Si-OH) groups on the glass surface;

Stage 2: the increase in pH leads to the dissolution of silica, in the form of silicic acid, $Si(OH)_4$, into the solution, and the continued formation of Si-OH groups on the glass surface;

Stage 3: condensation and polymerization of an amorphous SiO_2-rich layer on the material's surface depleted of alkali and alkaline-earth cations;

Stage 4: Ca^{2+} and $(PO_4)^{3-}$ ions migrate through the silica layer and from the solution to the surface, forming an amorphous calcium-phosphate layer on top of the SiO_2-rich layer;

Stage 5: with the continuous biomaterial dissolution, $CaO\text{-}P_2O_5$ layer incorporates OH^- and $(CO_3)^{2-}$ anions from the solution and crystallizes into a HCA layer.

Depending on the glass composition and the number of Si-O-Si bonds available, the five stages can occur from a few hours to several days.

***

Besides contributing to the bioactivity, ionic dissolution products from the bioactive glass are also responsible for the osteoconductive and osteoinductive behaviours of the 45S5 glass, as well as their ability to promote angiogenesis [4,13,38,39]. The material degrades and, consequently, releases calcium (Ca^{2+}), phosphate $(PO_4)^{3-}$ and silicon ions that activate and up-regulate gene expression in osteogenic cells. This leads to the proliferation and differentiation of osteoblasts, giving rise to rapid bone regeneration [4]. Regarding the angiogenic properties, the ions released from the BG stimulate the secretion of angiogenic growth factors in fibroblast, such as VEGF and bFGF [4,31,38–40]. Studies showed that surfaces coated with Bioglass produced a significant increase in the secretion of VEGF and bFGF [4,39]. As mentioned before, in TE it is important for a biomaterial to be able to promote angiogenesis, a necessary process for rapid revascularization in order to ensure the survival of tissues [13,39]. Therefore, BGs have an angiogenic potential and can be an alternative to the application of growth factors, that have been associated with some problems such as the cost, duration and efficiency of their release in the surrounding tissue [4].

In this way, BG exhibit attractive properties compared to other traditional bio-inert and non-degradable bioceramics, for tissue engineering applications. In the market, there were presented some commercial materials based on the Bioglass ®, like PerioGlass®, Biogran®, BonAlive® and NovaMin ®, all of which are available in particles instead of monolithic materials [3,41]. In the form of particles, granules or putties can be more easily pressed into a defect [3,33]. Usually, surgeons mix these particles with blood from the defect site, and then put them in the defect. The blood will help bone repairment, since it gives natural growth factors and cells to the mixture. Current applications are in orthopaedics, dentistry (tooth enamel remineralization, prevention of dentinal hypersensitivity) and craniomaxillofacial surgery [33].

In addition to silicate glass, other bioactive glasses with different compositions have been developed to improve physical characteristics and therapeutic effects, like bioactivity, rate of HA formation and angiogenic potential [13,33,37,42]. Since 45S5 (silicate) bioactive glass has a slow rate of HA conversion or undergoes incomplete conversion, after an *in vivo* implantation, one trend is the incorporation of different elements into the composition of the glass. In this way, the material's composition can be changed by incorporating other ions to form the glass system, which consequently results in the change of the dissolution behaviour of the material and in their reactivity (biological performance) when immersed in biological fluids [33]. Besides Ca, Si and P, there are many trace elements in the human body (such as Mg, Zn, B) that are known to participate in bone metabolism [34]. In this way, there have been new approaches, namely through the introduction of these active ions into the glass network in order to use their therapeutic effects and to improve the biological performance of the materials [34].

For example, this is the case of borate and borosilicate glasses, based on B_2O_3 ions as the main network formers, in which the incorporation of boron (B) ions in the BG demonstrated higher properties than silicate glasses [4,42]. In this way, the ions present in the glass network, and that will be released from it, play important roles in the formation, growth and repairment of the bone [37].

2.3.1.1. Importance of ionic dissolution products from BG

As seen in bioactive glasses, when it is in contact with simulated body fluids, the material degrades and releases inorganic ions, that are responsible for the enhancement of the bioactivity of the material and are determinant for the expression of genes involved in osteogenesis and angiogenesis [2,4,33–35,39]. The incorporation of certain elements as therapeutic agents, in bioactive glass, is getting significant attention in TE and increasing evidence in the literature indicates that ionic dissolution products from inorganic materials are the key to understand the behaviour of these materials *in vivo* and in *vitro* [34]. The degradation rates of the bioactive glasses will depend on their

composition, which ions are present, whether they are in the form of network formers or modifiers, and its amount.

Calcium ions

Calcium (Ca) is known to be involved in the bone metabolism, angiogenesis and growth and mineralization of bone tissue [34,39]. Inclusively, as said before, Ca and P are the main constituents of biological apatite - the inorganic phase of human bone. In this way, it is obvious that their presence in the bioactive glass is essential for bone formation.

In the silica network, Ca^{2+} ions behave as network modifiers, which disrupt the glass network by breaking the Si-O-Si bond and generating a non-bridging oxygen species (NBO).

Silicon ions

Silicon can be found in bone and connective tissues in the body, and it is known to be essential for the mineralization of the bone and gene activation [2,43,44]. In the early stages of the biomineralization process, silicon is present in active calcification stages, and during the later stages, silicon in aqueous orthosilicic acid, $Si(OH)_4$ form, induces HA precipitation [34,43,44].

In vivo experiments with rats showed a relationship between Ca and Si in bone formation: with low calcium intake, dietary Si increased the rate of mineralization [34,43,45]. Also, i*n vivo* outcomes have shown that substituting silicon for HA granules results in a higher bone ingrowth than pure HA granules [2]. In addition, Si has revealed stimulatory effects on cellular activities: osteoblastic proliferation and differentiation; formation of collagen I (protein in bone matrix) in human osteoblast cells; and osteogenic differentiation of mesenchymal stem cells [34,44]. Aside from the potential osteogenic benefits, silicon may have angiogenic capabilities as well [39,44]. Zhai *et al.* [46] reported that, in addition to bioactive glasses, a Si-containing bioceramic enhanced angiogenesis of human aortic endothelial cells.

Boron ions

Boron is one of the trace elements in the human body that is known to be involved in the bone metabolism (bone growth and maintenance), wound healing *in vivo*, stimulation of growth factors and cytokines, and to play a physiological role in angiogenesis [33,47,48].

In studies using rats, boron deprivation has decreased bone volume fraction, trabecular thickness and led to changes in rat behaviour and brain mineral composition [47,49]. In the human body, boron can be essentially found in bones, nails and hair, and its total content ranges from 3 to 20 mg [47,49,50]. Its presence is fundamental for the bone metabolism process and to prevent bone loss, osteoporosis, which generally occurs in post-menopausal women and in old men [47]. Researches have

observed that there is a difference in the concentration of boron in arthritic bones (3 ppm) and in healthy bones (56 ppm) [4,47,50].

In this way, it is of special interest to incorporate boron ions in bioactive glass, for their release in the human body for bone health and bone regeneration [47]. Borosilicate glass is an example of these bioactive materials, in which B_2O_3 replaced part of SiO_2, in silicate 45S5, being the main glass-forming component [47]. The electronic structure of boron and silicon is different, boron is trivalent, and silicon is quadrivalent, so the physio-chemistry and biological property of the materials will be different as well. The conversion mechanism of borosilicate glasses to HA is similar to the one described for 45S5 Bioglass ®, and this conversion was found to be influenced initially by the dissolution of the glass and later by the diffusion of ions to the reaction surface [47,51]. However, according to some authors, replacing the SiO_2 in the silicate based 45S5 bioactive glass with varying amounts of B_2O_3 produced glasses with controllable conversion rates of HA when immersed in physiological fluid [52,53]. Thus, the conversion rate and bioactive character of BGs depend on the B_2O_3:SiO_2 molar ratio and for higher B_2O_3 content in the silicate glass, the quicker is the conversion obtained [51–53]. This could be explained by its low chemical durability, which makes the material degrade rapidly and convert to HA more completely and at a more controllable rate than bioactive silicate glasses [50,54–56]. The bioactivity will be higher, as well as the bone formation, and the rate of bone tissue formation will be close to the degradation rate of the material. With all of this, borosilicate glass is useful in the field of bone TE.

Several studies, including Balasubramanian *et al.* [50], Saranti *et al*. [57] and Ryu *et al.* [58], have confirmed that boron in the glass network has a catalytic effect at favouring bioactivity, is noncytotoxic for the cells, in certain amounts, and may even improve mechanical properties [59]. Ohtsuki *et al.* [60] reported that CaO-SiO_2-B_2O_3 glass was bioactive as well as biodegradable, and the addition of a small amount of B_2O_3 (substitution of Si_2O for 30 mol% B_2O_3) into the CaO-Si_2O system increased the rate of dissolution of glass ceramics and the formation of Si-OH groups on the surface, providing nucleation sites for the HCA. Through *in vitro* tests, the materials were proven to be non-cytotoxic for cells. Accordingly, Brown *et al.*[61] and Hakki *et al.* [49] demonstrated that a higher B_2O_3 content (over 1 mg/L in the latter case) in the glass results in an inhibition of cell proliferation under static culture conditions and, consequently, in no biocompatibility for the osteoblast cells. Nevertheless, for lower boron amounts the inhibition of cell proliferation was alleviated.

Besides enhancing new bone formation, boron has been considered a promising therapeutic alternative in the enhancement of vascularization [4,33]. Bioactive glasses containing boron have demonstrated *in vivo* and *in vitro* capacity of stimulating the secretion of pro-angiogenic growth factors, including VEGF and β-TGF, and proliferation of endothelial cells, due to its ionic dissolution products [33]. The combination of Si and B ions might have a synergistic effect, and the rapid

degradation of these glasses leads to the release of pro-angiogenic ions, such as boron itself, improving angiogenesis [33]. Thus, Durand *et al.* [13,62] produced a bioactive glass 45S5 enriched with 2% B_2O_3, and confirmed that the boron ions released from the material stimulates human umbilical vein endothelial cell (HUVEC) proliferation and migration, and stimulates *in vitro* secretion of pro-angiogenic cytokines, such as IL-6 and b-FGF.

Cytotoxicity (Cytocompatibility)

The mineralization of bone is created by the osteoblasts when the cells are exposed to critical concentrations of the soluble ionic constituents released from bioactive glasses. The release of the inorganic ions into the surrounding fluid needs to be at a controlled rate, in order to avoid cytotoxicity [36]. When dissolution rates are too fast, the ionic concentrations are too high to be effective; and when the rates are too slow, the concentrations are too low to stimulate cellular proliferation and differentiation. A controlled release rate is the key.

Maeno *et al.* [63] found that low (2-4 mM) Ca concentrations are suitable for proliferation and survival of osteoblasts; medium (6-8 mM) Ca concentrations favour osteoblast differentiation and extracellular matrix mineralization; whereas higher concentrations (>10 mM) are cytotoxic. This cytotoxicity is due to an increase in Ca^{2+} accumulation. The authors even consider that the better value of Ca^{2+} concentrations is around 5 mM, which is useful for both HA deposition and osteoblast behaviour [63]. However, other studies believe that to encourage new bone formation, the target concentration of calcium in the local body fluid is 88-100 ppm and for Si is 17-20 ppm [36,64]. The natural levels of Si in the human body are low – 0.6 ppm for serum and 41 ppm for muscle - and therefore, the excretion of the Si is important [3].

The toxicity of boron is another concern that must be taken into account. Its release into the solution can be as borate ions, $(BO_3)^{3-}$. In the conventional "static" *in vitro* culture conditions, some of the glasses revealed to be toxic to the cells, but in "dynamic" conditions this toxicity was diminished [4,33,55]. A supposed explanation for this is the existence of a constant flow of oxygen and cells, which allow the renewal of the medium. Also, some studies have alleviated concerns about the toxicity of B *in vivo* cells [13,50]. Lin *et al.* [65], implanting high amounts (up to 1120 mg/animal) of 13.93B3 borate glass microfibers containing 53 wt% of B_2O_3 in rats, showed that no toxicity was evident in the kidney tissue. In addition, Balasubramanian *et al.* [50] conclude that borosilicate scaffolds containing 12.5 wt% B_2O_3 exhibited a moderate release of ions which support suitable cell proliferation and attachment (cytocompatibility), as well as good mechanical properties and rapid HA deposition. On the other hand, the authors also concluded that for higher B_2O_3 content, the glass stability and chemical durability decreased, resulting in faster dissolution, causing a rapid release of boron ions into the solution. The solution was found to be cytotoxic. Therefore, an optimum content

of B needs to be achieved in order to have a moderate release of ions which support suitable cell proliferation and attachment. In other study from Balasubramanian *et al.* [11], the material was defined as having cytotoxic behaviour *in vitro* for a boron release higher than 50 ppm, and a controlled release of boron in the range of 0-10 ppm.

***

Going back to the subject of biomaterials, in particular bioactive glasses, although they serve as reservoir for sustained delivery of active ions, they are far from ideal since they are still brittle, have higher elastic moduli than human bones. Therefore, they are not suitable for all grafting applications, such as sites that are under cyclic loads [35,66].

Composite materials of bioactive glass with a polymer would be a solution for inducing toughness. However the two phases degrade at different rates and, when in contact with body fluids, the polymer phase mask the bioactive phase, making it difficult to release ions and be in contact with the host bones [35,64].

Hence, a promising approach is the synthesis of inorganic-organic hybrid materials, with a bioactive glass (inorganic phase) chemically combined with a polymer (organic phase) at the molecular level [8,67]. They can be more attractive since they can overcome the weaknesses of bioactive glasses, such as fragility or low mechanical resistance in bending, by using a polymer and, at the same time, deliver the biological benefits of the glasses.

2.3.2. Hybrids

Hybrid materials are generally made of organic and inorganic components combined over length scales ranging from a few Ångstroms (10^{-10} m) to a few tens of nanometres [64,68]. The two phases are chemically bonding, forming an interpenetrating network of inorganic and organic components that interact at the nanoscale, not being able to be distinguished, unlike composites [2,3,69].

The development of hybrid organic-inorganic materials was mainly due to the progress in sol-gel science, in the 1980s, where the mild conditions allowed the combination of inorganic and organic domains [68–71].

2.3.2.1. Background of sol-gel method

Sol-gel process is a chemical synthesis method that involves two distinct phases: solution (sol) and gelation (gel). As the name implies, a sol is a colloidal suspension of solid particles in a liquid, while a gel is a porous, three-dimensional continuous solid network enclosing a liquid phase

[71,72]. The formation of solid materials occurs through gelation of solutions by chemical reactions and at low temperatures, in the presence of water [71,72]. This process is based on inorganic polymerization reactions that makes use of alkoxides precursors, $M(OR)_n$, where M represent a network-forming element such as Si, Ti, B, and OR an alkoxy group OC_nH_{2n+1} [9,71]. The most commonly used precursors are metal alkoxides once they react readily with water and the most used is the silicon alkoxide, in particular tetraethyl orthosilicate (TEOS), $Si(OC_2H_5)_4$ [71,72]. The process begins with the hydrolysis of alkoxide precursors introducing a reactive hydroxy group (-OH) to the metal, forming silanol (Si-OH) groups. Then, it occurs condensation of the hydroxy groups forming Si-O-Si units (siloxane bonds) with the loss of water or alcohol molecules. This type of condensation can continue to build a larger silicon-containing molecule through the process of polymerization [71].

Once the hydrolysis reaction has been initiated, generally both the hydrolysis and condensation occur simultaneously, by nucleophilic substitution (S_N) mechanisms [9,71,72]. The sol can be transformed into a gel through continuous polycondensation and solvent evaporation, i.e., gelation starts to occur. A drying step proceeds to remove the liquid by-products that remain in the pores and, consequently, shrinkage of the gel network occurs. If the evaporation happens under normal conditions, the amorphous solid structure formed is called xerogel [71]. A subsequent thermal treatment (sintering) may be performed to remove nitrates or silanols; to enhance mechanical properties by removing the existing pores; and to incorporate ions, such as calcium and boron, into the glass network toward the formation of a single-phase [3,70,72,73]. Thus, sintering causes further densification of the glass and reduces the mesoporosity, transforming the xerogel to a solid crystalline material [73]. However, one problem in the sol-gel route, compared to the melt process, is the difficulty to obtain crack-free monoliths, during drying: evaporation of the pore liquid gives rise to capillary stress within the pore network, causing shrinkage of the gels and cracking, which may lead to poor mechanical properties [3,71].

From a physical perspective, the sol-gel method permits the production of materials with various sizes, shapes, formats, i.e., with different configurations, such as monoliths, films for coatings, foams, powders, fibbers, by altering its process parameters [3,72]. Figure 3 represents a scheme of the sol-gel process and the possible products that can be formed [74].

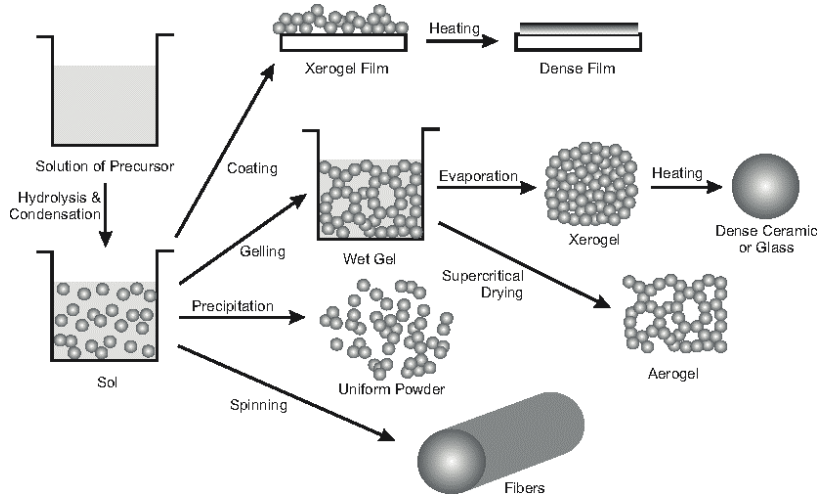

Figure 3 - Scheme of the sol-gel process and the products that can be obtained. Adapted by [74]

The diversity of morphologies that can be obtained, made the sol-gel route useful in several domains of research, including optics, electronics and, specially, biomaterials [72]. In the biomedical applications, this method has already been used in the preparation of inorganic materials, such as silica-based bioactive glasses, exhibiting beneficial properties associated with an ideal material for tissue regeneration. Properties like higher surface area and porous structure, which result in higher degradation rates as well as higher rates of HA formation and better capacity to bond to bone tissue, compared to the ones produced by melt-quenching [3,72]. Sol-gel chemistry not only offers an access to ceramic and glasses with better and new properties, but also to a novel class of materials. The advantageous processing conditions of sol-gel process, particularly the low reaction temperatures, allows the introduction of organic components into the inorganic network, leading to the synthesis of organic-inorganic hybrid materials [72]. These materials present high degree of homogeneity and purity at a molecular level, as well as unique physical and chemical properties [3,9,75].

2.3.2.2. ORMOSILS

The new family of materials made by sol-gel technique was explored by Philip and Schmidt [76], in 1984, who called them organically modified silicates (ORMOSILS). For the past decade, ORMOSILs have become an expanding field of investigation, due to its wide range of possible applications as biomaterials, anti-corrosion coatings and drug-delivery systems [7,68,70,77–80]. From a materials science point of view, the bone is an example of a hybrid structure with an extracellular matrix mainly consisting of an organic (collagen) and an inorganic (hydroxyapatite) phases with molecular interactions between them [3,64]. In this way, ORMOSILS have gained much interest in bone tissue engineering, since they can combine the bioactive properties of inorganic glasses and the

mechanical properties of polymers by chemical bonding, achieving superior properties than a single phase material can provide [70,81]. The introduction of the polymer will lower the elastic modulus value, making it closer to the one of human bones and, hence, the brittleness of the inorganic network is reduced, and the stress shielding is avoided. Furthermore, the interactions at molecular level between the two domains will lead to the material behaving as a single phase, resulting in a controlled congruent degradation and allowing the cells to contact the inorganic and organic phases simultaneously , contrary to composites [3].

Classification of hybrids

The properties of hybrid materials are not only the sum of the individual contributions of both phases but also their interactions [3,77,82]. During the preparation of hybrids by sol-gel method, different interactions can occur between the organic and inorganic phases. Thus, the nature of these interface interactions, as well as the chemical nature and content of both phases, influence the structure, the degree of organization and the relative properties of hybrid inorganic-organic materials [68,72,83]. Generally, the tendency is to increase interfacial interactions by creating an intimate mixing between organic and inorganic network, to minimize phase separation [67,68,83,84]. Subsequently, hybrids materials can be classified in two classes based on the type of interaction that exist at the hybrid interface [67,68,75,77,82]:

Class I: organic and inorganic compounds are linked by weak bonds, such as Van der Waals forces, hydrogen bond, π- π interaction or electrostatic forces. In this class, the polymer is mechanically entrapped into a silica glass network during condensation. One consequence of these weak interactions is the occurrence of phase separation in the material, and its rapid dissolution when in contact with water, since water molecules separate the chains [3,64,67,68,82].

Class II: hybrid structures in which the two phases, or at least parts of them, are bonded to each other by strong chemical bonds, such as covalent or ionic-covalent bonds. These covalent bonds contribute to the production of a material with better mechanical properties and controlled congruent degradation, because the fine scale interaction leads to the hybrids acting as a single phase at the molecular level, being more stable and homogeneous. Cross-linking is considered the key feature of this class [3,64,70,82,83]. Figure 4 schematize a silica-polymer Class II hybrid material [64].

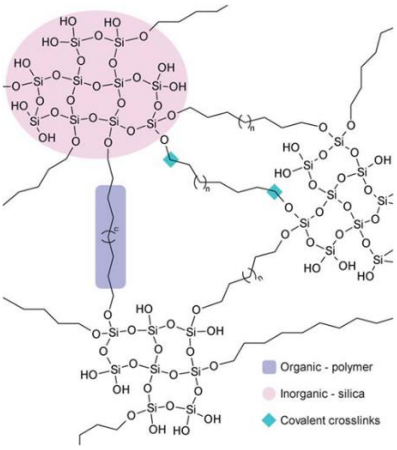

Figure 4 - Schematic of a silica-polymer Class II hybrid material. Adapted by [64]

Several hybrids have been studied based on the combination of bioactive glass with polymers, polymers like poly(ε-caprolactone (PCL) [85,86], poly(vinyl alcohol) (PVA) [87], poly(tetramethylene oxide) (PTMO) [9,10] gelatin [88,89] or polydimethylsiloxane (PDMS) [3,9,14,17,90–92]. A great range of ORMOSILs using PDMS, as the organic compound for the TEOS/PDMS system, have been prepared [6,16,93].

2.3.2.2.1. PDMS-TEOS system

Several studies have been reported in the literature, using tetraethylorthosilicate (TEOS) as the inorganic precursor and PDMS as the organic one for the preparation of ORMOSILs, by sol-gel process [9,94–97]. Figure 5 shows a schematic representation of the ORMOSILs structure using TEOS and PDMS.

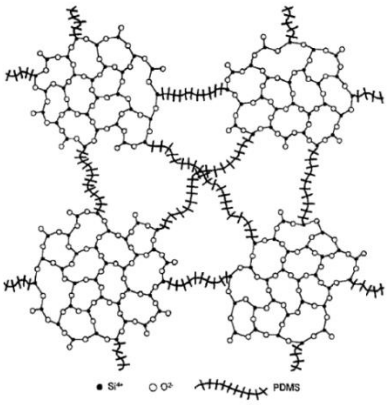

Figure 5 - Schematic representation of the silica network linked with PDMS. Adapted by [6]

The choice of TEOS is governed by its controllable hydrolysis reaction rate, through simple variations in the synthesis conditions, and the ease of incorporation of organic species into the system [72]. TEOS has been the typical silicate precursor used in silicate bioactive sol-gel glass [3].

Currently, the most common way to introduce an organic group into an inorganic silica network is by using an organo-alkoxysilane (organically modified alkoxysilanes) molecular precursor, $(OR)_{4-n}Si\text{-}R'\text{-}Si(OR)_{4-n}$ with n=1,2,3. While OR will be hydrolysed to yield the inorganic framework, the organic group R', which can be an organofunctional group, introduces new properties to the inorganic network, like flexibility and hydrophobicity [68]. Silanol-terminated poly(dimethylsiloxane) (PMDS) is generally chosen as the organic component for the synthesis of hybrids, special for Class II [9,64]. In this class it is normally used a polymer that contains silane bonds, like PDMS [64]. Despite this polymer not being soluble in water, it has a silica backbone with organic side groups, and when it is added to the sol, its terminal methyl groups hydrolyse, forming silanol (Si-OH) groups. These groups can condense with other silanol groups from hydrolysed TEOS, resulting in covalently bonded network [3,64,88,98–101]. The similarity of the hydrolysis products of both PDMS and TEOS makes them highly chemical compatible, allowing the formation of co-condensation bonds by covalent links between the two domains [8,9,102]. Other beneficial features of PMDS, such as its inertness, good thermal stability, high elasticity of the siloxane backbone and non-toxicity, makes it useful to be used in the production of a biomaterial. It can already be found in clinical applications such as contact lenses, medical devices or even in implants.

Previous researches from several authors, such as Wilkes [9,103], Mackenzie [6,14,99,104–106], Babonneau [107–109] and Beaucage [8,92,110,111], were fundamental for understanding the sol-gel process of this binary system and the ways in which it could be modified in order to obtain different structures and microstructure and thus, the desired properties. In this way, various factors, such as reaction parameters, control the morphology and the properties of the final materials. The most important processing variables influencing hydrolysis and condensation reactions, and their respective rates, are [9,112]:

- Type and content of precursor(s);
- Molecular weight of the organic precursor (PDMS);
- pH (catalyst and its content);
- Alkoxide/H_2O ratio;
- Type and content of solvent;
- Order of components addition.

In respect to the precursors used, it has been found that the alkoxide nature influences the development of the siloxane network, since it act as a cross-linking reagent [113]. In the PDMS-SiO_2 hybrid system, TEOS acts as a cross-linking agent, avoiding the growth of PDMS chains [113]. After the hydrolysis of TEOS and PDMS, Si-OH and $Si(CH_3)^2$-OH ending groups co-condensate, leading to the formation of $D_{(Q)}$ structural groups – tetrafunctional Q^n (n=3,4) structural units (SiO_4) cross-linked to difunctional D^n (n=1,2) structural units ($(CH_3)_2.SiO_2$), where *n* is the number of bridging oxygen atoms surrounding Si [114]. This reaction takes place at the same time of TEOS self-condensation. In this way, the organic and inorganic precursors can suffer hydrolysis, co-condensation and self-condensation reactions, and these reactions rates, as well as their extents, depend on the composition of the system and the reactions' conditions [105], and they will determine the structure of the final products [9].

PDMS/TEOS ratio

The PDMS/TEOS ratio is one of the factors that mainly influence the materials properties, like elastic modulus or stiffness, as well as the morphology. The incorporation of PDMS can reduce the stiffness and brittleness of the silica network, conferring toughness and flexibility to the product. Over a critical PDMS concentration (approximate 35 wt%), the ORMOSILs exhibit rubbery behaviour [6]. Besides, the increase in PDMS content leads to an increase in the material porosity [6]. The polymer chains break up the continuity of the SiO_2 network, creating "voids", that when the material is under compressive load, the silica gel species have space to move, being arranged via the flexible PDMS without breakage [6,106]. By adding the polymer, this break in the continuity of the silica network, gives rise to an increase in porosity [6].But the low PDMS content results in a system with higher modulus and with higher tendency to cracking and shrinkage, making it difficult to prepare dense monolithic materials [9].

Furthermore, PDMS leads to a network structure on the micron-scale, contributing to the formation of a material in the bulk (monolith) form [6,92]. The presence of the polymer is critical for the development of monolithic morphologies in PDMS-TEOS hybrid system, partially due to their multiple size-scale morphologies, ranging from Angstroms to micrometers. [92]. This organosiloxane provides a micrometer-scale morphology, that protects the nanometer-scale porous structure from collapse during drying, contributing to the monolith structure [6,92,106]. While TEOS influences the nanometer-scale primary particle growth, PDMS influence the micrometer-scale domain growth [8,92].

PDMS molecular weight

The molecular weight and amount of the polymer is other aspect that needs to be considered. In the literature has been reported that, for the same PDMS amount, low molecular weight (500-1700 g/mol) leads to more PDMS silanol functional groups, i.e., more reacting sites on PDMS [9]. Reacting sites on the polymer are important for the co-condensation between TEOS, which becomes faster with the increase of these sites. Thus, the system will gel at a shorter time and lead to enhanced micrometer-scale growth and limited nanometer-scale growth [92]. Besides, a low molecular weight of PDMS results in a more compacted ORMOSILs due to the shorter chain length in the polymer compared to larger molecular weight PDMS. The solubility is higher, which leads to better dispersion and uniformity of PDMS in the system, and so, higher homogeneity of the final material [9,102]. Another way to reach a better dispersion of PDMS in the network is by using an acid catalyst, which will influence the micrometer-range structure, as will be explained bellow.

H_2O/ TEOS and Catalyst

Water content (H_2O/ TEOS molar ratio *r*) and the type and concentration of catalyst are other sol-gel parameters that will influence the chemistry of TEOS hydrolysis and condensation process, particularly the co-condensation between PDMS and TEOS. As it is known from the sol-gel chemistry of silica, the hydrolysis-condensation reaction rates are generally increased using a catalyst, either an acid or a base, since the silicon alkoxides are not very reactive (low electrophilicity) [9,67]. The addition of an acid or base is around the isoelectric point of the silica acid (pH < 2). Bioactive sol-gel glasses, as well as hybrids in PDMS-TEOS system, have been synthesised under acidic catalysis, since it promotes the hydrolysis rate of TEOS and, consequently, more PDMS is incorporated into the silica network. In this way, a better dispersion of the polymer in the final network can be achieved [9,100] and the material's structure (porosity and pore size) will be influenced by the acid, especially HCl, which is the most used in PDMS-SiO_2 system [100].

Using a high *r*, the silica alkoxide hydrolysis rate is also favoured relatively to condensation, which promotes a higher number of TEOS hydrolysed monomers and the PDMS self-condensation [92,102,107]. Besides, for higher H_2O content it is observed a more porous material, with an increase in the pore volume and in the surface area [107]. Sometimes, the immiscibility of PDMS with water can cause an initial phase separation, which normally can be shown by a cloudy solution [8].

Studies have confirmed that the gelation rate of a PDMS-TEOS hybrid system increased with the amount of H_2O and HCl [92]. In addition to the hydrolysis and the gelation of the silica network, pH also affects the functionalization of the polymer. Under extreme pH values the polymer can degrade, so during sol preparation it may be necessary to raise the pH from less than 2 to close to 7, providing that the polymer maintains the molecular weight and integrity [3].

Thus, several factors control the structure, morphology and, consequently, the properties of hybrid materials [92,102,104,115]. The relation between composition, structure, and property, as well as the process of nanostructure formation of materials has been investigated.

***

In order to improve the properties of the PDMS-SiO_2 hybrid system, specially the biological ones, it may be necessary to introduce a third or a fourth basic compound in the system, like calcium or boron.

The introduction of these ions, in the form of metal oxides (M'_xO_y) within the network, by Si-O-M' bonds, changes the final structure and morphology of the material [114]. Generally, in binary metal oxide systems, it is assumed that a high level of homogeneity can be achieved with the formation of M-O-M', with M and M' being two different metals [19]. However, some metals can cause a heterogeneous structure of the gel, due to the different chemical nature and reaction rate of the molecular precursors, as well as the different structure and size of the ion itself which will give rise to instability. All of these lead to the formation of M-O-M and M'-O-M' bonds or M-O-M' oxo-bridges with low stability, which can cause separation [19,114]. For example, metals like titanium and zirconia, that have a higher reactivity than silicon. According to Julián *et al.* [113,114], the stability of the Si-O-M' linkages in the liquid state influence the degree of dispersion of the cross-linking metal within the siloxane matrix. Thus, these parameters play an essential role in the structural arrangement of the hybrid material [113].

2.3.2.2.2. CaO in PDMS-TEOS system

Earlier works from several authors, such as Tsuru *et al.* [14,100], Mackenzie *et al.*, Qi Chen *et al.*[116] , Salinas *et al.*[101,107,117] and Kamitakahara *et al.* [66,118], have pointed out the hybrid materials based on the PDMS-TEOS system, prepared by sol-gel, as being potentially bioactive especially when calcium is added to the composition, depositing spontaneously apatite on their surfaces in SBF [94,116]. As previously mentioned, for osteoconductive or osteoinductive applications, the presence of Ca^{2+} ions in the biomaterials is a requirement for the enhancement of bioactivity and osteogenesis, as well as silanol groups once they provide sites for calcium phosphate nucleation [100]. In addition, in some works using calcium in the system [66,117,118] monolithic samples were obtained with mechanical properties analogous to those of human cancellous bones and with excellent apatite-forming ability. This was observed when CaO:TEOS molar ratio was 0.1:1 and H_2O:TEOS molar ratio was 4:1. Besides, it was proved that a high PDMS amount do not let Ca^{2+} ions incorporate into the silica

network and, consequently, decreases the bioactivity of the material. Also, from the work of Tsuru *et al.* [100], hybrid materials, which were confirmed by the co-polymerization between TEOS and PMDS, have showed that the bioactivity not only depends on the calcium contents but also on the amount of HCl. As more HCl was mixed, more Ca^{2+} could be incorporated into the structure. Besides, the catalyst modifies the structure of the hybrids by controlling porosity and pore size, i.e., an increase of HCl amount leads to an increase in the specific area and pore size [100].

One of the biggest challenges is the incorporation of calcium into the hybrid network, at low temperatures and without any toxic effect. The most common source of calcium in hybrid system has been calcium nitrate ($Ca(NO_3)_2$) due to its high solubility, but the nitrate by-products are cytotoxic [3,64]. In the sol-gel glass processing, the glass is thermally heated at temperatures above 600ºC to remove the nitrates, and the calcium could enter the silica network at 400ºC, becoming a network modifier. However, this is not possible for hybrid synthesis, because these temperatures are too high for the organic components, provoking its degradation (PDMS decomposition temperature is near 350ºC). So, other calcium sources for organic-inorganic hybrid systems have been tested as alternatives, but some processing related problems still persisted. For example, it is the case of calcium chloride ($CaCl_2$) used for the synthesis of silica-calcium-PVA hybrids, that does not enter the bulk of materials recrystallizing on the surface during ageing and drying process, even though toxic by-products were avoided [3,64,119]. In this thesis, during experimental works, the same happened when it was used calcium chloride (Annex II).

Recently, this problem was solved with the use of calcium acetate monohydrate, $Ca(CH_3CO_2)_2{\cdot}H_2O$, as a precursor. In works from Almeida *et al.*[96,120], calcium acetate was used for the synthesis of PDMS-SiO_2-TiO_2-CaO hybrid systems and it was possible to obtain a homogeneous incorporation of calcium into the silica network as well as a potential bioactive and cytocompatible material. In the present work, calcium acetate will be the calcium precursor used for the preparation of PDMS-TEOS-B_2O_3-CaO system.

2.3.2.2.3. B_2O_3 in PDMS-TEOS-CaO system

In the literature, there are already studies about bioactive hybrid materials based on the PDMS-SiO_2-CaO [95,118] and PDMS-SiO_2-B_2O_3 [17–19,108,121] systems, but no hybrid system with both calcium and boron oxide (PDMS-SiO_2-B_2O_3-CaO) have been developed yet.

Boron's structure

The structure of borosilicate glasses has been often described in terms of their chemical short-range order (CSRO) between framework cations. The CSRO has strong implications for the kinetic stability of glasses in contact with aqueous solutions [122]. The importance of the extent of

disorder between the framework cations and other aspects of structural disorder has stimulated a significant number of experimental and theoretical studies. Boron-11 nuclear magnetic resonance (NMR) spectroscopy has been used for the study of the atomic configurations of alkali borate and borosilicate glasses, since ^{11}B is 80% naturally abundant and exhibits high sensitivity in NMR experiments [123]. This technique allows the collection of information about short-range structure as well as connections among various network structural units [122,124].

Boron in glasses can be either three or four-fold coordinated ($^{[3]}B$ and $^{[4]}B$, respectively), and, generally, amorphous borates consist of a network of interconnected $^{[3]}B$ and $^{[4]}B$ with oxygen units, whose charge is balanced by network modifying cations [123,125,126]. The trigonal boron species can be either in the form of a boroxol rings, which consist in a ring of three BO_3 entities linked, or nonrings, while the tetrahedral boron species ($^{[4]}B$) can have two, three and four Si neighbours (iB,(4-i)Si) for i=0,1,2 [127]. The fraction of these species can be determined by boron-11 NMR as well as the first and second neighbour population around the boron units and the effects of modifier type and content on the materials' structure [127,128]. Besides FT-IR, NMR spectroscopy is another technique frequently used to detect borosiloxane bonds and, usually both methods are used together to complement themselves. These two techniques have played a prominent role in the study of the structure of borate and borosilicate glasses, as well as ORMOSILs containing boron [18,19,123–125,129–131].

Like in FT-IR, NMR has specific signals that correspond to fingertips of the atoms' neighbours. The borosiloxane bonds generally appears in ^{11}B resonance as a signal around δ=12.8 ppm, corresponding to BO_3 non-ring sites [19]. While the BO_3 ring (boroxol) is characterized by a signal near 18 ppm.

***

In the glasses, binary SiO_2-B_2O_3 gels have been studied as precursors for borosilicate glasses, mainly based on TEOS and triethyborate (TEB) or trimethylborate (TMB). However, the integration of boron atoms into the silica network at molecular levels, forming borosiloxane (B-O-Si) bonds, is not easy at room temperature [130,132]. The problem was that a large amount of boron (about 25%) was lost during the gel synthesis, in the form of acid boric, $B(OH)_3$, and not during the densification step of the xerogel. Likewise, Irwin and co-workers [132] reported a NMR study of the structural evolution of samples obtained from TEOS or tetramethyl orthosilicate (TMOS), $Si(OCH_3)_4$, and TMB, and they demonstrated that only a small amount of B-O-Si groups existed in the final gels dried at room temperatures. In addition, they reported that the majority of boron atoms precipitated in the form of $B(OH)_3$. This could be explained by the reactivity of the B-O-Si bonds toward hydrolysis, because trigonal boron is very electrophilic, being preferentially hydrolysed in the presence of water, forming

boric acid, and it is also very susceptible to nucleophilic attack. Even if B-O-Si bridges form in the early stages of the sol-gel process, they are easily broken at the end, owing to the increasing amount of water produced via condensation reactions [132–134]. The easy hydrolysis of borosiloxane bonds by water may be one of the reasons why boron is leached from the gel systems [134]. In addition, the porous nature of the material, i.e, a high surface area facilitate the easy exit of boric acid [134].

The effect of the PDMS

Nevertheless, studies from Sorarù *et al.* [19,130] have showed that the synthesis of SiO_2-B_2O_3 is favoured by using a organo-modified silicon alkoxide, that allows a homogeneous incorporation of boron atoms in the hybrid siloxane network. The formation of these borosiloxane bonds can be described by the following possible reactions:

$$= B - OH + \equiv Si - OR' \rightarrow = B - OR' + \equiv Si - OH \quad (1)$$

$$= B - OH + \equiv Si - OH \rightarrow = B - O - Si + H_2O \quad (2)$$

$$= B - OH + \equiv Si - OR' \rightarrow = B - O - Si \equiv \ + R'OH \quad (3)$$

where R' represents an alkyl group. An explanation for the retention of B-O-Si bonds in the hybrid borosilicate gels was explained by the authors [19,130], as being due to:

(i) The low hydrolysis ratio in the sol-gel synthesis (H_2O/Si=1.5);
(ii) The presence of organic groups closes to the B-O-Si bridges, which act as in situ protection of the borosiloxane bonds from water attack: Si-R groups gives a hydrophobic character to the hybrid siloxane network, favouring the removal of water and, consequently, preventing the hydrolytic cleavage of the B-O-Si groups;
(iii) The higher electron density of the silicon atoms in the organically substituted gels, which strengthens the Si-O bonds.

Hence, it is possible that the organic substituent, as well as some synthesis parameters can have a possible influence, such as the pH of the hydrolysis water and the boron load, plays an important role in the formation of homogeneous borosilicate gels containing B-O-Si bonds, [19].

Some authors even named ormoborosil (organically modified borosilicate) materials to the products in which boron was incorporated into the silica hybrid network, as the forming cation [18,129,131]. In works from Penã-Alonso *et al.* [129,131], ormoborosils materials were successfully

synthesized from TEOS, triethylborate (TEB, the boron precursor) and PDMS (1750 $g.mol^{-1}$), through sol-gel method [18,129]. The FT-IR results showed the presence of hybrid bonds between TEOS and PDMS (Si-O-Si), which were characterized by the appearance of a band at 850 cm^{-1}. In IR spectra, it was also observed the formation of borosiloxane (B-O-Si) bonds in the dried gels, located at 881 cm^{-1} for D units (PDMS) and at about 940 cm^{-1} for Q units (TEOS) [18]. These results were in accordance with the ones from Sorarù *et al.* [19,130], who synthesized hybrid SiO_2-B_2O_3 gels by reacting modified silicon alkoxides (R-Si$(OE)_3$, R=Me, Et, Vi) with TEB and boric acid. Their results showed the presence of B-O-Si bonds in the gels due to the absorption peak in the FT-IR spectra at 880-890 cm^{-1} and from a resonance peak at -12.8 ppm in the ^{11}B MAS NMR spectra. The author also verified that the increase in B content as well as in the pH of the hydrolysis water (from 1 to 2.5) intensify the absorption peak around 880 cm^{-1}. This means that more trigonal boron units (BO_3) are incorporated into the siloxane network via B-O-Si bridges [130]. Additionally, the chemical analysis indirectly suggested the incorporation of boron into the siloxane network instead of the evaporation of boric acid [19].

The effect of the network modifier

As it is known from borate and borosilicate glasses, the content of alkaline atoms has a direct impact on the boron coordination number, acting as network modifiers when they are located close to a BO_3 unit or a SiO_4 unit [123,125,127]. At low concentrations of the modifier cation, trigonal boron species (BO_3) are converted to four-coordinated tetrahedral species (BO_4). As the concentration of the oxide modifier in the composition increases, the bridging oxygens (BO), on the trigonal planar boron, are converted into nonbridging oxygens (NBOs) [123,125]. NBOs are defined as oxygens bonded to one framework cation (network-forming), and bridging oxygens (BO) as oxygens linking two network cations [135]. Besides, above a certain amount of boron in the system (30%), the boron will preferably coordinate in the trigonal form and, therefore lower fractions of $^{[4]}B$ units and higher of non-bridging oxygens (NBOs) are generated. This is known as "boron anomaly" [136].

Hence, modifier cations are large and are of low valence, forming weaker bonds with oxygens. Moreover, there is a tendency for the higher strength field modifier cation to promote the formation of bridging BO_4 units, therefore changing the boron coordination [137]. Brinker observed that in the presence of a sufficiently strong nucleophile, boron adopts a tetrahedral coordination with sp^3 hybridization via nucleophilic addition reaction (A_N) [71]. Calcium ions act as a network modifier in the silica network, disrupting the glass network by breaking the Si-O-Si bond, and promoting the change in boron coordination [126]. Although water can cause hydrolysis of B-O-Si, it is not sufficiently nucleophilic, like Ca^{2+}, to change the boron coordination [71].

Influence of boron in the microstructure

Boron is trivalent, and silicon is quadrivalent, in this way, it is expected that the incorporation of boron, to substitute the silicon, will have an influence in the physio-chemistry and biological properties of the material. In a study from Chengtie Wu *et al.* [48], it was observed that the incorporation of boron (5% and 10% mol) into a mesoporous bioactive glass (MBG) scaffold, by sol-gel method, slightly decreased the specific surface area and nano-pore volume. The replacement of SiO_4^{4-} with BO_3^{3-} may disrupt the ordered orientation of SiO_4^{4-} during the self-assembly reaction, which may be due to the valence difference between SiO_4^{4-} and BO_3^{3-}. This difference cause defects in atomic arrangement, manifesting itself by altering the mesopore structure (surface area and pore volume). On the other hand, the addition of boron did not influence the release of SiO_4^{4-} ions, which indicates that it does not change the dissolution of MBG scaffolds, as silicon is the main component (>70%) in MGB. Furthermore, boron was released in a controllable way, and at concentrations lower than 8 ppm, which may have contributed to the improvement of the proliferation and bone-related gene expression (Col I and Runx2) of the osteoblast.

***

In the present work it is described the synthesis, by sol-gel procedure, and characterization of a mesoporous hybrid monolithic material based on the PDMS-SiO_2-B_2O_3-CaO system, for biological applications. According to the literature, this is a novelty. Thus, the main challenges in this work are the incorporation of boron and calcium in the silica network, at low temperatures (≤ 150ºC), without occurring phase separation. Hence, the objectives of this work are:

- ✓ To obtain a homogeneous incorporation of calcium and boron ions in the hybrid system, by firstly defining the experimental protocol (the preparation conditions);
- ✓ To study the effect of calcium and boron ions in the materials' structure, microstructure and macrostructure, by changing its concentration in the system;
- ✓ To obtain a material with the ability to release calcium and boron ions when in contact with SBF and in cellular medium;
- ✓ To obtain a bioactive and biocompatible material;
- ✓ To study the effects of boron on the cell viability, proliferation and morphology;

Chapter 3

Experimental Procedure

In this chapter it is detailed the material and experimental procedure used to prepare the samples in the PDMS-SiO_2-B_2O_3-CaO system, by the sol-gel process. Also, the techniques used to characterize the obtained materials, in terms of their structure and microstructure, as well as their *in vitro* bioactivity, are presented and summarized in this chapter.

3.1. Materials

In the preparation of the hybrid monolithic materials, there were used different reagents that are described in Table 1 in terms of chemical formula, purity and brand.

Table 1 - Reagents, chemical formula, purity and brand.

Reagents	Chemical Formula	Purity (%)	Brand
Tetraethyl orthosilicate (TEOS)	$C_8H_{20}O_4Si$	> 99.0 %	Sigma-Aldrich
Isopropyl alcohol (IPA or iPr-OH)	C_3H_7OH	> 99.5 %	Sigma-Aldrich
Hydrochloric acid (HCl)	HCl	-	Panreac
Acetone (Acet)	C_3H_6O	> 99.5 %	Sigma-Aldrich
Polydimethylsiloxane silanol terminated (550 g/mol average molecular weight) (PDMS)	$(C_2H_6OSi)_n$	-	Sigma-Aldrich
Trimethyl borate (TMB)	$B(OCH_3)_3$	> 99.0 %	Fluka
Calcium acetate monohydrate (CaAc)	$Ca(CH_3CO_2)_2 \cdot H_2O$	> 99.0 %	Sigma-Aldrich

3.2. Sample preparation

To fulfil the previously described objectives of this work, five different compositions based on PDMS-SiO_2-B_2O_3-CaO system were prepared, always using the same reagents but varying the molar ratio of boron and calcium precursors. In this way, the parameter that was changed and evaluated in this system was calcium and boron contents. Table 2 shows the composition of the materials, in molar ratio, and the samples' notation. Samples were named "B*x*C*y*" being *x*= $B(OCH_3)_3$/TEOS and *y*= $Ca(CH_3CO_2)_2.H_2O$/TEOS, in units of 1/100 mol. The inorganic part of these

hybrid materials was supplied by the tetraethyl orthosilicate (TEOS), calcium acetate (CaAc) and the trimethyl borate (TMB), while the organic part by polydimethylsiloxane silanol terminated (550 g/mol). The materials were prepared with the following fixed molar ratio compositions: H_2O:TEOS=2:1, IPA:TEOS=3.75:1, PDMS:TEOS=0.18:1, HCl:TEOS=0.25:1 and Acetone:TEOS=3.75:1.

Table 2 - Composition (in molar ratio) of five samples.

Notation	**Composition (in molar ratio)**	
	***x* (TMB/TEOS)**	***y* (CaAc/TEOS)**
B5C5	0.05	0.05
B10C0	0.10	0
B10C10	0.10	0.10
B15C10	0.15	0.10
B20C10	0.20	0.10

Preliminary works were performed before the achievement of the final protocol procedure (Annex II). In the first attempts, it was used a different calcium precursor, calcium chloride; however, a non-homogeneous morphology was observed in the samples. After the drying, the gel exhibited precipitates in the surface, which could correspond to calcium precipitates. But when the calcium precursor was changed, from calcium chloride to acetate one, the solution demonstrated no signs of immiscibility or precipitates in the final gel. Therefore, after several efforts, a procedure was reached without an immiscible solution and the presence of precipitates in the final sol-gel material.

The experimental protocol used and defined to produce the hybrid materials is shown in Figure 6. As can be seen in the figure, two solutions were prepared separately:

- Solution A: 10.4 mL of PDMS, 22.3 mL of TEOS and *x* of TMB were added on 80% acetone, always under continuous magnetic stirring, and at room temperature;
- Solution B: 28.1 mL of isopropanol (IPA) was used to dissolve *y* of calcium acetate (CaAc). The medium was acidified with 0.25 mol of hydrochloric acid (HCL), the catalyst of the hydrolysis/condensation process. Then, it was added 20% of the acetone amount and 2 mol of distilled water;

After the preparation of each solution, they were mixed together and then stirred for 3 hours at room temperature. During this time, it occurred hydrolysis and condensation reactions. In the composition without calcium (B10C0) the procedure was the same, with the only difference being the absence of the calcium acetate step.

After stirring, the final suspension (sol) was putted into petri dishes and kept at room temperature during 24 hours, for aging, remaining liquid and transparent. Afterwards, the suspension was placed in an oven at 60ºC during 3 days to transform in gel, followed by drying at 150ºC for 1 hour, to ensure a complete loss of solvents. All compositions resulted in white opaque monolithic samples, with some cracks. Figure 7 shows the monolithic samples obtained after the drying step. Furthermore the samples were stored in a desiccator until use, since the samples demonstrated to be very hygroscopic, particularly the ones containing calcium in the composition.

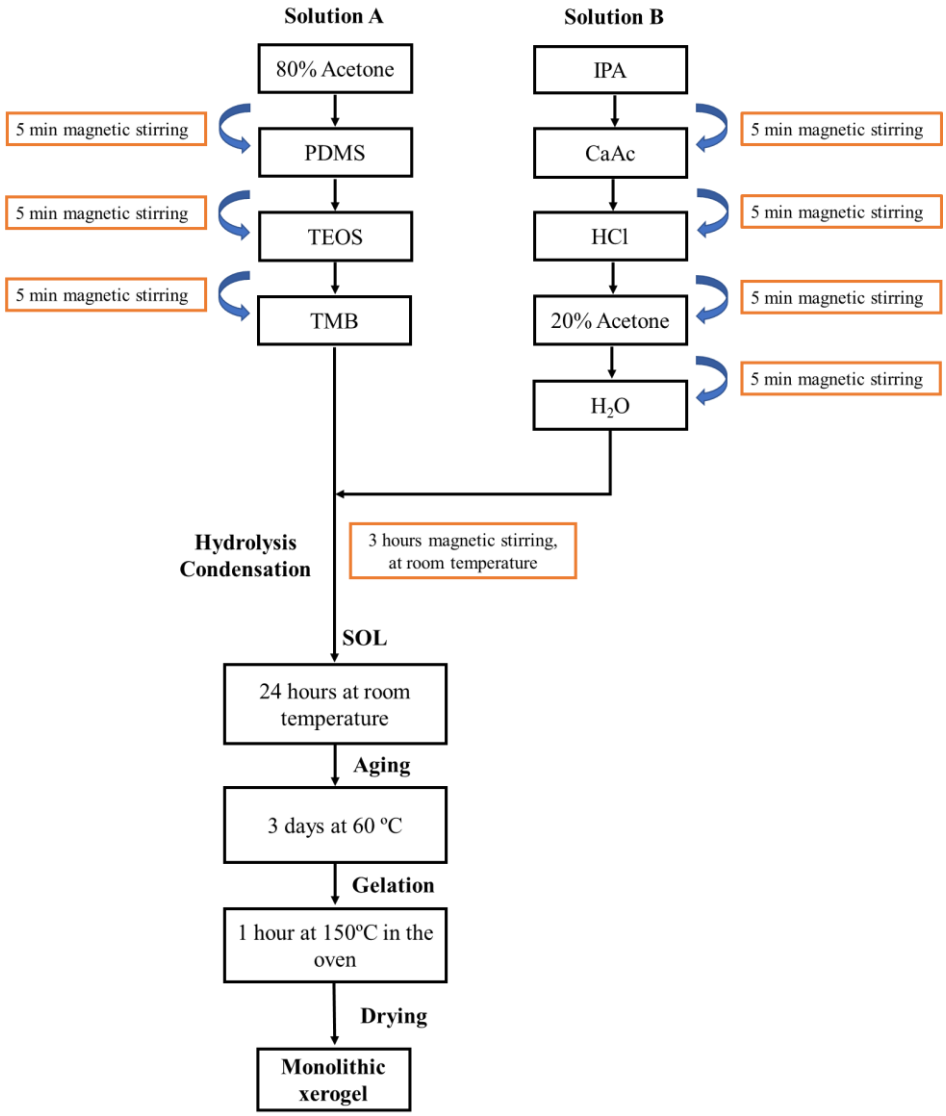

Figure 6 - Experimental procedure used to prepare the hybrid materials with different compositions.

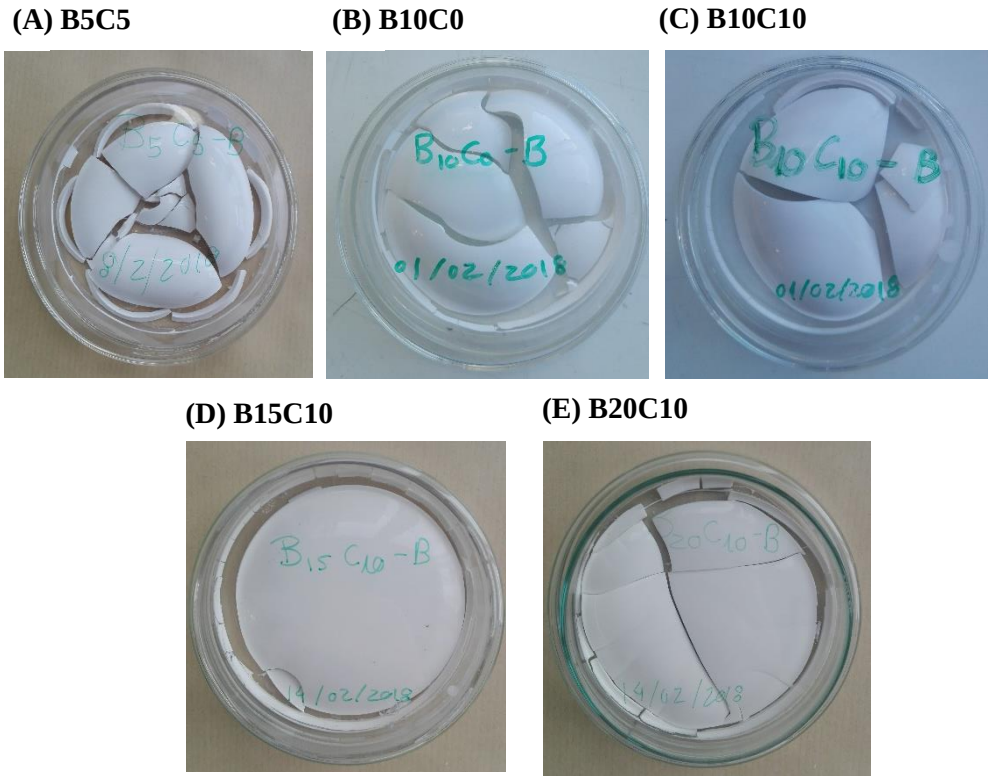

Figure 7 - Monolithic samples obtained after dried at 150ºC, in petri dishes: (A) B5C5, (B) B10C0, (C) B10C10, (D) B15C10 and (E) B20C10.

3.3. Characterization techniques

The obtained monolith samples were characterized with some experimental techniques described in this chapter, in order to analyse their structure and morphology. But to perform the characterization analyses, the monolithic samples were first grounded in a mortar in order to create thin powders.

3.3.1. Fourier transform infrared spectroscopy (FT-IR)

The chemical bonds and molecular structure in the material can be determined by FT-IR, based on the spectrum absorption bands. This characterization method allows the determination of the functional groups present in the sample, since the intensity and position of each peak corresponds to the vibrational mode of a specific chemical bond. This is a fast and non-destructive technique that permits to perceive the local symmetry of the material under analysis.

In this study, some infrared spectra were recorded on a *Bruker model Tensor 27* in the region of 350-4000 cm^{-1} with a 4 cm^{-1} resolution and 128 scans; and others in the range of 750-1300 cm^{-1} with a 2 cm^{-1} resolution using 250 scans.

Prior to analysis, each powder sample was mixed and grinded with a small amount of potassium bromide (KBr) and pressed to produce disks. The sample spectra were obtained by using the pure KBr spectrum and they were reported in transmittance mode. These analyses were carried out in the laboratory of the Department of Chemistry of the University of Aveiro.

3.3.2. Nuclear magnetic resonance spectroscopy (NMR)

Nuclear magnetic resonance (NMR) is a spectroscopic technique used to observe local magnetic fields around atomic nuclei. The intramolecular field around an atom, in a molecule, changes the resonance frequency, and the chemical shift provides detailed information about the structure of a molecule and its individual functional groups. In the NMR spectra different functional groups can be distinguishable, as well as identical functional groups with different neighbouring substituents.

For this study, the samples B10C0, B10C10, B15C10 and B20C10 were investigated to determine the boron coordination in the samples. Samples were characterized by solid-state ^{11}B HAHN-ECHO NMR, using a Bruker Avance III HD 700MHz (16.4 T), with a pulse length of 6.25 μ. The data from the literature [19,124,130] was used to assign the peaks associated with boron trigonal ($^{[3]}B$) in rings and nonrings, and boron tetrahedral ($^{[4]}B$). Spectra were simulated using DMFIT software and data from the literature, and the relative percentage of each structure was calculated [138].

3.3.3. X-ray diffraction (XRD)

The X-ray diffraction (XRD) is a non-destructive technique used to identify and quantify crystalline phases in the material. Thus, it gives information about the crystalline or amorphous nature of the material.

In this work, XRD was used to verify the amorphous character of the hybrid materials, and after bioactivity tests, to verify the presence of crystalline phases of calcium phosphate. For the analysis it was used *Pan Analytical -X'pert-PRO* diffractometer equipped with a copper anode (Cu), which operates with a current of 40 mA and a voltage of 45 kV, emitting a radiation Kα1 of λ=1.540598 Å and Kα2 of λ=1.544426 Å. The spectra were recorded through a continuous scan from the smallest possible angle, which was 2θ=2°, up to 2θ=40°, with a step size of 0.0263° and at room temperature. The identification of the crystallographic phases was made using the Powder Diffraction

File (PDF) data provided by JCPDS/ICDD (Joint Committee on Powder Diffraction Standards/International Centre for Diffraction Data ICDD).

3.3.4. Sieving technique

To perform the cellular tests, there were needed samples with a specific particle size, from 0.180 to 0.355 mm size. Therefore, the monolithic compositions were grinded to fine powders of 0.180-0.355 mm size, using a mortar and pestle of agate. The sieves used were from *Filtra Vibration* with a diameter of 200 mm. The specific surface area of each sample, in this interval of size, was determined by BET to calculate the available area.

3.3.5. Specific surface area by Brunauer-Emmet-Teller (BET) method

The specific surface areas (SSA) of the hybrid materials produced were determined by the method of physical adsorption of nitrogen gas, developed by Brunauer, Emmet and Teller (BET). The surface area of a given material is defined as the surface area of a solid particle per unit mass, usually expressed in m^2/g. This method consists in passing a mixture of gases composed of nitrogen and helium on the sample, which makes the particles adsorb a molecular layer of nitrogen. The amount adsorbed, as a function of the relative pressure of gas (p/p0), is defined by isothermal adsorption curve, where p0 is the saturation vapor pressure of the adsorbed substance at the temperature in which the assay is performed. To perform this assay a *Micromeritics – Germini 2370V5* equipment was used in order to determine the specific surface areas. Before the determination of the volume of adsorbed gas, the samples were degassed at 150 ºC for 12 hours and cooled to room temperature. At least 30 points were acquired with an equilibrium time set of 5 seconds.

According to the International Union of Pure and Applied Chemistry (IUPAC), the type of porosity in the material can be defined based on the isotherms, which comprise six different types, each one corresponding to a specific adsorption mechanism [139]. Figure 8 shows the six types of isotherms and Table 3 their description [139].

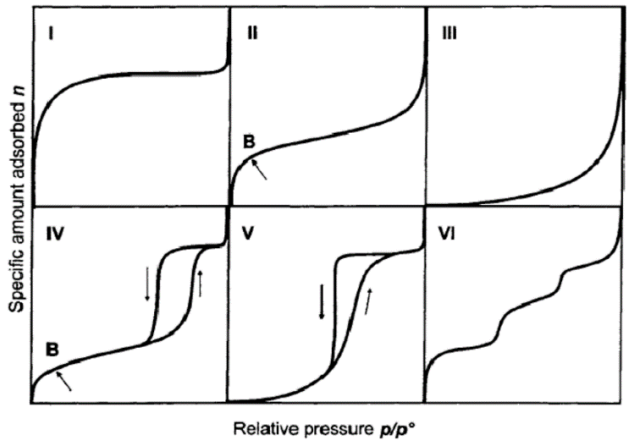

Figure 8 - Six types of gas adsorption isotherms, according to the IUPAC classification.

Table 3 - Types of gas isotherms and their description.

Type	Description
I	Microporous materials. Relatively small external surfaces.
II	Non-porous or macroporous materials. Point B is the stage at which the monolayer is complete and the multilayer adsorption is about to begin.
III	Nonporous materials. Weak adsorbent-adsorbate interaction and in multilayers. Uncommon.
IV	Mesoporous materials, high porosity and occurrence of capillary condensation. There is a hysteresis loop. The initial part corresponds to the monolayer-multilayer adsorption.
V	Micro and mesoporous materials. Low gas-solid interaction. Uncommon.
VI	Non-porous surface. Adsorption mechanism in multilayers.

In type IV and V isotherms, a phenomenon called hysteresis can occur, in which the adsorption curve does not coincide with the desorption curve [139]. There are four types of hysteresis, illustrated in Figure 9, and each type represents a pore shape. In the graphics, *a* represents the amount adsorbed and *P/P0* the relative pressure.

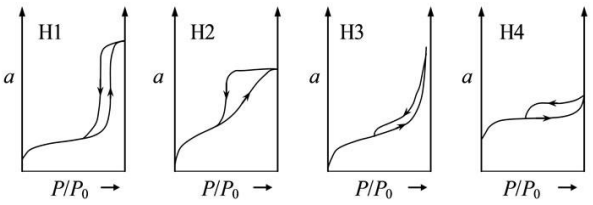

Figure 9 - Four different types of possible hysteresis.

H1 type hysteresis is characteristic of porous materials with rigid agglomerates and spherical shaped particles. The hysteresis type H2 corresponds to materials with bottle-shaped pores, while H3 type hysteresis presents particles with plaque morphology, giving rise to slit-shaped pores. H5 type hysteresis is associated with narrow and slit-shaped pores [139].

3.3.6. Scanning electron microscopy (SEM) and energy dispersive x-ray spectroscopy (EDS)

The scanning electron microscopy (SEM) is one of the most used surface analysis techniques, which can obtain high resolution images of a sample surface at a nanometer scale. In this way, this technique was used to perform the microstructural characterization of all samples.

The SEM equipment used is a *Hitachi model SU-70* microscope, which operates with an acceleration voltage of 25 KeV. This equipment is provided with an energy dispersive X-ray spectroscopy (EDS) system with a tungsten filament, which allows a qualitative analysis of the elemental composition. The powder samples were fixed in an aluminium sample holder, with double-sided carbon tape. To increase the electrical conductivity of the samples, they were coated with a thin carbon film using an *Emitech K950* carbon depositor. The microscope used to perform the analysis was from the Department of Materials and Ceramic Engineering of the University of Aveiro.

3.4. *In vitro* mineralization assays

As referred in the previous chapter, the first indication of a potentially bioactive material is its ability to precipitate apatite (calcium-phosphate) on the surface, which can be evaluated by performing *in vitro* assays on simulated body fluid (SBF). For this purpose, the samples were immersed in Kokubos's simulated body fluid (SBF) for 1, 7 and 14 days. After this test, it was possible to verify the surface modifications in the materials as well as the ionic concentration variation in the solution.

3.4.1. Simulated body fluid (SBF) tests

The SBF test was carried out following the Kokubo protocol [140]. In this way, 1000 ml of SBF solution was prepared, and its composition as well as the order of addition of the reagents and their concentrations, are shown in Table 4. The SBF is an aproteic and acellular solution that intends to simulate human plasm, presenting similar pH and ionic concentrations to the benchmark. Table 5 presents the ion concentrations (mM) and pH of human blood plasma and of SBF solutions based on Kokubo protocol [140,141].

Table 4 - Order, chemical formula and concentration of reagents for preparing 1000 ml of SBF.

Order	Reagent	Chemical formula	Concentration (g/L)
1.	Sodium chloride	NaCl	7.996
2.	Sodium hydrogen carbonate	$NaHCO_3$	0.350
3.	Potassium chloride	KCl	0.224
4.	Di-potassium hydrogen phosphate trihydrate	$K_2HPO_4^{2-}\cdot 3H_2O$	0.228
5.	Magnesium chloride hexahydrate	$MgCl_2\cdot 6H_2O$	0.305
6.	Hydrochloric	HCl (1M)	40 ml
7.	Calcium chloride dihydrate	$CaCl_2\cdot 2H_2O$	0.548
8.	Sodium Sulphate	Na_2SO_4	0.071
9.	Tris-hydroxymethyl aminomethane	$(HOCH_2)_3CNH_2$	6.057

Table 5 - Nominal ion concentration (Mm) and pH value of SBF in comparison with those in human blood plasma.

	Na^+	K^+	Mg^{2+}	Ca^{2+}	Cl^-	HCO_3^-	HPO_4^{2-}	SO_4^{2-}	pH
Plasma	142.0	5.0	1.5	2.5	103.0	27.0	1.0	0.5	7.2-7.4
SBF	142.0	5.0	1.5	2.5	147.8	4.2	1.0	0.5	7.40

Firstly, 700 ml of ultrapure water was placed in a goblet at 37ºC under continuous stirring and, slowly, the numerically identified reagents were added one by one, in the order presented in Table 4. The SBF solution was placed in a previously cleaned 1000 ml volumetric flask and the remaining HCl, diluted to pH values of 7.4, was added to be equal to the physiological pH. Finally, the prepared SBF solution was preserved in a sterile container and saved in the refrigerator (3ºC).

Bioactivity tests were performed by immersing the samples, in powder form, in SBF, using a ratio of 75 mg ratio, of each material, to 50 ml of SBF solution. The mixture was stored in polypropylene containers, previously sterilized, and placed in an oven for different periods of time: 1, 7 and 14 days. The oven temperature was 37ºC to simulate body temperature. At the end of each soaking time, the supernatant liquid was removed by filtration, using a sterile syringe and a 0.22-micron filter, to remove any traces of solid material. The SBF solution was stored at ~ 3ºC, in polypropylene containers, for further analysis. The solid materials deposited at the end of the containers were withdrawn and transferred to tubes with the aid of ultrapure water, then centrifuged

for 5 minutes at 3000 rpm, with water and with acetone. Finally, the material was dried for a few hours in an oven at 60ºC to remove traces of acetone.

3.4.2. Apatite layer characterization

After SBF, to verify the deposition of an apatite layer on the materials' surface and the possible formation of crystalline phases of apatite, microstructural and structural analyses were performed by SEM/EDS and XRD, respectively. The chemical structure of the hybrid materials after SBF immersion was also analysed by FT-IR spectroscopy, to confirm the presence of functional groups characteristic of calcium-phosphate links. The equipment used was the same as mentioned above.

3.4.3. Inductively coupled plasma optical emission spectroscopy (ICP-OES)

Inductively coupled plasma optical emission spectroscopy (ICP-OES) is an analytical technique used for the detection of trace elements in solid or liquid samples. In this study, it was used with the aim of determining the concentrations of calcium, boron, silicon and phosphorus ions present in the supernatant liquid, after soaking the hybrid samples, being measured as a function of the immersion time (1, 7 and 14 days).

The spectrometer used was ICP-optical emission *Jobin Yvon Activa M* from the Central Laboratory of Analysis of the University of Aveiro.

Chapter 4

Results and Discussion

In this chapter, the results obtained by different techniques are analysed and discussed. It starts with the hybrid structural characterization, moving forward to its microstructure analysis and finishing with the bioactivity tests on acellular medium.

4.1. Hybrid structure and microstructure analysis

4.1.1. FT-IR analysis

FT-IR studies of the PDMS-SiO_2-B_2O_3-CaO hybrid samples were acquired in the spectral range of 350-4000 cm^{-1}. All samples exhibit infrared bands in the region of 399-3469 cm^{-1}, which were previously reported by other authors as being characteristic of hybrid materials of the PDMS-SiO_2 [93,101], PDMS-SiO_2-CaO [16,96] and PDMS-SiO_2-B_2O_3 [18,19,129,130] systems. The assignment of absorption bands to each sample, is shown in Table 6. The bands were identified according to the literature data. The data are divided in three figures, representing each one a different interval.

Figure 10 shows the IR spectra of all the compositions in the spectral range of 350-4000 cm^{-1}. As can be seen in the figure, the absorption bands characteristic of the adsorbed water are presented, in the 3000-3500 cm^{-1} region, and correspond to the bending (δ) vibrational modes of O-H bonds [95,96,142,143]. The band at *ca.* 1635 cm^{-1} is assigned to the stretching (ν) vibrational modes of O-H bonds from the water as well as from KBr [95,96,142,143]. The presence of water bands can be due to the existence of residual Si-OH groups (silanols), which are potential sites for water absorption. Consequently, the samples demonstrate high hydrophilicity [143]. Observing the spectra, the presence of calcium in the samples made the peaks related to water become sharper than without the presence of calcium (B10C0). This can be due to the hygroscopic effect that calcium provides to the material.

In Figure 10 there are also presented the absorption bands related to the organic PDMS molecules. These bands are detected at *ca.* 1265, 1416 and 2968 cm^{-1}, and they are assigned to symmetric and asymmetric bending of CH_3 in $Si(CH_3)_2$ structure, and to asymmetrical C-H stretching vibrations from CH_2 groups, respectively [93–95,97,129,131].

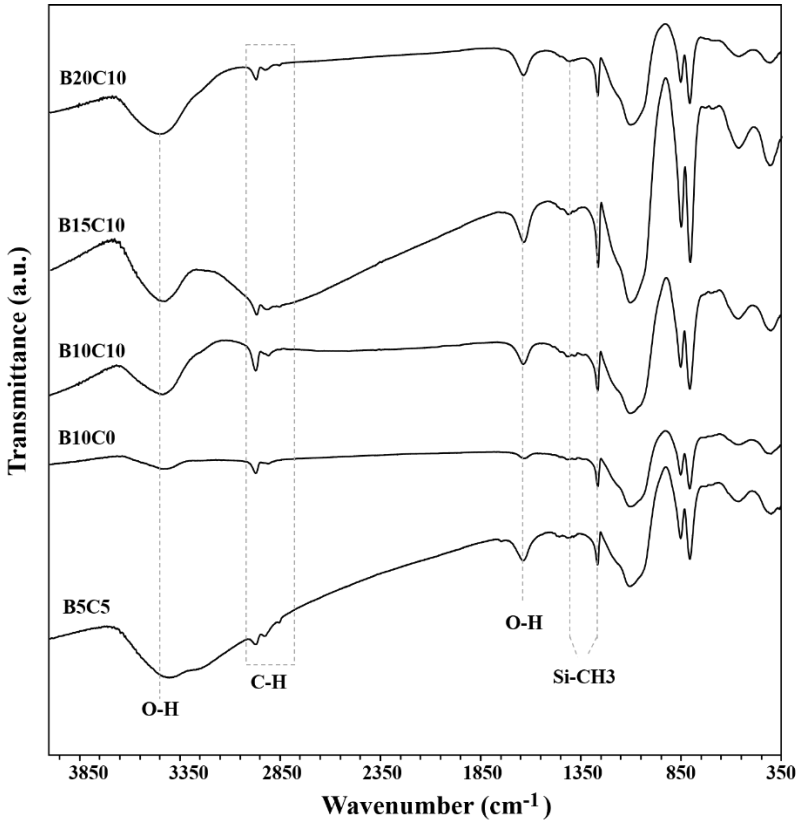

Figure 10 - FT-IR spectra for the five compositions in the interval of 350-4000 cm^{-1}.

Figure 11 shows the spectra of the five compositions in two different intervals: in 350-1550 cm^{-1} (Fig.11-A) and in 750-1300 cm^{-1} (Fig.11-B) spectral region, and the respective bonds assignment. In this figure it is possible to have a better view of the peaks, particularly from hybrid D-Q and borosiloxane bonds, and of the differences between the samples.

In Fig.11-A, the bands at *ca.* 564, 805 and 1103 cm^{-1} are respective due to the vibration of Si-O-Si bonds in 4-fold rings, in tetrahedron rings with symmetric stretching (ν_s) modes and to Si-O-Si symmetric stretching in linear structures [10,16,121,144,145]. These bands are already observed in silica-gels and PDMS-SiO_2 based hybrid materials [94,146]. The band located at 805 cm^{-1} is attributable to PDMS in tetrahedral chains, and the increase in the intensity of the band can be due to the increase in cyclic PDMS molecules [129]. On the other hand, the organic precursor (PDMS) can contain cyclic and linear structures in the reaction medium and so the band values are different for each one [17]. Apart from the other peaks that seem very similar, the peak centred at 1103 cm^{-1} shows some slight differences in its shape and intensity [121,145]. With the increase of the boron amount, the peak becomes more defined, being attributed to the linear structure of PDMS. Yet, around this peak, two shoulders are present near 1050 cm^{-1} and 1170 cm^{-1}, which can be assigned to the stretching of Si-O-Si bonds in both PDMS and TEOS molecules [18,95,121,129]. At the same time, these bands can be related to the presence of Si-O-C, C-O-C and Si-C bonds [121,147]. According to some authors, the differences in the

"shape" of this region can indicate that the relative position of the peaks is quite sensitive to the geometry and size of the siloxane condensed species, which depend on the sol-gel experimental parameters [94,96]. By comparing the spectra of the five compositions, it seems that the shape and intensity of the shoulders changes with the concentration of boron in the system. Another absorption band that appears, and is associated with PDMS, is at *ca.* 700 cm^{-1}, being assigned to symmetrical stretching of Si-CH, although this band is not so clearly distinguishable in all spectra. Comparing to the sample's spectra, it is observed that, in that region, its shape is changing from one rising line to one declining, as the boron content increases in the composition.

Tellez *et al.* [148] have associated the bands at approximately *ca.* 400 cm^{-1} and *ca.* 850 cm^{-1} to hybrid cross-linked SiO_2 (Q units) – PDMS (D units) structures. The first band is present in all spectra (Fig. 11-A) and it is related to the interruption of the silica network with the hybrid SiO_4-$(CH_3)_2$·SiO_2 bonds, since its value dropped when compared to values obtained for pure silica gel (usually close to ca. 460 cm^{-1}). In the same way and according to literature, PDMS pure chains exhibit weak bands at *ca.* 860 cm^{-1}, corresponding to symmetrical rocking of CH_3 groups. However, in this study this value shifted to lower values (*ca.* 850 cm^{-1}) due to co-polymerization reactions between PDMS molecules and hydrolysed Si-OH groups of TEOS (Q structural groups) [16,96,129]. These bands were obtained for all spectra. In this way, the formation of hybrid structures is confirmed by the existence of bonding between the organic and the inorganic parts (D-Q bonds) of the material.

The incorporation of boron into the hybrid TEOS-PDMS network leads to the formation of new bonds: B-O-B and Si-O-B links. The hydrolysis of TMB forms B-OH (boranol) groups, which can either self-condensate and form B-O-B bonds, or occur co-polymerization between B-OH groups and Si-OH from TEOS or PDMS molecules [19,131,142]. However, some of these B-OH groups can remain uncondensed, as it happens with Si-OH groups [19]. In the literature, the main adsorption bands typical of boron bonds remain around 720 cm^{-1} and in the 1300-1550 cm^{-1} spectral region, being assigned to B-O-B bending vibration and B-O stretching of BO_3 units, respectively [19,130,143,149]. These bands could be clearly found in spectra of the Fig.12-A, although with some slight shifts. The first value moved to higher values around *ca.* 725 cm^{-1}. In the 1300-1550 cm^{-1} region some peaks appear, at *ca.* 1385 cm^{-1} and *ca.* 1448 cm^{-1}, which are characteristic of B-O stretching vibrations where B is in planar trigonal coordination [134,142]. These bands can be used to confirm the presence of boron in the final gels, and the appearance of B-O-B bonds suggests that there is still boron in the skeleton linked between each other.

Besides forming B-O-B groups, the introduction of boron atoms can also form Si-O-B bonds. The characteristic peaks of borosiloxane (Si-O-B) links are present in these five compositions at *ca.* 673 cm^{-1}, 891 cm^{-1} and 927 cm^{-1} [19,129,150]. The first peak can be detected in the Fig.11-A, while the other two peaks are present in the Fig.11-B, which represent the IR bands in the interval of

750-1300 cm^{-1}. The former band corresponds to the bending of the Si-O-B bonds [19]. Despite no observation of the other two peaks of Si-O-B bonds in the first spectra (Fig.11-A), the peaks clearly appear in the spectra of Fig.11-B, being obtained by altering the conditions in FT-IR spectrometer, by increasing the scanning, from 128 to 250 $scans^{-1}$, and the resolution, from 4 cm^{-1} to 2 cm^{-1}. According to the literature [18,19,131,134], the shoulder around *ca.* 891 cm^{-1} corresponds to the stretching of Si-O-B bonds, in which the silicon atoms correspond to D units; while the peak at *ca.* 927 cm^{-1} is assigned to Si-O-B bonds, but with the silicon atoms being from Q units (TEOS).

Regarding the effect of boron load in the bands associated to the boron, there are no visible changes for the case of Si-O-B linkages at *ca.* 927 cm^{-1}, but at *ca.* 673 and *ca.* 891 cm^{-1} the peak becomes more distinct for higher boron contents, particularly for B10C10, B15C10 and B20C10 (Fig.11-B). A similar behaviour is verified for B-O and B-O-B linkages, except for B20C10 in which these two peaks are disappearing.

In this way, the existence of these borosiloxane bridges in the samples' spectra suggest that trigonal boron atoms are incorporated into the siloxane structure, forming a homogeneous borosilicate network. The link between the boron and the silica precursors was possible even without the heat treatment, just by using low processing temperatures (< 150ºC).

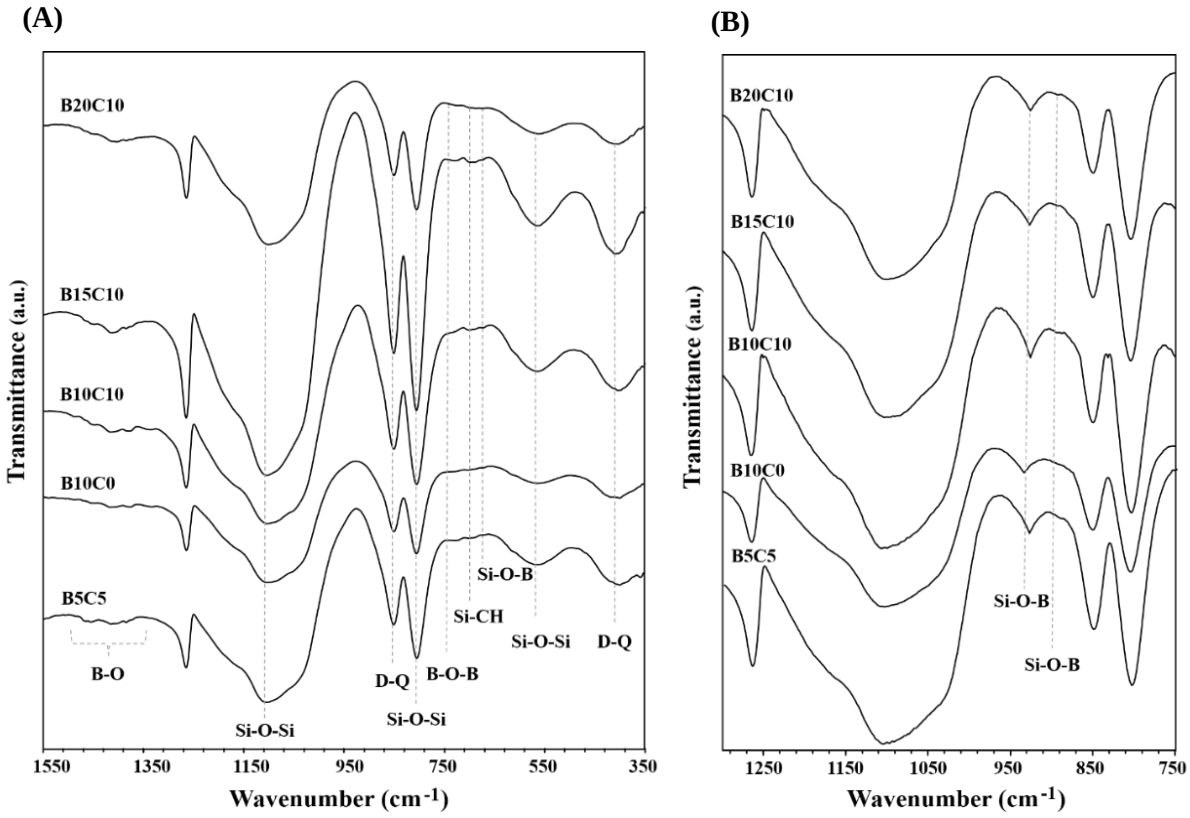

Figure 11 - FT-IR spectra of the five compositions in the interval of (A) 350-1550 cm-1, with a resolution of 4 cm-1 and 128 scans; and (B) 750-1300 cm-1, with resolution of 2cm-1 and 250 scans.

The bands related to the calcium acetate, like C-O vibrational modes, were not detected by FT-IR. The absence of these vibration modes, which are common in acetate-based materials, was due to the reaction between the acetate and the acid used in the synthesis, causing protonation of the carboxylic group of calcium acetate. From here, it is produced acetic acid that reacts with the 2-propanol (IPA) present in the solution originating an ester (2-propyl ethanoate) [94,96]. This ester has a boiling point lower than the temperature that the materials were subject to, and so it is evaporated when the material is dried at 150 ºC [96]. The calcium acetate used demonstrated a hygroscopic behaviour which leads to the physically adsorbed water in the samples with Ca content. This precursor not only adsorbs moisture from the air but also dissolves itself in that moisture, undergoing a change of state. Ultimately, the most important IR bands that characterize the co-polymerization between TEOS (inorganic precursor) and PDMS (organic precursor), and the presence of borosiloxane bridges, are present in all the prepared hybrids.

Table 6 - Band assignments for the five compositions and respective references.

Assignment	Wavenumber (cm^{-1})					
	B5C5	**B10C0**	**B10C10**	**B15C10**	**B20C10**	**References**
ν O-H in H_2O	3409	3417	3434	3429	3458	[95]
ν_a C-H in CH_3	2970	2970	2971	2968	2968	[94,95,130]
ν O-H in H_2O	1639	1635	1637	1637	1635	[95,134]
ν B-O in BO_3	1456	1448	1448	1449	-	[130,134]
δ_a CH_3 in $Si(CH_3)_2$	1416	1417	1416	1415	1414	[94,95]
ν B-O in BO_3	1385	1376	1378	1385	1385	[47,130,131,134]
δ_s CH_3 in $Si(CH_3)_2$	1265	1265	1265	1265	1265	[18,93–95,129]
ν_s Si-O-Si	1105	1103	1103	1104	1101	[121]
ν Si-O-B	930	934	927	928	927	[18,19,129,131]
ν Si-O-B	888	-	891	892	889	[18,19,131]
D-Q units	851	851	851	851	850	[18,95,129,131]
ν_s Si-O-Si	805	806	805	805	805	[18,95,129,151]
δ B-O-B in BO_3	729	725	729	730	722	[143,149]
ν_s Si-C	701	698	701	697	694	[47,147]
δ Si-O-B	669	669	671	673	674	[19,134]
Si-O-Si	562	564	563	564	563	[95,151]
D-Q units	399	399	403	409	402	[95,130]

4.1.2. ^{11}B NMR analysis

In order to complement the IR results, the structure of PDMS-SiO_2-B_2O_3-CaO hybrid materials was also investigated through solid-state NMR analysis, which was performed on the B10C0, B10C10, B15C10 and B20C10 samples. ^{11}B NMR HAHN-ECHO spectra recorded for each sample are presented in Figure 12, and in Table 7 is represented the relative percentages of each boron structure, for each sample. The aim of this analysis is to provide structural information about the boron units and how the concentration of trigonal and tetrahedral boron species was changing between the different samples. The B5C5 sample was not used for this analysis, because the objective was to observe the effect of boron addition in the structure, while maintaining fixed all the other compounds, including calcium; the B10C0 sample was used to compare the presence and absence of CaO in the boron structure. Si-29 NMR was not performed because it is not very informative to investigate the formation of borosiloxane network [19].

As can be observed in Figure 12, hybrids present different structural arrangements of boron which are confirmed by the presence of two peaks corresponding to distinct groups of B structural units. The first one is between 13 to 18 ppm and it is assigned to trigonal BO_3 ($^{[3]}$B) units, in which a broad peak near δ=13 ppm can be attributed to BO_3 nonring sites, while the shoulder with a chemical shift near 18 ppm corresponds to boron in rings of three planar BO_3 groups, known as boron in boroxol rings [123,124,127]. The other boron group was observed near 1.3 ppm, for the compositions with calcium in the system (B10C10, B15C10 and B20C10). This peak is assigned to tetrahedral BO_4 ($^{[4]}$B) units [19,124,130,131].

In this way, the presence of $^{[4]}$B units are related to the addition of calcium into hybrid system, since this signal only appears when calcium is presented (B10C10, B15C10 and B20C10 samples).

Samples (Table 7) presented a higher fraction of $^{[3]}$B units than $^{[4]}$B units, because boron is a network former and its stable form in nature is trigonal. By adding a modifier cation (calcium), a small fraction of boron trigonal tends to change to BO_4 (metastable form). In respect to the effect of the boron load, as boron amounts increase in the composition, maintaining fixed the calcium content, more boron units are available in the system for the calcium to transform the boron trigonal in tetrahedra. For instance, this is the case of samples B15C10 and B20C10, where the former (with less boron amount) presents 15% of $^{[4]}$B, and the latter 20%.

These results are in accordance with the ones from other authors [71,126,137], which assumed that, in borosilicate glasses, the presence of a strong nucleophilic cation, such as lithium or calcium, makes boron change its coordination from $^{[3]}$B to $^{[4]}$B units. Indeed, Silver *et al* [126], who study the NMR spectrum of B^{11} in several glassy materials containing boron oxide, including borosilicate glasses, concluded that the boron atoms may have at least two coordination numbers. Moreover,

authors determined, that the presence of the BO_4 tetrahedra only appears when a modifier is present. Besides, they also showed that the percent of three- and four-coordinated atoms depend on the modifier concentration.

Additionally, the ^{11}B resonance signal at δ=13 ppm and at δ=18 ppm appear as the fingerprints for the formation of borosiloxane bonds [19,124,130,131]. The development of borosiloxane bonds in the hybrids prepared can be identified directly from the FT-IR and ^{11}B NMR results.

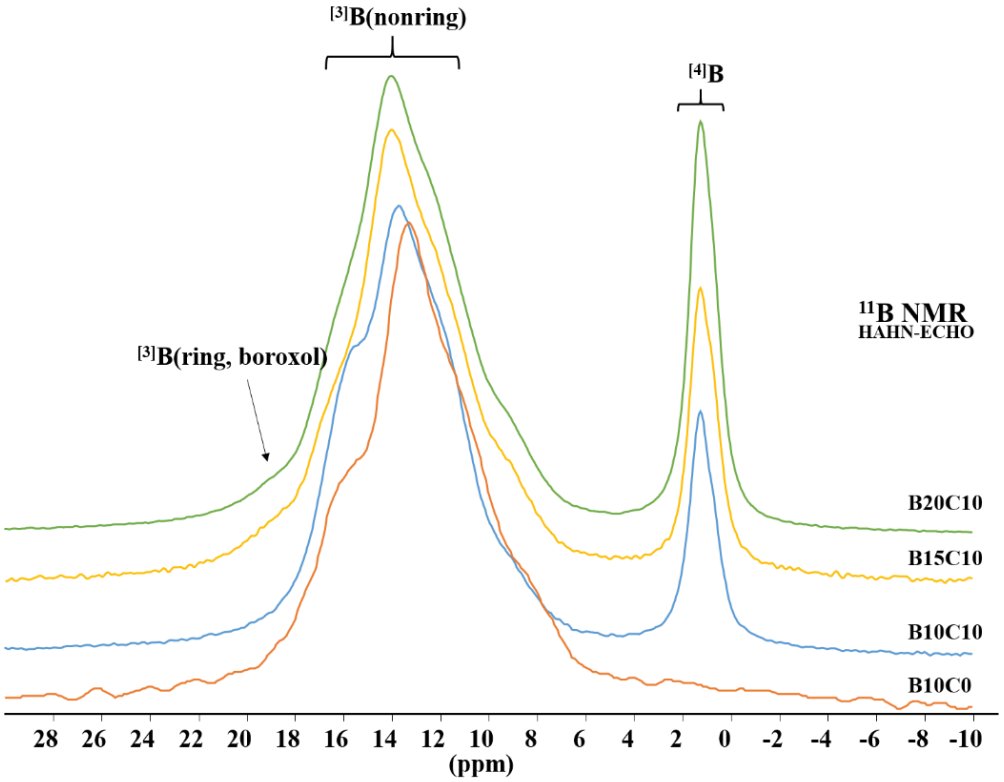

Figure 12 – ^{11}B NMR spectra of the samples B10C0, B10C10, B15C10 and B20C10.

Table 7 - Relative percentages of $^{[3]}B$ and $^{[4]}B$ in each sample.

Sample	% Fraction	
	$^{[3]}B$	$^{[4]}B$
B10C0	100	0
B10C10	88	12
B15C10	85	15
B20C10	80	20

4.1.3. XRD analysis

Figure 13 shows the XRD spectra of each sample. From the figure it can be inferred that all the prepared samples are amorphous and that there is one broad, undefined peak around 2θ ~ 8º which corresponds to a value of the Bragg d-spacing of around ~11 Å. The low angle value corresponds to the characteristic distance between silica domain centres, and to the way in which the boron is arranged with the silica groups. This is related to the coordination level, which influences the peak definition [91]. Observing the spectra, it is possible to verify that this peak, situated at 2θ=8º, only varies in width with the amount of boron added, becoming narrower with the decrease of its content. Therefore, increasing the amount of boron results in less definition of the peak and less coordination. This can be due to the boron entering in the inner network. The compositions with the highest and defined peak are B10C0 and B10C10.

Table 8 shows the angle at the maximum for each composition. The difference in the angle between each composition is minimal, always around 2θ=8°, corresponding to a d=11 (Å). This value of 11 Å is close to the value of 13 Å calculated by Brus and Dybal [152] for a primary silica domain size in a similar hybrid system. Since the present sol-gel procedure is a one-step process, in which network formation and particle generation are simultaneous processes, water will diffuse to friendly sites. Namely, sites with high polarity, such as domains with a high concentration of hydroxyl groups. Therefore, nucleation will occur at the cross-links [110].

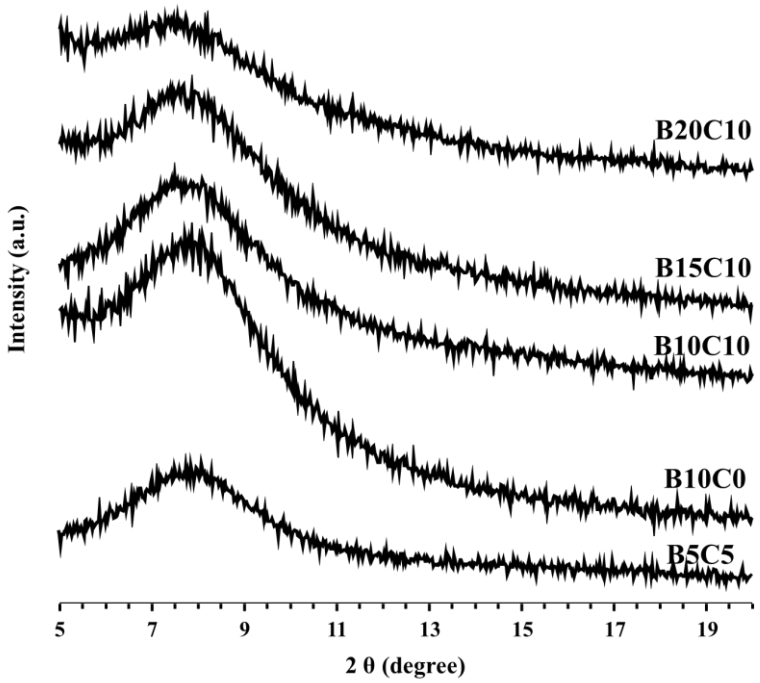

Figure 13 - XRD spectra of the five samples after dried at 150ºC.

Table 8 - Values of the maximum angle of the five samples.

Sample	2θ (°)
B5C5	8.1
B10C0	8.1
B10C10	7.5
B15C10	7.9
B20C10	7.7

4.1.4. BET specific surface area

Specific surface areas (SSA) of porous samples were obtained from the nitrogen adsorption-desorption isotherms using the Braunauer-Emmet-Teller (BET) method (Figure 14). The SSA results are presented in Table 9. Observing the isotherms of Figure 14, it is possible to assume that the composition with the highest quantity of gas adsorbed is B5C5, followed by B10C0 sample. The composition with the lowest quantity of gas adsorbed is B20C10, that is the composition with the highest amount of boron, presenting almost a line graphic compared to the other samples. Wherefore, as the content of boron in the hybrid composition increases, the adsorbed volume of nitrogen gas decreases, consequently lowering the percentage of porosity. This result is the first indication that the incorporation of TMB reduces the pore volume and then, the specific surface area.

According to the types of isotherms, the obtained graphics for all the compositions reveal a type IV isotherm (IUPAC classification), which is usually related to a mesoporous material (2 nm < pore diameter < 50 nm). These isotherms show type H3 hysteresis loop, which extends to low pressures. The morphology of these materials is in a lamellar way and the pores are in the form of slits. According to the literature, this type of low pressure hysteresis, in which the final value of the adsorption curve does not coincide with its initial value, is associated with the expansion of the non-rigid porous structure.

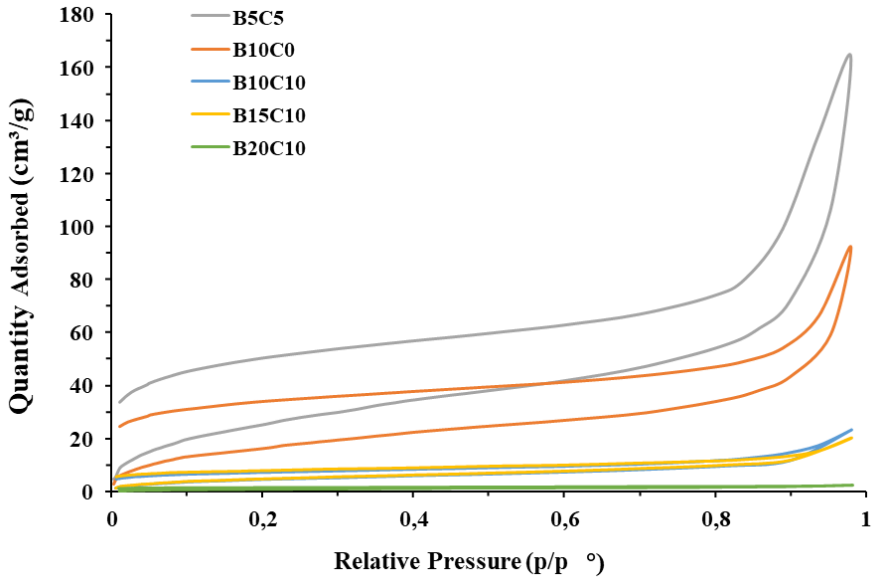

Figure 14 - Isotherms of each composition by BET method.

Table 9 shows the BET specific surface area (m^2/g) of each composition, with a particle size in the range of 180 to 355 µm, and the values agree with the isotherms analysed above. The table shows that increasing the boron concentration leads to a decrease in the value of the specific surface area. By comparing the B10C10 sample with the B20C10, the B10C10 sample has a surface area of almost double than the B20C10, 16.7 and 7 m^2/g, respectively. But the composition with the highest surface area is B5C5, which may be related not only to the amount of boron but also to the amount of calcium in the system. In this way, it is possible to assert that the B5C5 sample presents a highly mesoporous structure and that SSAs values exhibit a decrease with the addition of TMB to the hybrid material. Guo *et al.* [92] and Peña-Alonso *et al.*[131] already showed the presence of multiple size-scale morphologies, form nanometers to micrometers, in hybrid TEOS-PDMS materials [8]. They also proved that as the boron precursor increases, the surface area decreases while pore volume and pore size increase [131]. With the addition of TMB, the mesopore volumes decrease and macropore volumes increase [131].

Table 9 - Values of surface area calculated from the nitrogen adsorption isotherms, for the five samples.

	B5C5	**B10C0**	**B10C10**	**B15C10**	**B20C10**
BET surface area (m^2/g)	95.2	61.8	16.7	17.5	7.0

4.1.5. SEM and EDS analysis

The structure of the hybrids with different compositions were observed by scanning electron microscopy (SEM) and analysed by EDS. Figure 15 shows the hybrid micrographs and the respective EDS for all the samples, using a magnification of 10.0k and 20.0k, with an energy of 20.0 kV and 15 kV, respectively.

As can be seen in Figure 15, the samples with higher boron content, B15C10 (Fig.15-D1, D2) and B20C10 (Fig.15-E1, E2), show a larger porous structure compared to the others. At first sight it seems that the increase in the amount of boron contributes to the formation of more porous structures and, consequently, a less dense material. It can be stated that the porosity present in the material is related to the boron element. Nevertheless, the BET results show a decrease in the values of surface area with the concentration of boron in the system, as well as a decrease in the mesoporosity. As can be seen in the micrographs, the B15C10 and B20C10 samples have more boron in the system and present a larger pore structure and a lower surface area. Since the BET method only measures mesoporous structures and SEM cannot measure the mesoporosity, the porosity that is visible in these samples (B15C10 and B20C10) can be due to macrosized pores on the surface. The other samples exhibit mesosized pores on the surface, or even nanosized. So, the B5C5, B10C0 and B10C10 samples present a mesoporous structure, and the B15C10 and B20C10 samples a macroporous structure. Although the B10C10 and B15C10 samples present a similar surface area value, the SEM micrographs show a different microstructure.

By observing the microstructures, it is clear that the addition of boron to the composition affects the final morphologies of the hybrids, being more evident for higher contents of boron (B20C10). Accordingly, as boron content increases, the structure tends to the formation of a macroporous material. As known in the sol-gel chemistry [133], the atoms situated in the surface of silica secondary particles, rather than in the primary ones, act as “poisoned” sites and slow down the condensation process leading to a highly branched structure. This can give rise to porous microstructures with low values of specific surface area, as observed for the B20C10 sample.

The EDS analysis was performed to confirm the elements present in the samples. It can be observed that the spectra are similar and present peaks from Si, Ca, Cl, O, due to the compounds used to prepare the samples.

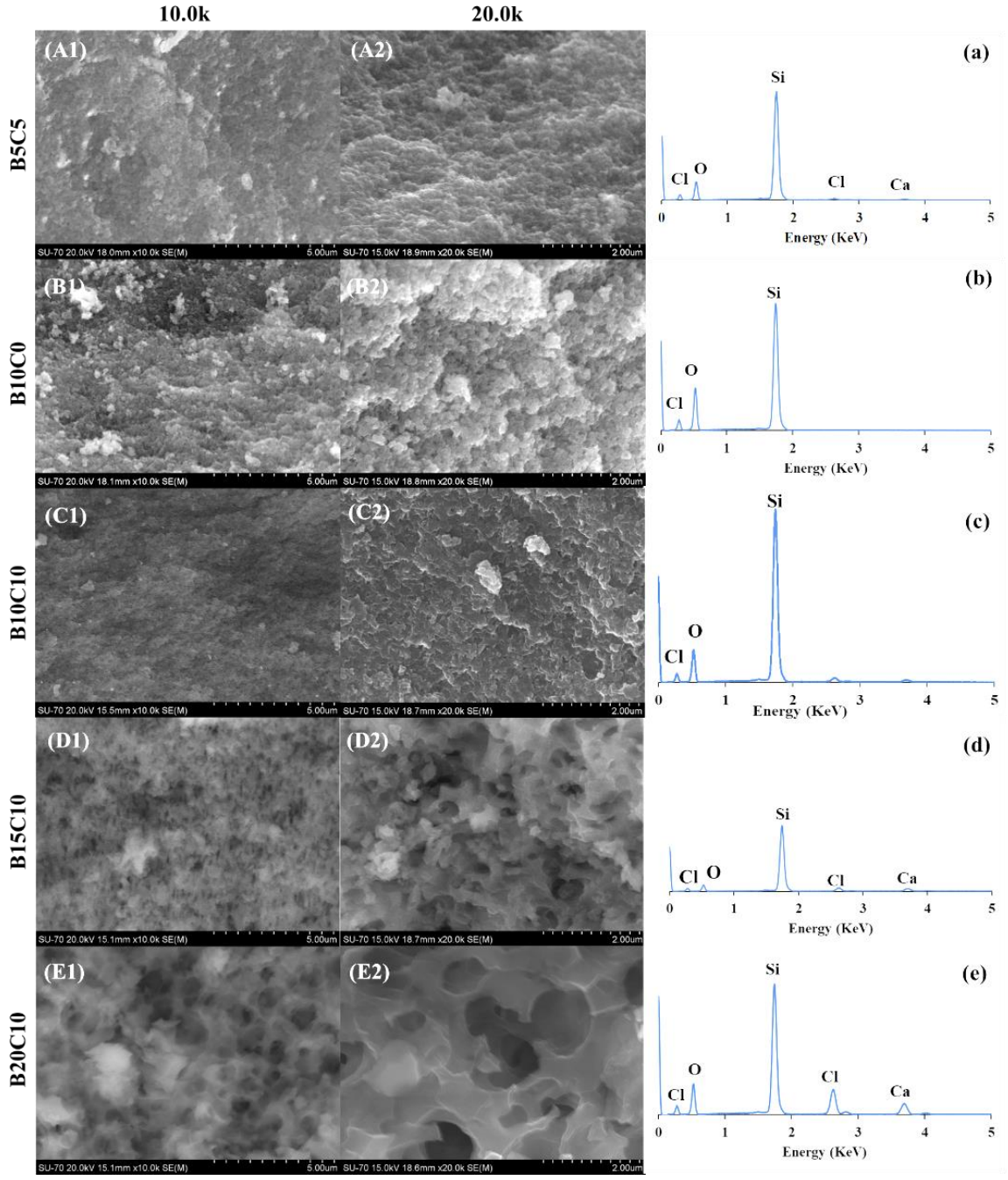

Figure 15 - SEM micrographs, with different magnification of 10.0k and 20.0k, and the respective EDS of the five samples dried at 150ºC: B5C5 (A1,A2, a), B10C0 (B1, B2, b), B10C10 (C1, C2, c), B15C10 (D1, D2, d) and B20C10 (E1, E2, e).

4.2. Bioactivity assays

In vitro acellular bioactivity of biomaterials is usually assessed by monitoring the rate of apatite formation on samples after immersion in SBF. Thus, after soaking the samples in Kokubo's simulated body fluid (SBF) for 1, 7 and 14 days, they were analysed by FT-IR, XRD and SEM with EDS, to verify the presence of crystalline HA or calcium phosphate aggregates on the surface of the samples. The supernatant liquid was analysed by ICP to confirm the degradation of the material and, consequently, its ability to release boron ions.

4.2.1. FT-IR analysis

As FT-IR is a sensitive technique used to detect the local structure of glasses, it becomes a convenient method to analyse the HA formation on samples after SBF immersion. The IR analysis was later carried out to evaluate the possible changes that the material might have suffered and determine the bonds established, indicative of hydroxyapatite. According to the literature, the bonds that can be considered the main characteristic peaks of crystalline HA, or amorphous calcium-phosphate aggregates, are P-O bending bands located around 600 cm^{-1} [153,154]. Figure 16 show the IR spectra of each composition obtained before (0 d) and after immersion in SBF for 1,7 and 14 days, and the respective band assignments. The IR spectra represented are in the interval of 350-2000 cm^{-1}, where the most noticeable changes occur.

Although the underlying mechanism towards HA formation is identical in the glasses, their reaction times differ strongly, depending on the composition used. This happens for the compositions in this study, in which the presence of HA peaks differs each time. But for all the samples, a new peak located near 600 cm^{-1} was detected after immersion, which can confirm the presence of amorphous phosphate species or HA layer on the surface. In the B5C5 (Fig. 16-A) sample, after 14 days, there was detected a small peak at 601 cm^{-1}, whereas in the B10C0 (Fig. 16-B) sample this small peak was observed 1 day after being immersed in SBF. In Fig.16-C, which presents the spectra of the B10C10 sample, it is clear the appearance of a new peak assigned to the P-O bonds, after 7 and 14 days. The intensity of the characteristic peak (at *ca.* 600 cm^{-1}) became stronger as the immersion time in SBF increased. In the B15C10 (Fig.16-D) and the B20C10 (Fig.16-E) samples the characteristic peak only appears after 14 days.

Regarding the change in the bonds that were already present in the material before immersion (0 days), it is possible to observe some variations in the intensity of them, mainly in D-Q vibration (at *ca*. 400 cm^{-1} and *ca.* 850 cm^{-1}); in Si-O-Si vibrations (at *ca.* 564 cm^{-1}, *ca.* 805 cm^{-1} and *ca.* 1103 cm^{-1}); in Si-CH3 vibrations (1265 cm^{-1}); and in the regions assigned to boron bonds, such as B-O-B (at *ca*. 730 cm^{-1}) and B-OH vibrations (between 1300 and 1550 cm^{-1}). In most of the samples, after

a day in contact with the supernatant liquid, the intensity of these peaks decreased, which suggests that the number of Si-O-Si, Si-CH3, B-OH and B-O-B bonds in the material decreased as well, due to the release of Si and B ions in the solution. However, as the time of immersion increased, the intensity of the peaks related to silicon increased as well, due to the formation of a silica-rich layer [155]. Accordingly, the samples with more boron and calcium in the system, such as the B10C10, the B15C10 and the B20C10 compositions, are the ones that show a band at *ca.* 600 cm^{-1}, which is assigned to the bending of the P-O bond on the surface of these samples. This is the prime indication of the presence of calcium-phosphate aggregates in the material. Besides, with the increase in immersion time, the results from the samples suggest the presence of a silica-rich layer.

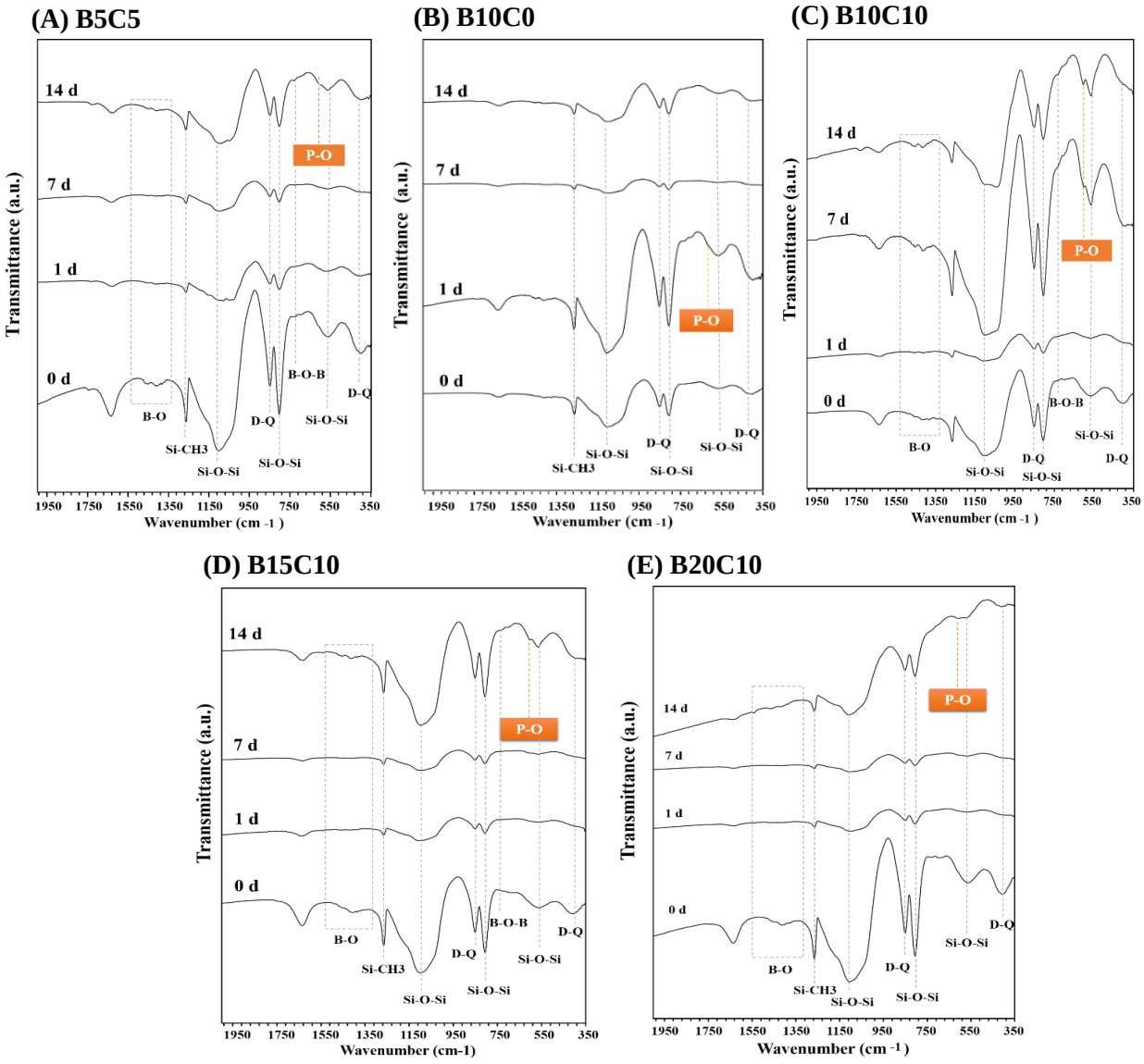

Figure 16 - FT-IR spectra of the five samples before (0 days) and after immersion in Kokubo solution during 1, 7 and 14 days: (A) B5C5 sample, (B) B10C0 sample, (C) B10C10 sample, (D) B15C10 and (E) B20C10 samples.

4.2.2. XRD analysis

The development of calcium phosphate aggregates or HA crystals cannot be identified solely based on the IR data. Therefore, X-ray diffraction analysis was performed to evaluate the presence of these precipitates. Figure 17 shows the X-ray diffractograms of samples B5C5 (Fig.17-A), B10C0 (Fig.17-B), B10C10 (Fig.17-C), B15C10 (Fig.17-D) and B20C10 (Fig.17-E) before (0 days) and after 1, 7 and 14 days of immersion in SBF. According to the literature, surface HA deposition is confirmed by the appearance of diffraction peaks at ~26º, ~32º, ~43º [153,155] .

As can be seen in Fig.17-A, corresponding to the B5C5 sample, no characteristic peak of the hydroxyapatite was detected after 1 day. However, after 7 days, the sample presented two peaks at 12º and 23º, which are characteristic of the calcium-phosphate that is deposited on the surface. Yet, after 14 days the peak disappears possibly due to the washes with ultrapure water and acetone that applied to the powder, before centrifugation.

In the B10C0 (Fig.17-B) composition no peak is detected. However, with the addition of calcium to the sample B10C10 (Fig.17-C) there appears a poorly defined peak at $2\theta=32^{o}$ after 14 days of immersion, but none appears at either 1 or 7 days. The compositions B15C10 (Fig.17-D) and B20C10 (Fig.17-E) do not show any representative peak of the apatite phase in any of the immersion times.

Therefore, considering the results obtained by XRD analysis, it is possible to deduce that no crystalline phase of calcium phosphate was formed, only some amorphous calcium-phosphate phases in some compositions. These results alone are not very conclusive and are not in line with the results obtained by FT-IR analysis, which detect the presence of phosphate links in all compositions.

The absence of crystalline phases is not exclusive of the existence of aggregates of calcium-phosphate, it depends on the concentration of each element and the time given to form these precipitations. And even when HA crystals do not appear, it is possible to obtain a bioactive and biocompatible material with only the presence of amorphous aggregates.

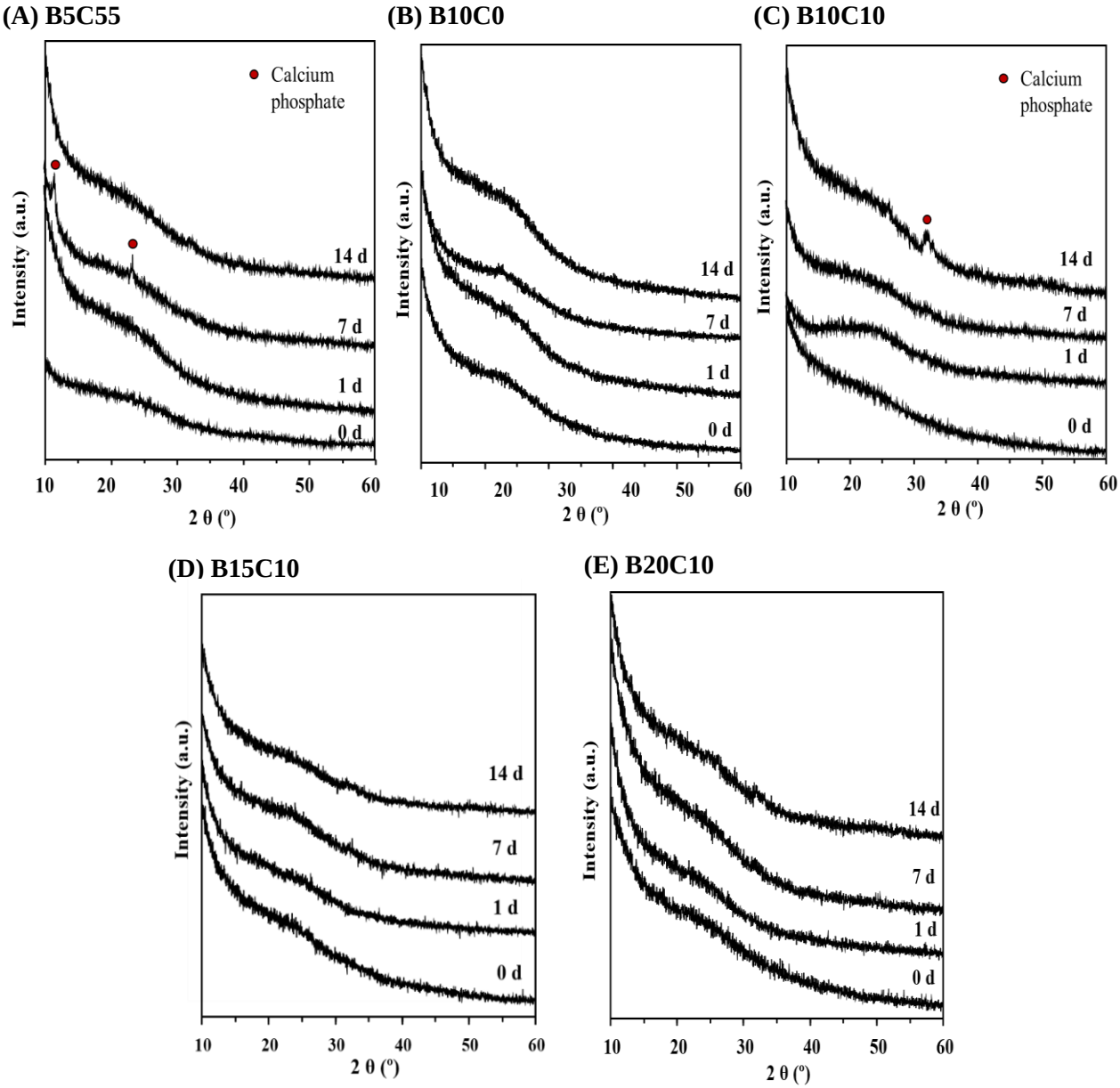

Figure 17 - XRD results from the samples before and after been immersed in SBF during 1,7 and 14 days: (A) B5C5, (B) B10C0, (C) B10C10, (D) B15C10, (E) B20C10.

4.3.3. SEM and EDS analysis

To complement the study of the material bioactivity in acellular medium, it was evaluated the surface of the samples dried at 150 ºC, after the samples were soaked in a simulated body fluid, by SEM and EDS. The SEM micrographs and respective EDS spectra of each composition surface, obtained after immersion in different time periods (1, 7 and 14 days), are represented below in the figures (Figures 18, 19, 20, 21, 22).

As can be observed in Figure 18, corresponding to the B5C5 sample, after 1 day of immersion (Fig.18-A1 and A2) there is no evidence of calcium or phosphorus in the materials, which is in accordance with its EDS (Fig.18-a). The calcium composing the material was not even detected, probably because Ca was released to the SBF solution. Though after 7 days (Fig.18-B1 and B2) it was detected a deposition of agglomerates in the surface of the material which, according to the EDS spectra (Fig.18-b), corresponds to a calcium-phosphate phase. As the time of immersion increased to 14 days, these granules of amorphous CaP-rich species continued to develop in the direction of HA crystals (Fig.18-C1 and C2). These results are in accordance with the ones from FT-IR and XRD, in which the appearance of a weak absorption band of P-O vibration and an calcium-phosphate phase were verified.

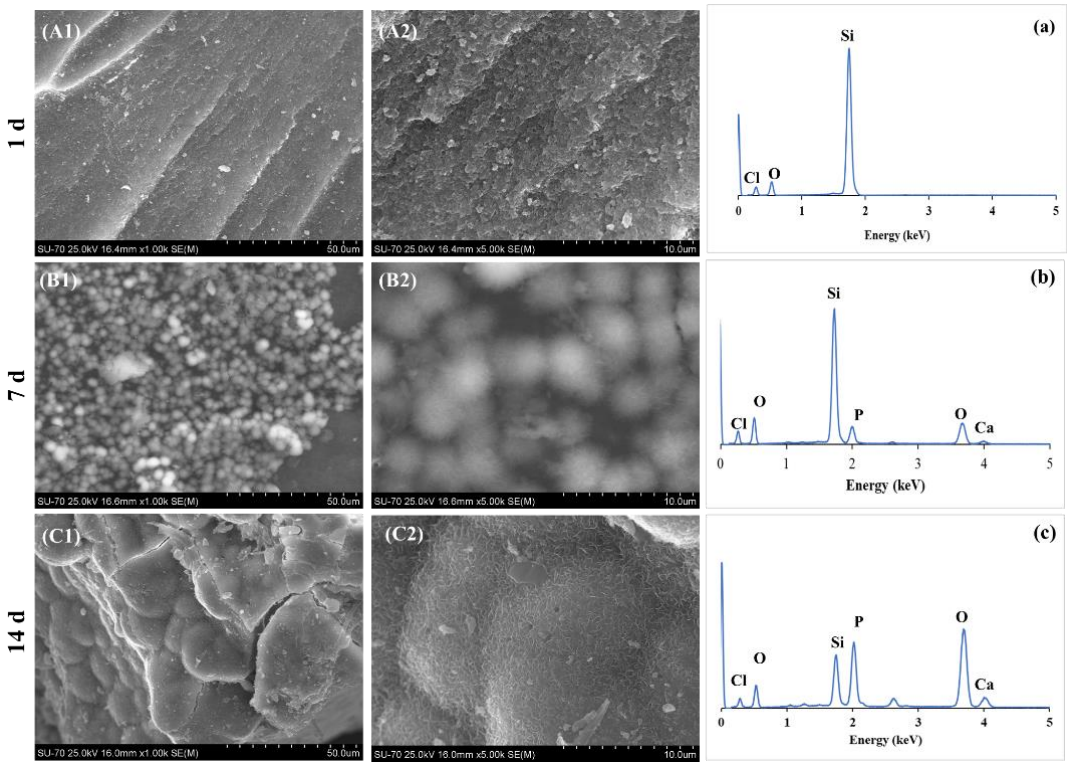

Figure 18 - SEM images, with magnification of 1.0k and 5.0k, and the respective EDS of the B5C5 composition dried at 150ºC after immersion in SBF for 1 day (A1, A2, a), 7 days (B1, B2, b) and 14 days (C1, C2, c).

Figure 19 corresponds to the B10C0 sample. Observing the SEM micrographs, there is no significant change at the microstructural level during immersion time. In the EDS spectra (Fig.19-a, b and c) no calcium or phosphorus ions were detected, just silicon ions belonging to the silica of the material. These results were expected since calcium was not present in this composition, making it difficult for the sample to form a calcium-phosphate layer. As said before, calcium ions are a requirement to promote the bioactivity of the material and, consequently, for the mineralization to occur.

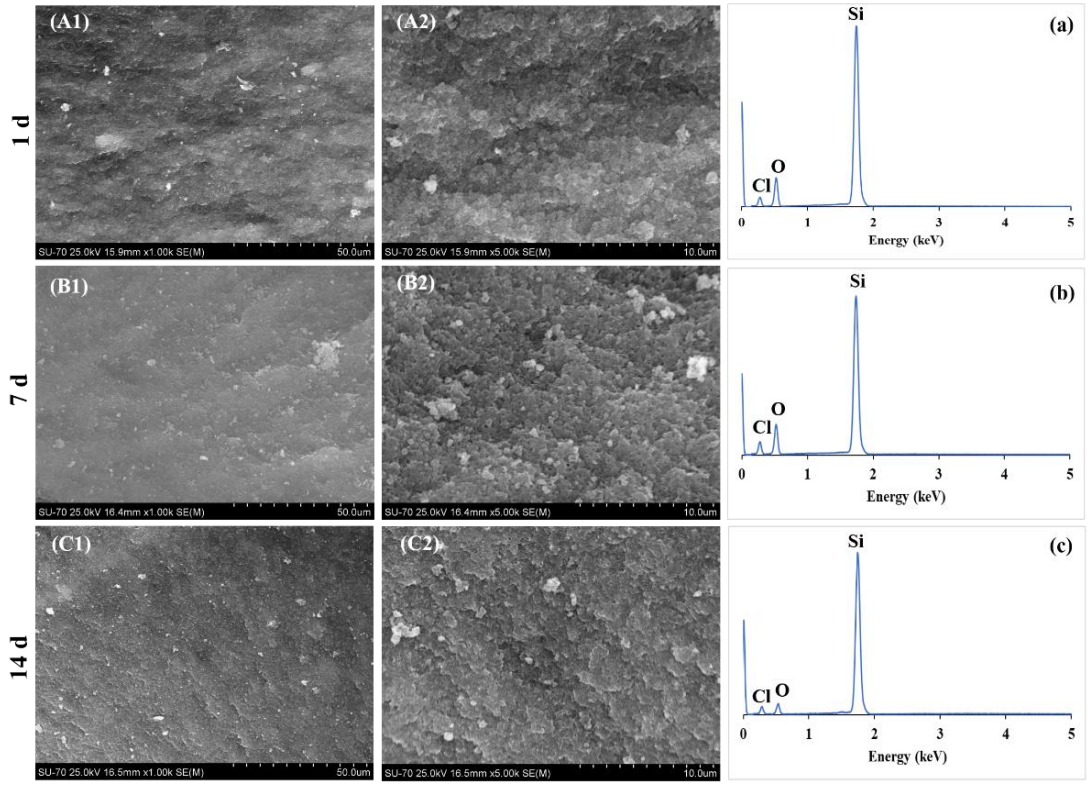

Figure 19 - SEM images, with magnification of 1.0k and 5.0k, and the respective EDS of the B10C0 composition dried at 150ºC after immersion in SBF for 1 day (A1, A2, a), 7 days (B2, B3, b) and 14 days (C1, C2, c).

Figure 20 shows the SEM images, with different magnifications, and the EDS spectra of the B10C10 sample after immersion in SBF for 1 day (Fig.20-A1, A2, A3 and a), 7 days (Fig.20-B1, B2, B3 and b) and 14 days (Fig.20-C1, C2, C3 and c). Observing the figures, the presence of precipitates in the surface of the material is detected in all immersion times. The change in the microstructure, before and after having been soaked in SBF, is accompanied by an obvious modification of the EDS spectra (Fig.20-a, b, c) which shows the appearance of characteristic peaks of Ca and P ions. These ions are attributed to the apatite-formation. Particularly, after immersion for 14 days, the images with

higher magnifications (Fig.20-C2 and C3) show the particles that covered the surface are formed with little crystals, that will presumably grow to HA-like crystals.

The EDS spectra also shows a peak of the Cl that is due to the HCl used in the samples' preparation.

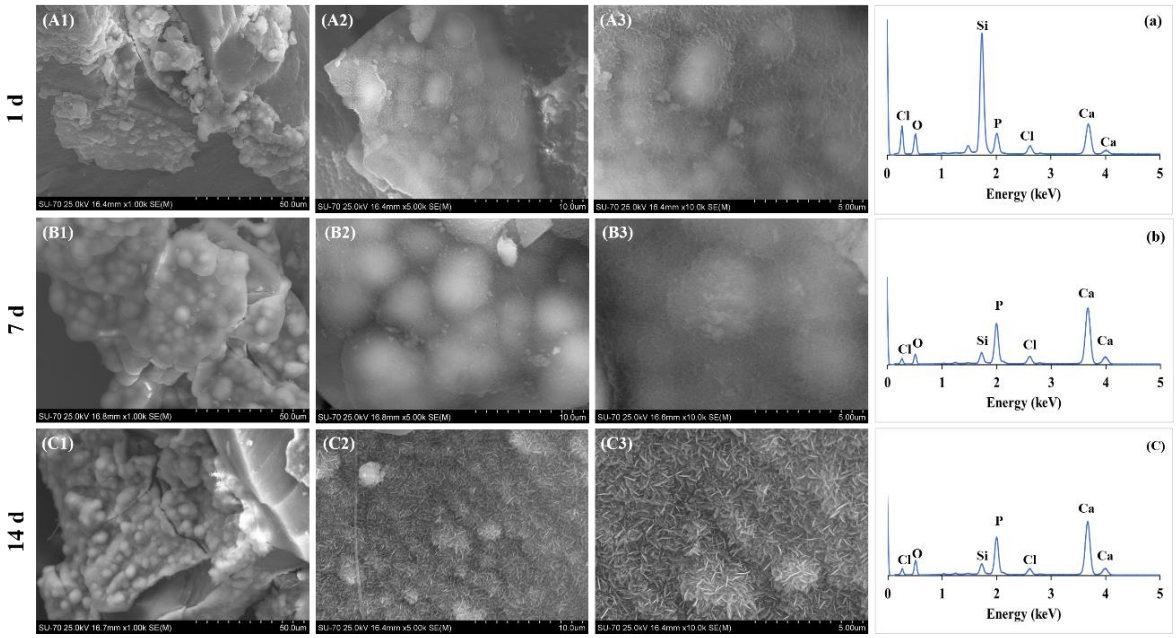

Figure 20 - SEM images, with a magnification of 1.0k, 5.0k and 10.0k, and the respective EDS of the B10C10 composition dried at 150ºC after immersion in SBF for 1 day (A1, A2, A3, a), 7 days (B1, B2, B3, b) and 14 days (C1, C2, C3, c).

The bioactivity analysis of the B15C10 sample is recorded in Figure 21, by SEM images, using different magnifications, and EDS spectra, for different immersion times: 1 day (Fig.21-A1, A2, A3, and a); 7 days (Fig.21-B1, B2, B3 and b); and 14 days (Fig.21-C1, C2, C3 and c). Observing the images, they revealed the presence of surface precipitates after soaking for three different times. After 1 day, it is observed, with a lower magnification (Fig.21-A1 and A2), a layer on the material's surface which, in agreement with EDS (Fig.21-a), is mainly composed of silicon, calcium and phosphorus ions. This could be the beginning of the calcium-phosphate layer's formation. The same happens for 7 days (Fig.21-B1 and B2) and 14 days (Fig.21-C1 and C2) of immersion, but the precipitates covering the surface are bigger.

Using a magnification higher than 5.0k (Fig.21-A3, Fig.21-B3, Fig.21-C3), one can state that the topography is changing during immersion time. The microstructure of the sample after 1 day (Fig.21-A3) is different from the ones after 7 (Fig.21-B3) and 14 days (Fig.21-C3), where the precipitates are forming into crystals, with lamellar form, which is typical of HA. This is in agreement with the FT-IR results after 14 days, which present a P-O bond characteristic of the formation of calcium-phosphate aggregates, although no visible apatite is observed in XRD.

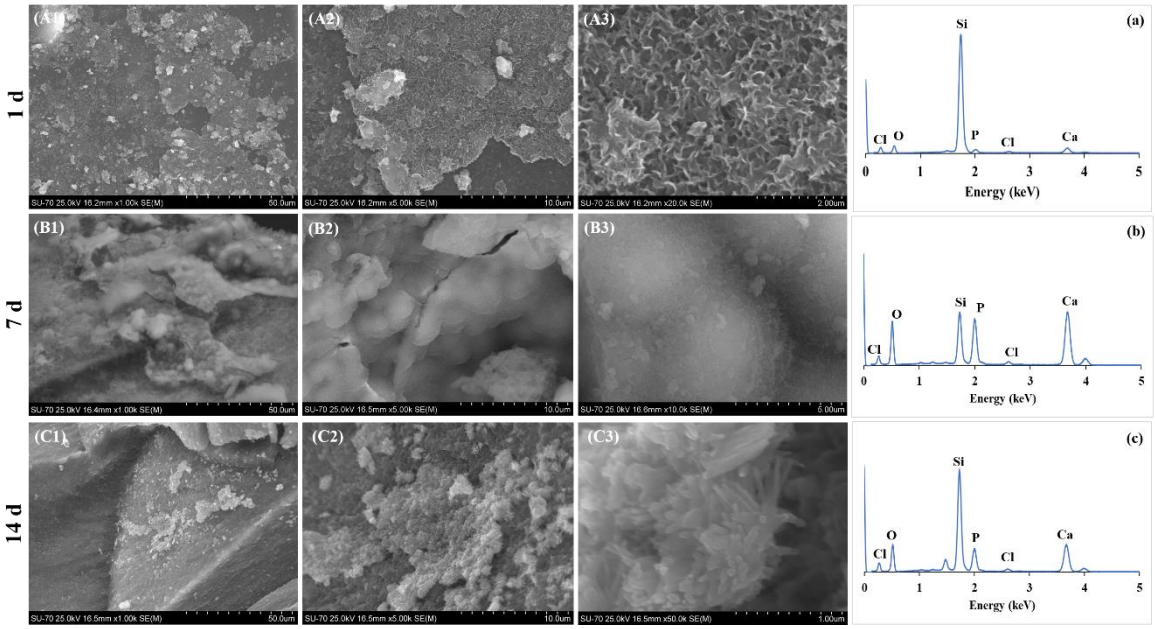

Figure 21 - SEM images and the respective EDS (a, b, c) of the B15C10 composition dried at 150ºC after immersion in SBF for 1 day (A1, A2,A3), 7 days (B1, B2, B3) and 14 days (C1, C2, C3), with three different magnifications.

Figure 22 is relative to the B20C10 sample, which also reveals the formation of apatite phase on the surface of the hybrid. Layers of calcium phosphate coat the powder samples (Fig.22-A1, Fig.22-B1 and Fig.22-C1), which are confirmed by the cauliflower-like shape of the crystals formed after 1 day (Fig.22-A2 and A3) and 14 days (Fig.22-C2 and C3). Again, the EDS spectra (Fig.22-a, b and c) confirm the existence of this phase. Although the SEM micrographs after 7 days of immersion (Fig.22-B2 and B3) do not reveal crystals with cauliflower like shape, there is still a presence of a calcium-phosphate phase. These images obtained from the material's surface can be relative to an area where the crystals are in development. This microstructure was also observed in the sample, B15C10, after 1 day.

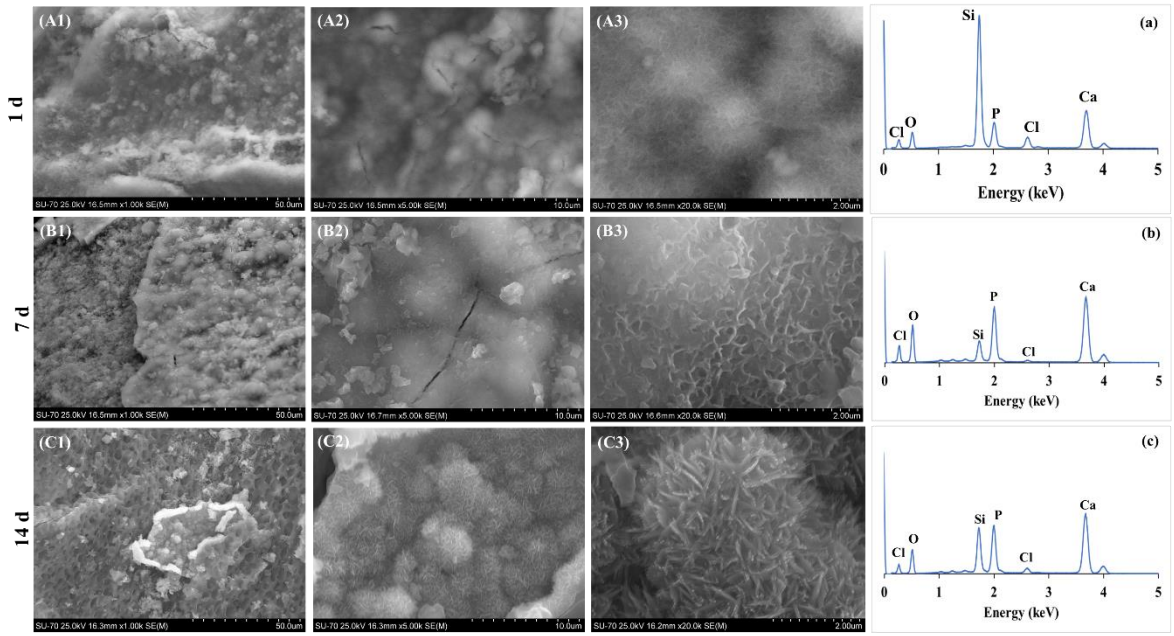

Figure 22 - SEM images and the respective EDS of the B20C10 composition dried at 150ºC after immersion in SBF for 1 day (A1, A2,A3), 7 days (B1, B2, B3) and 14 days (C1, C2, C3), with a magnification of 1.0k, 5.0k and 20.0k.

Although the XRD results do not show any considerable crystalline phases (peaks), throughout the various incubation times, the micrographs of SEM confirm the presence of aggregates in the hybrids' surfaces, corresponding to CaP phases. These results are supported by the FT-IR and EDS results, indicating the presence of a phosphate phase on the material, that is accompanied by an increase in calcium as well. The calcium-phosphate phase appears for all the samples containing calcium where it occurs a mineralization. These apatite precipitates are indicative of the material bioactivity potential. Thus, it is possible to have a bioactive material without crystalline phases, but with an amorphous calcium-phosphate phase.

The B10C0 sample, the one without calcium, was the only who exhibited no peaks of phosphorus in EDS, as well no precipitates in the surface of the hybrid material.

4.3.4. ICP analysis

ICP results are presented in Figure 23 which shows the variation of B (Fig.23-A), Ca (Fig.23-5B), P (Fig.23-C) and Si (Fig.23-D) ions concentration (ppm) in the supernatant liquid, for the five compositions, during different soaking times: 1, 7 and 14 days.

As shown in Fig.23-A, the boron concentration released from each sample increased throughout the immersion time and seems to be higher when more boron is in the composition. The B20C10 sample, which has the highest boron content, also reveals higher amounts of boron released, in the range of 7 ppm, for 7 and 14 days in SBF. The sample with the lowest amount of boron (B5C5) is also the one with the lowest concentration of boron released. In this way, with the increase of boron amount in the composition, more boron is released to the supernatant liquid, except for the cases of B10C0 and B10C10 samples. Although the two samples have the same amount of boron (0,10 mol), the B10C10 sample releases more boron than the B10C0.

Hence, these results suggest that the hybrids in the PDMS-SiO_2-CaO-B_2O_3 system can release boron when in contact with simulated body fluids. The values of the amount of boron released (from 1 to 7 ppm) from the samples are in the interval defined as optimum for a controlled release (0-10 ppm) [11]. Thus, according to the literature, these materials are probably capable of inducing osteoblasts activity and inhibit the osteoclasts bone resorption. At the same time, the boron's values are much lower than the one reported as cytotoxic (> 50 ppm) [11].

While boron concentration in the SBF increases with time, calcium (Fig.23-B) and phosphorus (Fig.23-C) concentrations decrease, which appears to be associated with the deposition of an amorphous calcium phosphate layer on the hybrid.

Regarding calcium concentration (Fig.23-B), all the samples containing calcium in the composition are capable of releasing this ion after 1 day of immersion, since the Ca ionic concentration of each sample, in the SBF is higher than the one for SBF standard, $[Ca]_{SBF\ standard}$ = 100 mg/L. With the time, the calcium concentration continues to decrease in all samples containing calcium, except for the B15C10 sample after 14 days, in which a different behaviour occurs. The B15C10 sample demonstrates a different behaviour comparatively to other samples after 14 days: the calcium concentration increases after 1 day, then decreases after 7 days and at day 14 increases drastically, while phosphorus ions stabilize. This rapid increase of Ca^{2+} can be due to the calcium saturation. Initially, the calcium ions diffuse through the hybrid and are released to the solution, explaining why the value of calcium after 1 day is higher than the SBF standard value. Then, occurs the link between the phosphate ions, forming an amorphous CaO and P_2O_5-rich film on the hybrid surface, so the calcium and phosphorus concentrations of the solution decrease. This process happens for all samples. The only difference is that at same point (at 14 days) in the B15C10 sample, the calcium in the material starts to be released to the solution, maybe due to the saturation of the surface.

As for silicon concentration in the SBF, with the exception of B10C0, it increases with the time of immersion, owing to the dissolution of soluble silica. According to the mechanism proposed by Hench [156], and explained before, the nucleation and precipitation of an apatite-like phase on the glass surface firstly begin with a cationic exchange. This exchange is between the cations within the hybrid and H^+ ions from the solution. This leads to the formation of silanol bonds (Si-OH) on the surface of the material. With the ongoing of the exchanging reaction, Si-O-Si bonds are attacked by hydroxyl ions, and when all four Si-O bonds of a single Si atom are broken, soluble silica, $Si(OH)_4$, is lost in the solution. Once again, a controlled release profile of silica ions is observed for B10C10 sample in the range of 1.7-16 ppm. For the composition with higher content of boron in the system (B20C10) it releases lower concentrations of silicon. This may be an indication that the bonds associated with silicon ions are strongly bonded, making it difficult to dissolve them in contact with physiological fluids. The sample without calcium, B10C0, do not present any change throughout time, maintaining the same value of silicon concentration, which is equal to the standard solution.

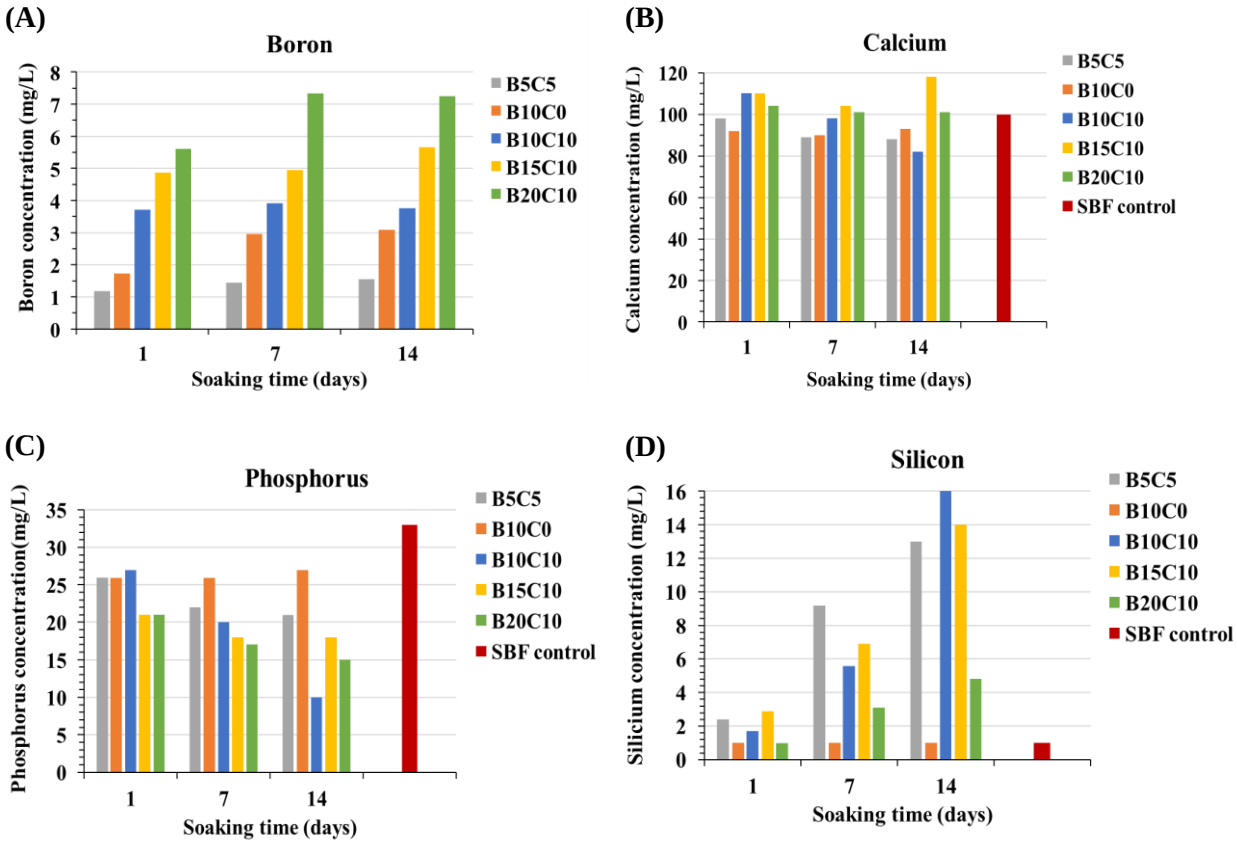

Figure 23 - Ionic concentration of (A) boron, (B) calcium, (C) phosphorus and (D) silicon in SBF medium at different soaking times (1, 7 and 14 days), and released from the five samples.

The ICP results are in agreement with the ones from SEM and FT-IR, since the decrease of calcium and phosphorous ions in the SBF solution suggest that these ions were used for the formation of a calcium-phosphate layer in the surface, confirmed by the appearance of precipitates in SEM micrographs as well as P-O vibrations in FT-IR spectra.

The pH of the supernatant liquid of the five samples, for each soaking time in SBF, was analysed. This analysis was useful to verify the effect of boron and calcium in the pH of the medium, when the sample is in contact with a simulated body fluid. Table 10 shows the pH values obtained for each composition, at different immersion times (1, 7 and 14 days). Observing the table, it is possible to confirm that there is not a significant variation in the pH values, remaining approximately neutral, pH~7.4 In addition, comparing the SBF standard (7.45) with the SBF with the ionic dissolution products of each sample, with different boron and calcium contents, the pH values are similar. In this way, these results may be advantageous, since boron ions did not acidify the medium, not occurring a significant variation of pH with the boron content.

Table 10 - pH values of each sample after being in SBF for 1, 7 and 14 days.

	B5C5	**B10C0**	**B10C10**	**B15C10**	**B20C10**
1 day	7.5	7.4	7.5	7.5	7.5
7 days	7.5	7.5	7.5	7.5	7.5
14 days	6.9	7.2	7.4	7.5	7.4

Chapter 5

Conclusions and Future Works

5.1. Conclusions

The two main objectives of the present work were: to prepare monolithic hybrid materials for bone tissue engineering based on a polydimethylsiloxane-silica (PDMS-SiO_2) system containing calcium and boron ions; and to achieve a better understanding of the relationship between calcium and boron addition and the obtained chemical structures, microstructure and macrostructure properties, and consequently the biological behaviour.

The first goal was accomplished, which was to define an experimental protocol to synthesize a homogeneous hybrid material. After some experimental work, it was possible to reach the ideal procedure where no precipitation was observed. The absence of precipitations was mainly due to the miscibility between the reagents used. Although water is important to start the hydrolysis-condensation process, not all the precursors used are miscible in water, like the case of PDMS. Though, PDMS is miscible in acetone as well as the TMB. Isopropanol was advantageous for the reaction with the ester, from the calcium acetate with HCl, which as eliminated during the drying step (150ºC).

In addition, this experiment allowed the formation of hybrid bonds (D-Q) between the organic (PDMS) and the silica inorganic precursor (TEOS) as well as the presence of borosiloxane bonds (B-O-Si). According to the literature, these links were confirmed by the appearance of bands near 400 and 850 cm^{-1}, and at *ca.* 880 and 925 cm^{-1} in the IR spectra of prepared samples, respectively. The last results were in accordance with the $^{[11]}$B NMR data, which demonstrates that samples with boron and calcium in the composition, such as B10C10, B15C10 and B20C10, revealed the presence of boron sites connected to SiO_4. In accordance with previous literature, the peaks obtained corresponded to trigonal boron units in non-ring and boroxol rings, and to tetrahedral boron structures. However, the sample without calcium (B10C0) did not present boron atoms in the BO_4 tetrahedral. Accordingly, this confirms that the presence of the CaO modifier influences boron's configuration, by changing the boron from BO_3 planar structures to BO_4 tetrahedra structures. The structure of the hybrid depends on the network former and modifier atoms.

Taking into account that the synthesis of the hybrid system was done at low processing temperatures, the B-O-Si bonds with four-coordinated borons revealed to be easily broken, since the

bond energy is weaker than the three-coordinated boron. In this way, the boron coordination can be in constant alternation between $^{[3]}B$ and $^{[4]}B$ sites [47].

In respect to the hybrid microstructure, it was noted that there was a microstructural difference between the samples, becoming this difference clearer with the increase of boron content used in the sol-gel preparation. BET analysis showed that the specific surface area and the mesoporosity of the material tend to decrease with the boron amount. Samples with higher amounts of boron demonstrated larger macropores, while the samples with low boron, a higher mesoporosity. Thus, it is possible to conclude that boron affects the microstructure of the material. The porosity observed in the SEM and BET specific surface area can be advantageous to the release of calcium and boron ions when in contact with body fluid, stimulating the formation of calcium-phosphate layer and the cell attachment, migration and vascularization. As referred before, vascularization of the tissue is important for bone repair and regeneration, and the ability to induce angiogenesis is considered one of the requisites for the devolvement of biomaterials.

Regarding the bioactive potential of the material, the results obtained by SEM, EDS and ICP are in agreement with the accepted mechanism of calcium phosphates formation in calcium-containing sols produced at room temperature. Samples with calcium in the system released it to the SBF medium over time, decreasing its ionic concentration and leading to the precipitation of calcium-phosphate. This was confirmed by SEM images, which demonstrated cauliflower aggregates on the sample's surface. The aggregates of calcium-phosphate were not deposited in a homogenous way, being instead dispersed throughout the surface. However, for the sample B10C0, which does not contain calcium in its composition, the concentration of this element in the SBF solution does not reach the threshold necessary to induce calcium phosphates crystallization, and consequently, no detection of aggregates was found in the SEM micrographs. Another goal was achieved: the production of a potential bioactive and biocompatible PDMS-SiO_2-B_2O_3-CaO hybrid.

From the ICP data, it was possible to verify that, for the same amount of boron, the presence of calcium in the system induces a higher release of boron from the material. This may be explained by the release of calcium from the system, when the material is in contact with body fluids, which will weaken the structure. Consequently, boron becomes more receptive to be released as well.

It must be noticed that although the SBF solution was been used to evaluate the capability of the materials to form calcium-phosphate on the surface, it presents several limitations as a technique to evaluate the material's bioactivity.

From the production and study of PDMS-SiO_2-B_2O_3-CaO hybrid system, there was two main conclusions achieved:

- The incorporation of boron in the hybrid system changes the materials' microstructure, by increasing the macro porosity and lowering the surface area;

- The presence of a network modifier in the hybrid structure changes the boron coordination from trigonal to tetrahedral.

5.2. Future works

The results obtained in the present work led to some suggestions for its continuation, as well as to the deepening of some aspects in the sense of clarifying certain results. In this way it is suggested:

- To evaluate if the calcium and phosphor ions are present in the ultrapure water and acetone applied to the powder, before centrifugation;
- To evaluate the cytocompatibility of the material in a cell media. These tests will be carried out in the laboratory of the University of Erlangen-Nuremberg, in Germany, in order to verify the possible cytotoxicity of the samples and their effect on the activity of osteoblastic cells. For that purpose, cell assays will be perform with the aim of measuring the cell viability, cell morphology, and release of angiogenic agents, such as vascular endothelial growth factor (VEGF), by the cells, when exposed to ionic dissolution products;
- To study the influence of sol-gel parameters, such as water, pH, TEOS and PDMS content, in the PDMS-SiO_2-B_2O_3-CaO hybrid system and, consequently, the modifications on the structure and microstructure of the material, as well as in the biological performance;
- To study the kinetic of Ca and B release.

References

(1) Langer, R.; Vacanti, J. P. Tissue Engineering. *Science (80-.).* **1993**, *260* (5110), 920–926.

(2) Pereira, M. M.; Jones, J. R.; Hench, L. L. Bioactive Glass and Hybrid Scaffolds Prepared by Sol–gel Method for Bone Tissue Engineering. *Adv. Appl. Ceram.* **2005**, *104* (1), 35–42.

(3) Jones, J. R. Review of Bioactive Glass: From Hench to Hybrids. *Acta Biomater.* **2015**, *23* (S), S53–S82.

(4) Rahaman, M. N.; Day, D. E.; Sonny Bal, B.; Fu, Q.; Jung, S. B.; Bonewald, L. F.; Tomsia, A. P. Bioactive Glass in Tissue Engineering. *Acta Biomater.* **2011**, *7* (6), 2355–2373.

(5) Salgado, A. J.; Coutinho, O. P.; Reis, R. L. Bone Tissue Engineering: State of the Art and Future Trends. *Macromol. Biosci.* **2004**, *4* (8), 743–765.

(6) Mackenzie, J. D.; Huang, Q. X.; Iwamoto, T. Mechanical Properties of Ormosils. *J. Sol-Gel Sci. Technol.* **1996**, *7* (3), 151–161.

(7) Yabuta, T.; Tsuru, K.; Hayakawa, S.; Osaka, A. Synthesis of Blood Compatible PDMS-Based Organic-Inorganic Hybrid Coatings. *J. Sol-Gel Sci. Technol.* **2004**, *31* (1–3 SPEC.ISS.), 273–276.

(8) Hyeon-Lee, J.; Guo, L.; Beaucage, G.; Macip-Boulis, M. A.; Yang, A. J. M. M. Morphological Development in PDMS/TEOS Hybrid Materials. *J. Polym. Sci. Part B Polym. Phys.* **1996**, *34* (17), 3073–3080.

(9) Wen, J.; Wilkes, G. L. Organic/Inorganic Hybrid Network Materials by the Sol-Gel Approach. *Chem. Mater.* **1996**, *8* (8), 1667–1681.

(10) Miyata, N.; Fuke, K.; Chen, Q.; Kawashita, M.; Kokubo, T.; Nakamura, T. Apatite-Forming Ability and Mechanical Properties of PTMO-Modified CaO-SiO2 Hybrids Prepared by Sol-Gel Processing: Effect of CaO and PTMO Contents. *Biomaterials* **2002**, *23* (14), 3033–3040.

(11) Balasubramanian, P.; Hupa, L.; Jokic, B.; Detsch, R.; Grünewald, A.; Boccaccini, A. R. Angiogenic Potential of Boron-Containing Bioactive Glasses: In Vitro Study. *J. Mater. Sci.* **2017**, *52* (15), 8785–8792.

(12) Newnham, R. E. Essentiality of Boron for Healthy Bones and Joints. *Environ. Health Perspect.* **1994**, *102* (SUPPL. 7), 83–85.

(13) Haro Durand, L. A.; Vargas, G. E.; Romero, N. M.; Vera-Mesones, R.; Porto-López, J. M.; Boccaccini, A. R.; Zago, M. P.; Baldi, A.; Gorustovich, A. Angiogenic Effects of Ionic Dissolution Products Released from a Boron-Doped 45S5 Bioactive Glass. *J. Mater. Chem. B* **2015**, *3* (6), 1142–1148.

(14) Tsuru, K.; Ohtsuki, C.; Osaka, A.; Iwamoto, T.; Mackenzie, J. D. Bioactivity of Sol-Gel Derived Organically Modified Silicates. Part I: In Vitro Examination. *J. Mater. Sci. Mater.*

Med. **1997**, *8* (3), 157–161.

(15) Camino, G.; Lomakin, S. M.; Lageard, M. Thermal Polydimethylsiloxane Degradation. Part 2. The Degradation Mechanisms. *Polymer (Guildf).* **2002**, *43* (7), 2011–2015.

(16) Tamayo, A.; Téllez, L.; Rodríguez-Reyes, M.; Mazo, M. A.; Rubio, F.; Rubio, J. Surface Properties of Bioactive TEOS-PDMS-TiO2-CaO Ormosils. *J. Mater. Sci.* **2014**, *49* (13), 4656–4669.

(17) Tellez, L.; Rubio, J.; Rubio, F.; Morales, E.; Oteo, J. L. Synthesis of Inorganic-Organic Hybrid Materials from TEOS, TBT and PDMS. *J. Mater. Sci.* **2003**, *38* (8), 1773–1780.

(18) Peña-Alonso, R.; Rubio, J.; Rubio, F.; Oteo, J. A FT-IR Study of the Synthesis of Boron Ormosils by Means of the Sol-Gel Process. *J. sol-gel Sci. …* **2002**, 255–263.

(19) Soraru, G. D.; Dallabona, N.; Gervais, C.; Babonneau, F. Organically Modified SiO2-B2O3 Gels Displaying a High Content of Borosiloxane (= B-O-Si) Bonds. *Chem. Mater.* **1999**, *11* (4), 910–919.

(20) Fu, Q.; Saiz, E.; Rahaman, M. N.; Tomsia, A. P. Bioactive Glass Scaffolds for Bone Tissue Engineering: State of the Art and Future Perspectives. *Mater. Sci. Eng. C* **2011**, *31* (7), 1245–1256.

(21) Moreno, M. S. M. da S. Engenharia de Tecidos Na Substituição de Tecido Ósseo, Universidade Fernando Pessoa, Porto, 2014.

(22) Henkel, J.; Woodruff, M. A.; Epari, D. R.; Steck, R.; Glatt, V.; Dickinson, I. C.; Choong, P. F. M.; Schuetz, M. A.; Hutmacher, D. W. Bone Regeneration Based on Tissue Engineering Conceptions — A 21st Century Perspective. *Bone Res.* **2013**, *1* (3), 216–248.

(23) Susmita Bose, Mangal Roy, and A. B. Recent Advances in Bone Tissue Engineering Scaffolds. *Trends Biotechnol.* **2012**, *30* (10), 546–554.

(24) Xia, Z. Tissue Engineering of Bone : The Role of Osteoblasts and Osteoclasts. **2004**, 1–4.

(25) Gutierres, M.; Ascensão Lopes, M.; Sooraj Hussain, N.; Trigo Cabral, A.; Almeida, L.; Domingos Santos, J. Substitutos Ósseos: Conceitos Gerais e Estado Actual. *Arq. Med.* **2005**, *19* (4), 153–162.

(26) Schicker, M.; Seitz, H.; Drosse, I.; Seitz, S.; Mutschler, W. Biomaterials as Scaffold for Bone Tissue Engineering. *Eur. J. Trauma* **2006**, *32* (2), 114–124.

(27) O'Brien, F. J. Biomaterials & Scaffolds for Tissue Engineering. *Mater. Today* **2011**, *14* (3), 88–95.

(28) Killian, M. L.; Cavinatto, L.; Galatz, L. M.; Thomopoulos, S. Recent Advances in Shoulder Research. *Arthritis Res. Ther.* **2012**, *14* (3).

(29) Dos, R.; Afonso, S. Interação Entre Biomateriais e Tecido Ósseo, Universidade do Porto, 1998.

(30) Nabiça, M. de S. M. S. Scaffolds Preparados Por Sol-Gel Para Aplicações Biomédicas, Universidade de Aveiro, 2013.

(31) Gerhardt, L. C.; Widdows, K. L.; Erol, M. M.; Burch, C. W.; Sanz-Herrera, J. A.; Ochoa, I.; Stämpfli, R.; Roqan, I. S.; Gabe, S.; Ansari, T.; et al. The Pro-Angiogenic Properties of Multi-Functional Bioactive Glass Composite Scaffolds. *Biomaterials* **2011**, *32* (17), 4096–4108.

(32) Cao, W.; Hench, L. L. Bioactive Materials. *Ceram. Int.* **1996**, *22* (6), 493–507.

(33) Kargozar, S.; Baino, F.; Hamzehlou, S.; Hill, R. G.; Mozafari, M. Bioactive Glasses: Sprouting Angiogenesis in Tissue Engineering. *Trends in Biotechnology*. 2018, pp 430–444.

(34) Hoppe, A.; Güldal, N. S.; Boccaccini, A. R. A Review of the Biological Response to Ionic Dissolution Products from Bioactive Glasses and Glass-Ceramics. *Biomaterials* **2011**, *32* (11), 2757–2774.

(35) Hench, L. L.; Jones, J. R. Bioactive Glasses: Frontiers and Challenges. *Front. Bioeng. Biotechnol.* **2015**, *3*.

(36) Hench, L. L. The Story of Bioglass®. *J. Mater. Sci. Mater. Med.* **2006**, *17* (11), 967–978.

(37) Rabiee, S. M.; Nazparvar, N.; Azizian, M.; Vashaee, D.; Tayebi, L. Effect of Ion Substitution on Properties of Bioactive Glasses: A Review. *Ceram. Int.* **2015**, *41* (6), 7241–7251.

(38) Mao, C.; Chen, X.; Miao, G.; Lin, C. Angiogenesis Stimulated by Novel Nanoscale Bioactive Glasses. *Biomed. Mater.* **2015**, *10* (2), 25005.

(39) Li, H.; Chang, J. Bioactive Silicate Materials Stimulate Angiogenesis in Fibroblast and Endothelial Cell Co-Culture System through Paracrine Effect. *Acta Biomater.* **2013**, *9* (6), 6981–6991.

(40) Keshaw, H.; Forbes, A.; Day, R. M. Release of Angiogenic Growth Factors from Cells Encapsulated in Alginate Beads with Bioactive Glass. *Biomaterials* **2005**, *26* (19), 4171–4179.

(41) Hench, L. L.; Roki, N.; Fenn, M. B. Bioactive Glasses: Importance of Structure and Properties in Bone Regeneration. *J. Mol. Struct.* **2014**, *1073* (C), 24–30.

(42) Bi, L.; Rahaman, M. N.; Day, D. E.; Brown, Z.; Samujh, C.; Liu, X.; Mohammadkhah, A.; Dusevich, V.; Eick, J. D.; Bonewald, L. F. Effect of Bioactive Borate Glass Microstructure on Bone Regeneration, Angiogenesis, and Hydroxyapatite Conversion in a Rat Calvarial Defect Model. *Acta Biomater.* **2013**, *9* (8), 8015–8026.

(43) Carlisle, E. M. Silicon: A Possible Factor in Bone Calcification. *Science (80-.).* **1970**, *167* (3916), 279 LP-280.

(44) Bose, S.; Fielding, G.; Tarafder, S.; Bandyopadhyay, A. Understanding of Dopant-Induced Osteogenesis and Angiogenesis in Calcium Phosphate Ceramics. *Trends Biotechnol.* **2013**, *31* (10), 594–605.

(45) Carlisle, E. M. Silicon: A Requirement in Bone Formation Independent of Vitamin D1. *Calcif. Tissue Int.* **1981**, *33* (1), 27–34.

(46) Zhai, W.; Lu, H.; Chen, L.; Lin, X.; Huang, Y.; Dai, K.; Naoki, K.; Chen, G.; Chang, J. Silicate Bioceramics Induce Angiogenesis during Bone Regeneration. *Acta Biomater.* **2012**, *8* (1), 341–349.

(47) Balasubramanian, P.; Büttner, T.; Miguez Pacheco, V.; Boccaccini, A. R. Boron-Containing Bioactive Glasses in Bone and Soft Tissue Engineering. *J. Eur. Ceram. Soc.* **2018**, *38* (3), 855–869.

(48) Wu, C.; Miron, R.; Sculean, A.; Kaskel, S.; Doert, T.; Schulze, R.; Zhang, Y. Proliferation, Differentiation and Gene Expression of Osteoblasts in Boron-Containing Associated with Dexamethasone Deliver from Mesoporous Bioactive Glass Scaffolds. *Biomaterials* **2011**, *32* (29), 7068–7078.

(49) Hakki, S. S.; Bozkurt, B. S.; Hakki, E. E. Boron Regulates Mineralized Tissue-Associated Proteins in Osteoblasts (MC3T3-E1). *J. Trace Elem. Med. Biol.* **2010**, *24* (4), 243–250.

(50) Balasubramanian, P.; Grünewald, A.; Detsch, R.; Hupa, L.; Jokic, B.; Tallia, F.; Solanki, A. K.; Jones, J. R.; Boccaccini, A. R. Ion Release, Hydroxyapatite Conversion, and Cytotoxicity of Boron-Containing Bioactive Glass Scaffolds. *Int. J. Appl. Glas. Sci.* **2016**, *7* (2), 206–215.

(51) Fu, Q.; Rahaman, M. N.; Fu, H.; Liu, X. Silicate, Borosilicate, and Borate Bioactive Glass Scaffolds with Controllable Degradation Rate for Bone Tissue Engineering Applications. I. Preparation and in Vitro Degradation. *J. Biomed. Mater. Res. - Part A* **2010**, *95* (1), 164–171.

(52) Huang, W.; Day, D. E.; Kittiratanapiboon, K.; Rahaman, M. N. Kinetics and Mechanisms of the Conversion of Silicate (45S5), Borate, and Borosilicate Glasses to Hydroxyapatite in Dilute Phosphate Solutions. *J. Mater. Sci. Mater. Med.* **2006**, *17* (7), 583–596.

(53) Yao, A.; Wang, D.; Huang, W.; Fu, Q.; Rahaman, M. N.; Day, D. E. In Vitro Bioactive Characteristics of Borate-Based Glasses with Controllable Degradation Behavior. *J. Am. Ceram. Soc.* **2007**, *90* (1), 303–306.

(54) Gu, Y.; Wang, G.; Zhang, X.; Zhang, Y.; Zhang, C.; Liu, X.; Rahaman, M. N.; Huang, W.; Pan, H. Biodegradable Borosilicate Bioactive Glass Scaffolds with a Trabecular Microstructure for Bone Repair. *Mater. Sci. Eng. C* **2014**, *36* (1), 294–300.

(55) Fu, Q.; Rahaman, M. N.; Bal, B. S.; Bonewald, L. F.; Kuroki, K.; Brown, R. F. Silicate, Borosilicate, and Borate Bioactive Glass Scaffolds with Controllable Degradation Rate for Bone Tissue Engineering Applications. II. In Vitro and in Vivo Biological Evaluation. *J. Biomed. Mater. Res. - Part A* **2010**, *95* (1), 172–179.

(56) El-Rashidy, A. A.; Roether, J. A.; Harhaus, L.; Kneser, U.; Boccaccini, A. R. Regenerating Bone with Bioactive Glass Scaffolds: A Review of in Vivo Studies in Bone Defect Models.

Acta Biomater. **2017**, *62*, 1–28.

(57) Saranti, A.; Koutselas, I.; Karakassides, M. A. Bioactive Glasses in the System CaO-B2O3-P2O5: Preparation, Structural Study and in Vitro Evaluation. *J. Non. Cryst. Solids* **2006**, *352* (5), 390–398.

(58) Ryu, H. S.; Lee, J. H. K.; Seo, J. H.; Kim, H.; Hong, K. S.; Kim, D. J.; Lee, J. H. K.; Lee, D. H.; Chang, B. S.; Lee, C. K.; et al. Novel Bioactive and Biodegradable Glass Ceramics with High Mechanical Strength in the CaO--SiO2--B2O3 System. *J.Biomed.Mater.Res.* **2004**, *68A* (1), 79–89.

(59) Yang, X.; Zhang, L.; Chen, X.; Sun, X.; Yang, G.; Guo, X.; Yang, H.; Gao, C.; Gou, Z. Incorporation of B2O3in CaO-SiO2-P2O5bioactive Glass System for Improving Strength of Low-Temperature Co-Fired Porous Glass Ceramics. *J. Non. Cryst. Solids* **2012**, *358* (9), 1171–1179.

(60) Chikara OHTSUKI , Yukio KOBAYASHI, K. T. and A. O. Compositional Dependence of Bioactivity of Glasses in the System Its in Vitro Evaluation. *J. Soc.* **1995**, *44*, 693–699.

(61) Brown, R. F.; Rahaman, M. N.; Dwilewicz, A. B.; Huang, W.; Day, D. E.; Li, Y.; Bal, B. S. Effect of Borate Glass Composition on Its Conversion to Hydroxyapatite and on the Proliferation of MC3T3-E1 Cells. *J. Biomed. Mater. Res. - Part A* **2009**, *88* (2), 392–400.

(62) Haro Durand, L. A.; Góngora, A.; Porto López, J. M.; Boccaccini, A. R.; Zago, M. P.; Baldi, A.; Gorustovich, A. In Vitro Endothelial Cell Response to Ionic Dissolution Products from Boron-Doped Bioactive Glass in the SiO_2–CaO–P_2O_5–Na_2O System. *J. Mater. Chem. B* **2014**, *2* (43), 7620–7630.

(63) Maeno, S.; Niki, Y.; Matsumoto, H.; Morioka, H.; Yatabe, T.; Funayama, A.; Toyama, Y.; Taguchi, T.; Tanaka, J. The Effect of Calcium Ion Concentration on Osteoblast Viability, Proliferation and Differentiation in Monolayer and 3D Culture. *Biomaterials* **2005**, *26* (23), 4847–4855.

(64) Valliant, E. M.; Jones, J. R. Softening Bioactive Glass for Bone Regeneration: Sol-Gel Hybrid Materials. *Soft Matter* **2011**, *7* (11), 5083–5095.

(65) Lin, Y.; Brown, R. F.; Jung, S. B.; Day, D. E. Angiogenic Effects of Borate Glass Microfibers in a Rodent Model. *J. Biomed. Mater. Res. - Part A* **2014**, *102* (12), 4491–4499.

(66) Kamitakahara, M.; Kawashita, M.; Miyata, N.; Kokubo, T.; Nakamura, T. Bioactivity and Mechanical Properties of Polydimethylsiloxane (PDMS)-CaO-SiO<inf>2</Inf> Hybrids with Different PDMS Contents. *J. Sol-Gel Sci. Technol.* **2001**, *21* (1–2), 1015–1016.

(67) Judeinstein, P.; Sanchez, C. Hybrid Organic - Inorganic Materials: A Land of Multidisciplinarity. *J. Mater. Chem.* **1996**, *6* (4), 511–525.

(68) Mammeri, F.; Le Bourhis, E.; Rozes, L.; Sanchez, C. Mechanical Properties of Hybrid

Organic-Inorganic Materials. *J. Mater. Chem.* **2005**, *15* (35–36), 3787–3811.

(69) Kickelbick, G. *Introduction to Hybrid Materials. Hybrid Materials*; 2007.

(70) Kickelbick, G. Hybrid Materials – Past, Present and Future. *Hybrid Mater.* **2014**, *1* (1), 39–51.

(71) Brinker, C. J.; Scherer, G. W. *Sol-Gel Science : The Physics and Chemistry of Sol-Gel Processing*; Academic Press: Boston, 1990.

(72) Owens, G. J.; Singh, R. K.; Foroutan, F.; Alqaysi, M.; Han, C. M.; Mahapatra, C.; Kim, H. W.; Knowles, J. C. Sol-Gel Based Materials for Biomedical Applications. *Prog. Mater. Sci.* **2016**, *77*, 1–79.

(73) Martin, R. A.; Yue, S.; Hanna, J. V.; Lee, P. D.; Newport, R. J.; Smith, M. E.; Jones, J. R. Characterizing the Hierarchical Structures of Bioactive Sol-Gel Silicate Glass and Hybrid Scaffolds for Bone Regeneration. *Philos. Trans. R. Soc. A Math. Phys. Eng. Sci.* **2012**, *370* (1963), 1422–1443.

(74) Nyamukamba, P.; Okoh, O.; Mungondori, H.; Taziwa, R.; Zinya, S. Synthetic Methods for Titanium Dioxide Nanoparticles: A Review. In *Titanium Dioxide - Material for a Sustainable Environment*; Yang, D., Ed.; 2018.

(75) Schubert, U.; Hiising, N.; Lorenz, A. Hybrid Inorganic-Organic Materials by Sol-Gel Processing of Organofunctional Metal Alkoxides. *Chem. Mater.* **1995**, *7* (11), 2010–2027.

(76) Philipp, G.; Schmidt, H. New Materials for Contact Lenses Prepared from Si- and Ti-Alkoxides by the Sol-Gel Process. *J. Non. Cryst. Solids* **1984**, *63* (1–2), 283–292.

(77) Vallet-Regí, M.; Colilla, M.; González, B. Medical Applications of Organic-Inorganic Hybrid Materials within the Field of Silica-Based Bioceramics. *Chem. Soc. Rev.* **2011**, *40* (2), 596–607.

(78) Schottner, G. Hybrid Sol-Gel-Derived Polymers: Applications of Multifunctional Materials. *Chem. Mater.* **2001**, *13* (10), 3422–3435.

(79) Kaya, S.; Cresswell, M.; Boccaccini, A. R. Mesoporous Silica-Based Bioactive Glasses for Antibiotic-Free Antibacterial Applications. *Mater. Sci. Eng. C* **2018**, *83* (May 2017), 99–107.

(80) Zhang, X.; Ye, H.; Xiao, B.; Yan, L.; Lv, H.; Jiang, B. Sol−Gel Preparation of PDMS/Silica Hybrid Antireflective Coatings with Controlled Thickness and Durable Antireflective Performance. *J. Phys. Chem. C* **2010**, *114* (47), 19979–19983.

(81) A. RaH mila, M. V.-R.; Departamento. Static and Dynamic in Vitro Study of a Sol-Gel Glass Bioactivity. *Biomaterials* **2000**, *22*, 2301–2306.

(82) Drisko, G. L.; Sanchez, C. Hybridization in Materials Science - Evolution, Current State, and Future Aspirations. *Eur. J. Inorg. Chem.* **2012**, No. 32, 5097–5105.

(83) Sanchez, C.; Rozes, L.; Ribot, F.; Laberty-Robert, C.; Grosso, D.; Sassoye, C.; Boissiere, C.;

Nicole, L. “Chimie Douce”: A Land of Opportunities for the Designed Construction of Functional Inorganic and Hybrid Organic-Inorganic Nanomaterials. *Comptes Rendus Chim.* **2010**, *13* (1–2), 3–39.

(84) Lebeau, B.; Maquet, J.; Sanchez, C.; Beaume, F.; Laupretre, F. Structural and Dynamical Studies of Hybrid Siloxane-Silica Materials. *J. Mater. Chem.* **1997**, *7* (6), 989–995.

(85) Chen, J.; Que, W.; Xing, Y.; Lei, B. Molecular Level-Based Bioactive Glass-Poly (Caprolactone) Hybrids Monoliths with Porous Structure for Bone Tissue Repair. *Ceram. Int.* **2015**, *41* (2), 3330–3334.

(86) Mondal, D.; Dixon, S. J.; Mequanint, K.; Rizkalla, A. S. Mechanically-Competent and Cytocompatible Polycaprolactone-Borophosphosilicate Hybrid Biomaterials. *J. Mech. Behav. Biomed. Mater.* **2017**, *75* (June), 180–189.

(87) Martín, A. I.; Salinas, A. J.; Vallet-Regí, M. Bioactive and Degradable Organic-Inorganic Hybrids. *J. Eur. Ceram. Soc.* **2005**, *25* (16), 3533–3538.

(88) Ren, L.; Tsuru, K.; Hayakawa, S.; Osaka, A. Novel Approach to Fabricate Porous Gelatin–siloxane Hybrids for Bone Tissue Engineering. *Biomaterials* **2002**, *23* (24), 4765–4773.

(89) Mahony, O.; Tsigkou, O.; Ionescu, C.; Minelli, C.; Ling, L.; Hanly, R.; Smith, M. E.; Stevens, M. M.; Jones, J. R. Silica-Gelatin Hybrids with Tailorable Degradation and Mechanical Properties for Tissue Regeneration. *Adv. Funct. Mater.* **2010**, *20* (22), 3835–3845.

(90) Kim, G. D.; Lee, D. A.; Moon, J. W.; Kim, J. D.; Park, J. A. Synthesis and Applications of TEOS-PDMS Hybrid Material by the Sol-Gel Process. *Appl. Organomet. Chem.* **1999**, *13* (5), 361–372.

(91) Almeida, J. C.; Wacha, A.; Bóta, A.; Almásy, L.; Vaz Fernandes, M. H.; Margaça, F. M. A.; Miranda Salvado, I. M. PDMS-SiO2 Hybrid Materials - A New Insight into the Role of Ti and Zr as Additives. *Polym. (United Kingdom)* **2015**, *72*, 40–51.

(92) Guo, L.; Hyeon-Lee, J.; Beaucage, G. Structural Analysis of Poly(Dimethylsiloxane) Modified Silica Xerogels. *J. Non. Cryst. Solids* **1999**, *243* (1), 61–69.

(93) Zhang, X. X.; Xia, B. B.; Ye, H. P.; Zhang, Y. L.; Xiao, B.; Yan, L. H.; Lv, H. B.; Jiang, B. One-Step Sol-Gel Preparation of PDMS-Silica ORMOSILs as Environment-Resistant and Crack-Free Thick Antireflective Coatings. *J. Mater. Chem.* **2012**, *22* (26), 13132–13140.

(94) Almeida, J. C.; Lancastre, J.; Vaz Fernandes, M. H.; Margaça, F. M. A.; Ferreira, L.; Miranda Salvado, I. M. Evaluating Structural and Microstructural Changes of PDMS -SiO2hybrid Materials after Sterilization by Gamma Irradiation. *Mater. Sci. Eng. C* **2015**, *48*, 354–358.

(95) Almeida, J. C.; Castro, A. G. B.; Lancastre, J. J. H.; Miranda Salvado, I. M.; Margaça, F. M. A.; Fernandes, M. H. V.; Ferreira, L. M.; Casimiro, M. H. Structural Characterization of PDMS-TEOS-CaO-TiO2 Hybrid Materials Obtained by Sol-Gel. *Mater. Chem. Phys.* **2014**,

143 (2), 557–563.

(96) Almeida, J. C.; Wacha, A.; Gomes, P. S.; Fernandes, M. H. R.; Fernandes, M. H. V.; Salvado, I. M. M. PDMS-SiO2-TiO2-CaO Hybrid Materials - Cytocompatibility and Nanoscale Surface Features. *Mater. Sci. Eng. C* **2016**, *64*, 74–86.

(97) Carlos Almeida, J.; Castro, A. G. B.; Miranda Salvado, I. M.; Margaça, F. M. A.; Vaz Fernandes, M. H. A New Approach to the Preparation of PDMS–SiO2 Based Hybrids – A Structural Study. *Mater. Lett.* **2014**, *128*, 105–109.

(98) Tsuru, K.; Hayakawa, S.; Osaka, A. Synthesis of Bioactive and Porous Organic-Inorganic Hybrids for Biomedical Applications. *J. Sol-Gel Sci. Technol.* **2004**, *32* (1–3), 201–205.

(99) Yabuta, T.; Bescher, E. P. P.; Mackenzie, J. D. D.; Tsuru, K.; Hayakawa, S.; Osaka, A. Synthesis of PDMS-Based Porous Materials for Biomedical Applications. *J. Sol-Gel Sci. Technol.* **2003**, *26* (1), 1219–1222.

(100) Tsuru, K.; Aburatani, Y.; Yabuta, T.; Hayakawa, S.; Ohtsuki, C.; Osaka, A. Synthesis and in Vitro Behavior of Organically Modified Silicate Containing Ca Ions. *J. Sol-Gel Sci. Technol.* **2001**, *21* (1–2), 89–96.

(101) Manzano, M.; Salinas, A. J.; Gil, F. J.; Vallet-Regí, M. Mechanical Properties of Organically Modified Silicates for Bone Regeneration. *J. Mater. Sci. Mater. Med.* **2009**, *20* (9), 1795–1801.

(102) Oh, E. O.; Chakrabarti, K.; Jung, H. Y.; Whang, C. M. Microstructures and Mechanical Properties of Organically Modified Silicate Prepared under Various Process Conditions. *Mater. Sci. Eng. B-Solid State Mater. Adv. Technol.* **2002**, *90* (1–2), 60–66.

(103) Glaser, R. H.; Wilkes, G. L.; Bronnimann, C. E. Solid-State Si-29 NMR of TEOS-Based Multifunctional Sol-Gel Materials. *J. Non. Cryst. Solids* **1989**, *113* (1), 73–87.

(104) Hu, Y.; Chung, Y. J.; Mackenzie, J. D. Gelation Kinetics of an Organically Modified Silicate. *J. Mater. Sci.* **1993**, *28* (24), 6549–6554.

(105) Hoshino, Y.; Mackenzie, J. D. Viscosity and Structure of Ormosil Solutions. *J. Sol-Gel Sci. Technol.* **1995**, *5* (2), 83–92.

(106) Hu, Y.; Mackenzie, J. D. Rubber-like Elasticity of Organically Modified Silicates. *J. Mater. Sci.* **1992**, *27* (16), 4415–4420.

(107) A. J. Salinas,1 J. M. Merino,1 F. Babonneau,2 F. J. Gil, 3 M. Vallet-Regı´1. Microstructure and Macroscopic Properties of Bioactive CaO–SiO2–PDMS Hybrids. *Biomed Mater Res Part B Appl Biomater 81B* **2006**, *83* (2), 340–344.

(108) Babonneau, F.; Maquet, J. Nuclear Magnetic Resonance Techniques for the Structural Characterization of Siloxane-Oxide Hybrid Materials. *Polyhedron* **2000**, *19* (3), 315–322.

(109) De Monredon-Senani, S.; Bonhomme, C.; Ribot, F.; Babonneau, F. Covalent Grafting of

Organoalkoxysilanes on Silica Surfaces in Water-Rich Medium as Evidenced By29Si NMR. *J. Sol-Gel Sci. Technol.* **2009**, *50* (2), 152–157.

(110) Breiner, J. M.; Mark, J. E.; Beaucage, G. Dependence of Silica Particle Sizes on Network Chain Lengths, Silica Contents, and Catalyst Concentrations Inin Situ-Reinforced Polysiloxane Elastomers. *J. Polym. Sci. Part B Polym. Phys.* **1999**, *37* (13), 1421–1427.

(111) Ulibarri, T. A.; Beaucage, G.; Schaefer, D. W.; Olivier, B. J.; Assink, R. A. Molecular Weight Dependence of Domain Structure in Silica-Siloxane Molecular Composites. *MRS Proc.* **2011**, *274* (June), 85.

(112) Schubert, U. Part One Sol – Gel Chemistry and Methods. *Sol-Gel Handb. Synth. Process.* **2015**, 1–28.

(113) Julián, B.; Gervais, C.; Cordoncillo, E.; Escribano, P.; Babonneau, F.; Sanchez, C. Synthesis and Characterization of Transparent PDMS-Metal-Oxo Based Organic-Inorganic Nanocomposites. *Chem. Mater.* **2003**, *15* (15), 3026–3034.

(114) Julián, B.; Gervais, C.; Rager, M. N.; Maquet, J.; Cordoncillo, E.; Escribano, P.; Babonneau, F.; Sanchez, C. Solid-State17O NMR Characterization of PDMS-MxOy(M = Ge(IV), Ti(IV), Zr(IV), Nb(V), and Ta(V)) Organic-Inorganic Nanocomposites. *Chem. Mater.* **2004**, *16* (3), 521–529.

(115) Tamayo, A.; Rubio, J. Structure Modification by Solvent Addition into TEOS/PDMS Hybrid Materials. *J. Non. Cryst. Solids* **2010**, *356* (33–34), 1742–1748.

(116) Chen, Q.; Miyaji, F.; Kokubo, T.; Nakamura, T. Apatite Formation on PDMS-Modified CaO-SiO2-TiO2 Hybrids Prepared by Sol-Gel Process. *Biomaterials* **1999**, *20* (12), 1127–1132.

(117) Salinas, A. J.; Merino, J. M.; Babonneau, F.; Gil, F. J.; Vallet-Regi, M. Microstructure and Macroscopic Properties of Bioactive CaO-SiO2-PDMS Hybrids. *J. Biomed. Mater. Res. Part B-Applied Biomater.* **2007**, *81B* (1), 274–282.

(118) Kamitakahara, M.; Kawashita, M.; Miyata, N.; Kokubo, T.; Nakamura, T. Bioactivity and Mechanical Properties of Polydimethylsiloxane (PDMS)-CaO-SiO2 Hybrids with Different Calcium Contents. *J. Mater. Sci. Med.* **2002**, *13* (11), 1015–1020.

(119) Rámila, A.; Balas, F.; Vallet-Regí, M. Synthesis Routes for Bioactive Sol-Gel Glasses: Alkoxides versus Nitrates. *Chem. Mater.* **2002**, *14* (2), 542–548.

(120) Almeida, J. C.; Wacha, A.; Gomes, P. S.; Alves, L. C.; Fernandes, M. H. V.; Salvado, I. M. M.; Fernandes, M. H. R. A Biocompatible Hybrid Material with Simultaneous Calcium and Strontium Release Capability for Bone Tissue Repair. *Mater. Sci. Eng. C* **2016**, *62*, 429–438.

(121) Rubio, F.; Rubio, J.; Oteo, J. L. A FT-IR Study of the Hydrolysis of Tetraethylorthosilicate (TEOS). *Spectrosc. Lett.* **1998**, *31* (1), 199–219.

(122) Lee, S. K.; Musgrave, C. B.; Zhao, P.; Stebbins, J. F. Topological Disorder and Reactivity of

Borosilicate Glasses: Quantum Chemical Calculations and 17O and 11B NMR Study. *J. Phys. Chem. B* **2001**, *105* (50), 12583–12595.

(123) Kroeker, S.; Stebbins, J. F. Three-Coordinated Boron-11 Chemical Shifts in Borates. *Inorg. Chem.* **2001**, *40* (24), 6239–6246.

(124) Du, L.-S.; Stebbins, J. F. Nature of Silicon−Boron Mixing in Sodium Borosilicate Glasses: A High-Resolution ^{11}B and ^{17}O NMR Study. *J. Phys. Chem. B* **2003**, *107* (37), 10063–10076.

(125) Möncke, D.; Tricot, G.; Winterstein-Beckmann, A.; Wondraczek, L.; Kamitsos, E. I. On the Connectivity of Borate Tetrahedra in Borate and Borosilicate Glasses. *Phys. Chem. Glas. Eur. J. Glas. Sci. Technol. Part B* **2015**, *56* (5), 203–211.

(126) Silver, A. H.; Bray, P. J. Nuclear Magnetic Resonance Absorption in Glass. I. Nuclear Quadrupole Effects in Boron Oxide, Soda-Boric Oxide, and Borosilicate Glasses. *J. Chem. Phys.* **1958**, *29* (5), 984–990.

(127) Du, L. S.; Stebbins, J. F. Site Preference and Si/B Mixing in Mixed-Alkali Borosilicate Glasses: A High-Resolution 11B and 17O NMR Study. *Chem. Mater.* **2003**, *15* (20), 3913–3921.

(128) Stebbins, J. F.; Oglesby, J. V; Xu, Z. Disorder among Network-Modifier Cations in Silicate Glasses; New Constraints from Triple-Quantum 17 O NMR. *Am. Mineral.* **1997**, *82* (11–12), 1116–1124.

(129) Peña-Alonso, R.; Rubio, J.; Rubio, F.; Oteo, J. L. FT-IR and Porosity Study of Si-B-C-O Materials Obtained from TEOS-TEB-PDMS Derived Gel Precursors. *J. Sol-Gel Sci. Technol.* **2003**, *26* (1–3), 195–199.

(130) Sorarù, G. D.; Dallabona, N. Hybrid RSiO1.5/B2O3 Gels from Modified Silicon Alkoxides and Boric Acid. *Tribol. Trans.* **1999**, *42* (3), 592–600.

(131) Peña-Alonso, R.;Tamayo, A.; Rubio, F. and Rubio, J. Influence of Boron Concentration on the Surface Properties of TEOS-PDMS Hybrid Materials. *J. Sol-Gel Sci. Technol.* **2005**, *36*, 113–124.

(132) Irwin, A. D.; Holmgren, J. S.; Jonas, J. Solid State 29Si and 11B NMR Studies of Sol-Gel Derived Borosilicates. *J. Non. Cryst. Solids* **1988**, *101* (2–3), 249–254.

(133) Brinker, C. J.; Scherer, G. W. *Sol-Gel Science: The Physics and Chemistry of Sol-Gel Processing*; Boston, 1990.

(134) Grandi, S.; Tomasi, C.; Cassinelli, V.; Cucca, L.; Profumo, A.; Mustarelli, P.; Balduini, C. SiO2-B2O3 Xerogels: The Problem of Boron Leaching. *J. Non. Cryst. Solids* **2012**, *358* (14), 1631–1637.

(135) Stebbins, J. F.; Zhao, P.; Kroeker, S. Non-Bridging Oxygens in Borate Glasses: Characterization by 11B and 17O MAS and 3QMAS NMR. *Solid State Nucl. Magn. Reson.*

2000, *16* (1–2), 9–19.

(136) Doweidar, H. Consideration of the Boron Oxide Anomaly. *J. Mater. Sci.* **1990**, *25* (1), 253–258.

(137) Wu, J.; Stebbins, J. F. Temperature and Modifier Cation Field Strength Effects on Aluminoborosilicate Glass Network Structure. *J. Non. Cryst. Solids* **2013**, *362* (1), 73–81.

(138) Massiot, D.; Fayon, F.; Capron, M.; King, I.; Le Calve, S.; Alonso, B.; Durand, J. O.; Bujoli, B.; Gan, Z. H.; Hoatson, G. Modelling One- and Two-Dimensional Solid-State NMR Spectra. *Magn. Reson. Chem.* **2002**, *40* (1), 70–76.

(139) Sing, K. S. W.; Everett, D. H.; Haul, R. A. W.; Moscou, L.; Pierotti, R. S.; Rouquerol, J.; Siemieniewska, T. Reporting Physisorption Data for Gas/Solid Systems with Special Reference to the Determination of Surface Area and Porosity. *Pure Appl. Chem.* **1985**, *57* (4), 603–619.

(140) Kokubo, T.; Takadama, H. How Useful Is SBF in Predicting in Vivo Bone Bioactivity? *Biomaterials* **2006**, *27* (15), 2907–2915.

(141) Bohner, M.; Lemaitre, J. Can Bioactivity Be Tested in Vitro with SBF Solution? *Biomaterials* **2009**, *30* (12), 2175–2179.

(142) Villegas, M. A.; Navarro, J. M. F.; Fernandez Navarro, J. M.; Navarro, J. M. F.; Fernandez Navarro, J. M.; Navarro, J. M. F. Characterization of B2O3-SiO2 Glasses Prepared via Sol-Gel. *J. Mater. Sci.* **1988**, *23* (7), 2464–2478.

(143) Soraru, G. D.; Babonneau, F.; Maurina, S.; Vicens, J. Sol-Gel Synthesis of SiBOC Glasses. *J. Non. Cryst. Solids* **1998**, *224* (2), 173–183.

(144) Peña-Alonso, R.; Sorarù, G. D. Synthesis and Characterization of Hybrid Borosiloxane Gels as Precursors for Si-B-O-C Fibers. *J. Sol-Gel Sci. Technol.* **2007**, *43* (3), 313–319.

(145) Han, Y.-H.; Taylor, A.; Mantle, M. D.; Knowles, K. M. Sol–gel-Derived Organic–inorganic Hybrid Materials. *J. Non. Cryst. Solids* **2007**, *353* (3), 313–320.

(146) Aguiar, H.; Serra, J.; González, P.; León, B.; Gonzalez, P.; Leon, B. Structural Study of Sol-Gel Silicate Glasses by IR and Raman Spectroscopies. *J. Non. Cryst. Solids* **2009**, *355* (8), 475–480.

(147) Samuneva, B.; Djambaski, P.; Kashchieva, E.; Chernev, G.; Kabaivanova, L.; Emanuilova, E.; Salvado, I. M. M.; Fernandes, M. H. V; Wu, A. Y. Sol-Gel Synthesis and Structure of Silica Hybrid Biomaterials. *J. Non. Cryst. Solids* **2008**, *354* (2–9), 733–740.

(148) Téllez, L.; Rubio, J.; Rubio, F.; Morales, E.; Oteo, J. L. FT-IR Study of the Hydrolysis and Polymerization of Tetraethyl Orthosilicate and Polydimethyl Siloxane in the Presence of Tetrabutyl Orthotitanate. *Spectrosc. Lett.* **2004**, *37* (1), 11–31.

(149) Lepry, W. C.; Nazhat, S. N. Highly Bioactive Sol-Gel-Derived Borate Glasses. *Chem. Mater.*

2015, *27* (13), 4821–4831.

(150) Beckett, M. A.; Rugen-Hankey, M. P.; Varma, K. S. Trimethoxyboroxine as an "oxygen-Transfer" Reagent: A Non-Aqueous "Sol-Gel" Route to Alkali-Free Borosilicate Glass. *Chem. Commun.* **2000**, No. 16, 1499–1500.

(151) Castro, A. G. B.; Almeida, J. C.; Salvado, I. M. M.; Margaca, F. M. A.; Fernandes, M. H. V. A Novel Hybrid Material with Calcium and Strontium Release Capability. *Mater. Lett.* **2012**, *88*, 12–15.

(152) Brus, J.; Dybal, J. Solid-State NMR Study of Structure, Size and Dynamics of Domains in Hybrid Siloxane Networks. *Polymer (Guildf).* **2000**, *41* (14), 5269–5282.

(153) Wang, X.; Cheng, F.; Liu, J.; Smått, J. H.; Gepperth, D.; Lastusaari, M.; Xu, C.; Hupa, L. Biocomposites of Copper-Containing Mesoporous Bioactive Glass and Nanofibrillated Cellulose: Biocompatibility and Angiogenic Promotion in Chronic Wound Healing Application. *Acta Biomater.* **2016**, *46*, 286–298.

(154) Peitl O, LaTorre GP, H. L. Effect of Crystallization on Apatite Layer Formation of Bioactive Glass 45S5. *J Biomed Mater Res* **1996**, *30*, 509–514.

(155) Yu, B.; Turdean-Ionescu, C. a.; Martin, R. a.; Newport, R. J.; Hanna, J. V.; Smith, M. E.; Jones, J. R. Effect of Calcium Source on Structure and Properties of Sol-Gel Derived Bioactive Glasses. *Langmuir* **2012**, *28* (50), 17465–17476.

(156) Hench, L. L. Bioceramics: From Concept to Clinic. *J. Am. Ceram. Soc.* **1991**.

(157) Lippmaa, E.; Magi, M.; Samoson, A.; Engelhardt, G.; Grimmer, A. R. Structural Studies of Silicates by Solid-State High-Resolution Si-29 Nmr. *J. Am. Chem. Soc.* **1980**, *102* (15), 4889–4893.

Annex

Annex I

Notation used for Si structural groups

In the present work it will be used a notation to represent silicon structural groups, which was developed by Lippmaa et al. [157] and adapted by Glaser et al [103].

Silicon-based tetrahedra containing oxygen and organic "R" groups, in the case of PDMS "R" is a methyl group (CH_3), can be represented by:

- "Q" quaternary (four) oxygen tetrahedral
- "T": ternary (three) oxygen and one organic group tetrahedral
- "D": "di" oxygen and two groups tetrahedral.

The numerical superscript indicates the number of other silicate structures attached to the one in question. Figure 24 represent a schematic representation of the notation used for Si functional groups.

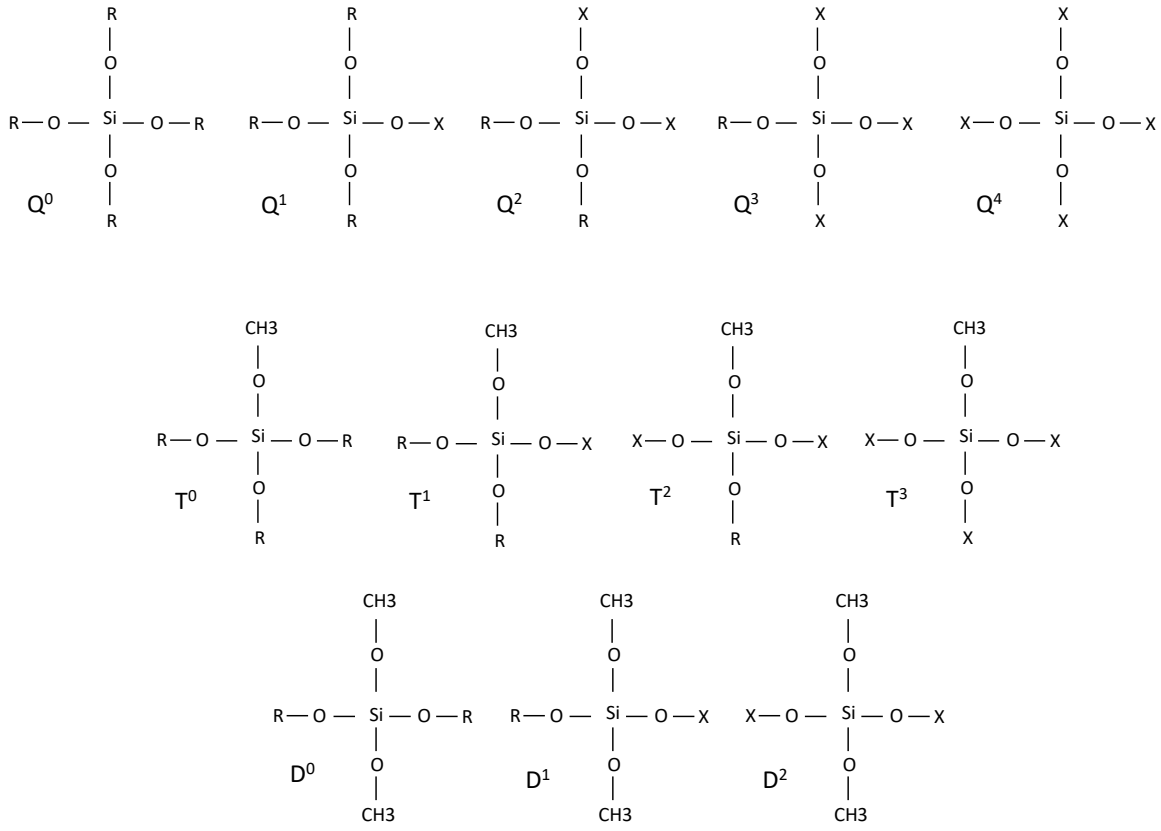

Figure 24 - Notation used for Si structural groups.

Annex II

Results from previous procedures

Before achieving the final protocol, same experimental attempts were made, using different procedures as well as different precursors than the ones used for the defined protocol described in this work. It was the case of calcium precursor. In Figure 25 it is presented images of samples dried at 150ºC, in petri dishes, using calcium chloride ($CaCl_2$) as calcium precursor and the formation of precipitates in the surface.

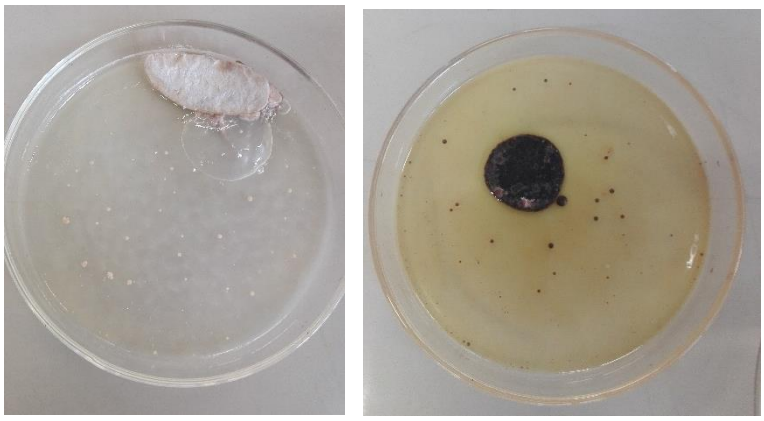

Figure 25 - Examples of samples dried at 150ºC, in petri dishes, using CaCl2 as calcium precursor.

Annex III

Scientific poster

A poster based in this thesis and entitled “Boron containing PDMS-SiO_2.CaO hybrid materials by sol-gel for bone tissue engineering”, was presented in the “V Congreso Hispano-Luso de Cerámic y Vidrio/LVI Congreso Nacional de la SECV” in Barcelona, Spain.

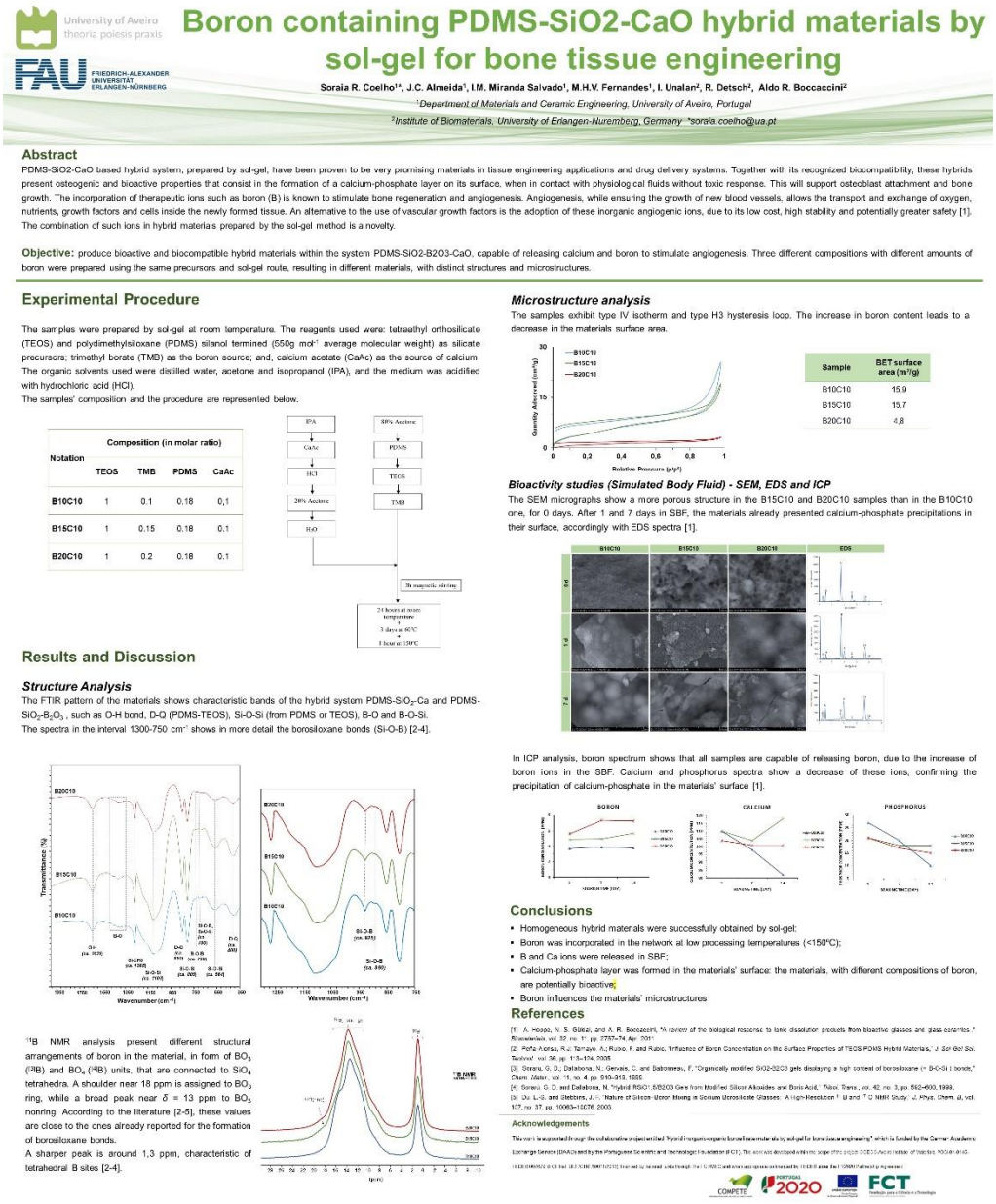

Figure 26 – Scientific poster based in this dissertation.